



THE HONG KONG
POLYTECHNIC UNIVERSITY

香港理工大學

Pao Yue-kong Library

包玉剛圖書館

Copyright Undertaking

This thesis is protected by copyright, with all rights reserved.

By reading and using the thesis, the reader understands and agrees to the following terms:

1. The reader will abide by the rules and legal ordinances governing copyright regarding the use of the thesis.
2. The reader will use the thesis for the purpose of research or private study only and not for distribution or further reproduction or any other purpose.
3. The reader agrees to indemnify and hold the University harmless from and against any loss, damage, cost, liability or expenses arising from copyright infringement or unauthorized usage.

IMPORTANT

If you have reasons to believe that any materials in this thesis are deemed not suitable to be distributed in this form, or a copyright owner having difficulty with the material being included in our database, please contact lbsys@polyu.edu.hk providing details. The Library will look into your claim and consider taking remedial action upon receipt of the written requests.

The Hong Kong Polytechnic University

Interdisciplinary Division of Biomedical Engineering

**Liver Fibrosis Assessment Using Transient
Elastography Guided with Real-time B-mode
Ultrasound Imaging: A Feasibility Study**

Tak-Man MAK

A thesis submitted in partial fulfilment of the requirements for
the degree of Master of Philosophy

July 2012

CERTIFICATE OF ORIGINALITY

I hereby declare that this thesis is my own work and that, to the best of my knowledge and belief, it reproduces no material previously published or written, nor material that has been accepted for the award of any other degree or diploma, except where due acknowledgement has been made in the text.

_____ (Signed)

Tak-Man MAK (Name of student)

ABSTRACT OF THESIS

“Liver Fibrosis Assessment using Transient Elastography Guided with Real-time B-mode Ultrasound Imaging: A Feasibility Study”

Submitted by Tak-Man MAK

for the degree of Master of Philosophy

at The Hong Kong Polytechnic University

in July 2012

Liver fibrosis is a kind of chronic damage of the liver and may lead to cirrhosis, one of the top 10 causes of death in the western world. The complications of cirrhosis may include liver failure, portal hypertension and hepatocellular carcinoma. The main causes of liver fibrosis are very common including hepatitis B virus (HBV) and hepatitis C virus (HCV) infection, alcohol abuse and non-alcoholic steatohepatitis (NASH). Thus, the demand for a noninvasive diagnostic system is high. Recently, a device called Fibroscan (Echosens, Paris, France) has been developed based on transient elastography, which shows promising results for liver fibrosis assessment. However, this device does not provide visual guidance of the liver during measurement, which affects the measurement accuracy and user-friendliness of operation. Our team has also developed a transient elastography system with real-time B-mode ultrasound imaging serving as visual guidance for liver fibrosis assessment, named as Liverscan. The aims of this MPhil study are (1) to design and fabricate specific probe for Liverscan to assess liver fibrosis non-invasively; (2) to systematically validate the new system and (3) to establish a measurement protocol for using the system.

The measurement probe was designed and fabricated with a B-mode ultrasound transducer (4.5 MHz) fixed along the axis of a mechanical vibrator. When the mechanical vibrator was activated, the ultrasound transducer vibrated accordingly to generate shear wave in tissue. The vibration frequency used in this study was 100 Hz and its amplitude was approximately 5 mm at the surface of the transducer, which were optimal for this system. The induced shear wave propagated through liver tissue; pulse-echo ultrasound acquisition was used to trace the shear wave. The propagation of the shear wave in tissue indicates the stiffness of liver. A higher shear wave velocity indicates a harder liver tissue that reveals the severity of fibrosis.

The measurement using Liverscan was validated by conventional mechanical indentation test on 15 custom-made agar-gelatin phantoms with different stiffness. An Instron machine was used to measure the force-indentation relationship of phantoms, and then their Young's modulus values were calculated and compared with the results obtained by Liverscan. A significant linear correlation of Young's moduli measured by the mechanical indentation test and the Liverscan ($r=0.97$, $p<0.001$) was found. This indicated that Liverscan was able to differentiate soft tissues with various stiffness.

In this study, totally 67 subjects including 34 male and 33 female (Age: 34 ± 13 years and BMI: 21.3 ± 2.8 kgm^{-2}) were recruited for different tests. Among them, 20 subjects had confirmed liver diseases while the rest has no history of any liver disease. 26 and 23 subjects participated in inter- and intra-observer tests for the Liverscan, respectively. 28 subjects were tested using both Liverscan and Fibroscan. In addition,

all the 67 subjects participated in the test of location dependence using Liverscan.

For the *in vivo* measurement using Liverscan, the subjects were tested using the following protocol. All the subjects fasted for at least 3 hours prior to any measurements. During the tests, the subjects were asked to lie down in supine position with their right arms in maximal abduction and placed behind their heads. Then, an area close to the projection of the rib cage was identified, i.e. the intercostal space between the 7th and 8th ribs and about 5 cm in distance from the projection. After the suitable location was identified, the measurement probe was applied. With the guidance of real-time B-mode ultrasound, we could select the depth and location of liver tissue to be assessed without any large blood vessels included by moving the cursor of region of interest (ROI). For the intra-observer test, the test was repeated by the same operator twice following the same protocol. The tests were conducted by two operators in the inter-operator test. In addition to the first location, another one was selected for applying the measurement probe to test the location dependence, which was at the intercostal space between 8th and 9th ribs. After the measurement using Liverscan, the selected subjects were tested again by the Fibroscan within one week at the centre of The Hong Kong Health Check. All the subjects fasted at least 3 hours before the measurement, and they were tested by the same operator at the centre.

The results showed excellent repeatability of the measurement using Liverscan with an intraclass correlation coefficient of 0.987 ($p<0.001$) and 0.988 ($p<0.001$) for the inter- and intra-observer tests, respectively. A high correlation between the liver stiffness values obtained by the Liverscan and the Fibroscan was found ($r=0.886$, $p<0.001$). This indicated that the Liverscan was able to perform reliable *in vivo* liver

stiffness measurement and capable of identifying liver with different stiffness. Based on the correlation and the result published for Fibroscan measurement, the calculated cut-off value of liver fibrosis was 14.0 kPa for the Liverscan. The location dependence test revealed no significant difference in the stiffness between the two tested sites ($p=0.178$) and the two sets of stiffness data showed significant correlation ($r=0.946$, $p<0.001$). This result demonstrated that both the locations were qualified to be included in the measurement protocol of the Liverscan.

In summary, this study has demonstrated that the Liverscan with a specifically designed B-mode probe is able to provide a reliable measurement of livers with different stiffness using the proposed measurement protocol. The real-time B-mode ultrasound imaging is useful as visual guidance which improves the measurement accuracy and efficiency. Future studies are required to further validate the system and demonstrate its clinical value by testing a large group of subjects with different degrees of liver fibrosis and by making comparison with biopsy.

Key words: Ultrasound, transient elastography, elasticity measurement, liver fibrosis, soft tissue

PUBLICATIONS ARISING FROM THE THESIS

Journal papers

1. **Mak T-M**, Huang Y-P, Zheng Y-P. Liver fibrosis assessment using transient elastography guided with real-time B-mode ultrasound imaging: A feasibility study, *Ultrasound in Medicine and Biology*, Vol. 39 (6), pp 956-966, 2013.

Conference proceedings

1. **Mak T-M**, Yu X, Zheng Y-P. Liver fibrosis assessment using transient elastography guided with real-time B-mode ultrasound imaging: Investigation of food intake effect, 10th International Tissue Elasticity Conference, Arlington, Texas, USA, pp 81, Oct, 2011.
2. Zheng Y-P, **Mak T-M**, Huang Z-M, Cheung C-WJ, Zhou Y-J, He J-F. Liver fibrosis assessment using transient elastography guided with real-time B-mode ultrasound imaging, BME 2010 Conference, Hong Kong, Nov, 2010.
3. Zheng Y-P, **Mak T-M**, Huang Z-M, Cheung C-WJ, Zhou Y-J, He J-F. Liver fibrosis assessment using transient elastography guided with real-time B-mode ultrasound imaging, 6th World Congress of Biomechanics (WCB 2010), Singapore, pp 1036-9, Aug, 2010.

ACADEMIC AWARDS

1. Hong Kong Medical and Healthcare Device Industries Association (HKMHDIA),
Student Research Award, 2nd Runner-up, Nov. 2010
2. BME 2010 Conference, Best Young Engineers' Paper Competition, Memorial
Award, Nov 2010.

ACKNOWLEDGEMENTS

Given this precious opportunity, I would like to express my sincere appreciation to the people who have helped me with their efforts to make this thesis possible.

First and foremost, I would like to acknowledge with my sincere gratitude to my supervisor, Prof. Yong-ping ZHENG. I always got plentiful suggestions, invaluable comments and kind guidance from him. This helped me a lot to make this thesis possible. With his rigorous scholarship and patient encouragement, I was able to finish this study. Moreover, his working attitude has infected me and pushed me to work hard and be serious and scientific to research. I thank him for pointing out the problems with me and teaching and sharing knowledge with me.

I would like to thank Dr. Thomas Ming-Hung LEE and Dr. Mo YANG for assessing my proposal and confirmation report, pointing out the existing problems and giving valuable suggestions to my study. I would also like to thank Dr. Eric WC TAM for allowing me to use the mechanical workshop for probe fabrication.

I gratefully acknowledge Mr. James CHEUNG for his guidance and comments, Mr. Zheng-Ming HUNG and Dr. Yong-Jin ZHOU for software support, Mr. Jun-Fung HE for his technical support, Ms. Xue YU for her help for *in vivo* measurement and Mr. Kung-Chee CHEN for his valuable comments on probe fabrication. At the early stage of my study, they really inspired me and helped me a lot. Great thanks are given to Ms. Sally Ding for her help on editing my thesis. I would also like to thank the engineers from SIUI for their technical support and all the subjects who participated in the study.

I am grateful to all of my colleagues, who learned along with me and stimulated me a lots, most notably Mr. Yanping HUANG, Mr. Like WANG, Mr. Louis LEE, Ms. Yen LAW, Mr. Tim TANG, Ms. Jing-Yi GUO, Mr. Cong-Zhi WANG, Mr. William Man-Wai CHIU, Mr. Guang-Quan ZHOU and Ms. Wei-Wei JIANG.

I would like to thank my beloved family for their support during my study period, especially my wife, Ms. Lai Yee CHOI, who always supports me for doing research.

Lastly, I would like to acknowledge the financial support from the Hong Kong Polytechnic University (J-BB69), and the HK Innovative Technology Fund (GHP/047/09).

TABLE OF CONTENTS

| | |
|---|-------------|
| CERTIFICATE OF ORIGINALITY | II |
| ABSTRACT OF THESIS | III |
| PUBLICATIONS ARISING FROM THE THESIS | VII |
| ACADEMIC AWARDS..... | VIII |
| ACKNOWLEDGEMENTS | IX |
| TABLE OF CONTENTS | XI |
| LIST OF ABBREVIATIONS | XIV |
| LIST OF FIGURES | XV |
| LIST OF TABLES | XIX |
| CHAPTER 1 INTRODUCTION | 1 |
| 1.1 BACKGROUND..... | 1 |
| 1.2 OBJECTIVES OF THE STUDY | 3 |
| 1.3 OUTLINE OF THE DISSERTATION..... | 4 |
| CHAPTER 2 LITERATURE REVIEW | 6 |
| 2.1 ANATOMY OF LIVER..... | 6 |
| 2.2 LIVER DISEASE: LIVER FIBROSIS | 7 |
| 2.3 ASSESSMENT OF LIVER FIBROSIS..... | 9 |
| 2.3.1 <i>Liver Biopsy</i> | 9 |
| 2.3.2 <i>Serum Marker Analysis</i> | 12 |
| 2.3.3 <i>B-mode Ultrasound Imaging</i> | 13 |
| 2.3.4 <i>Magnetic Resonance Imaging</i> | 17 |

| | |
|--|-----------|
| 2.3.5 <i>Elasticity Measurement of Liver</i> | 20 |
| 2.3.5.1 Real-time elastography | 20 |
| 2.3.5.2 Transient Elastography | 23 |
| 2.3.5.3 Magnetic Resonance Elastography | 27 |
| 2.3.5.4 Supersonic Shear Imaging | 30 |
| 2.3.6 <i>Summary</i> | 33 |
| CHAPTER 3 MATERIALS AND METHODS | 35 |
| 3.1 PROBE DEVELOPMENT AND FABRICATION..... | 35 |
| 3.2 TRANSIENT ELASTOGRAPHY SYSTEM WITH REAL-TIME B-MODE ULTRASOUND IMAGING..... | 38 |
| 3.3 SYSTEM VALIDATION USING AGAR-GELATIN PHANTOMS | 39 |
| 3.4 SUBJECTS | 43 |
| 3.5 IN VIVO ASSESSMENT PROTOCOL AND REPEATABILITY TESTS | 44 |
| 3.6 COMPARISON BETWEEN LIVERSCAN AND FIBROSCAN..... | 47 |
| 3.7 TESTS FOR LOCATION DEPENDENCE OF MEASUREMENT | 48 |
| 3.8 STATISTICAL ANALYSIS | 49 |
| CHAPTER 4 RESULTS | 50 |
| 4.1 AGAR-GELATIN PHANTOMS: CORRELATION BETWEEN LIVERSCAN AND MECHANICAL INDENTATION TEST..... | 50 |
| 4.2 INTRA- AND INTER- REPEATABILITY TESTS | 51 |
| 4.3 CORRELATION BETWEEN LIVERSCAN AND FIBROSCAN FOR IN VIVO MEASUREMENTS | 52 |
| 4.4 LOCATION DEPENDENCE OF MEASUREMENT..... | 57 |
| CHAPTER 5 DISCUSSION | 59 |

| | |
|--|-----------|
| 5.1 SUMMARY OF THE STUDY..... | 59 |
| 5.2 REAL-TIME B-MODE ULTRASOUND GUIDING | 60 |
| 5.3 EVALUATION OF THE STIFFNESS MEASURED BY LIVERSCAN | 62 |
| 5.4 EVALUATION OF THE MEASUREMENT PROTOCOL..... | 64 |
| 5.5 STAGES OF LIVERSCAN DEVELOPMENT | 66 |
| CHAPTER 6 CONCLUSIONS AND FURTHER SUTDIES | 68 |
| 6.1 CONCLUSIONS | 68 |
| 6.2 FURTHER STUDIES | 68 |
| 6.2.1 <i>Size of subject group</i> | 68 |
| 6.2.2 <i>Comparison with biopsy</i> | 69 |
| 6.2.3 <i>Measurement protocol: Fasting study</i> | 69 |
| 6.2.4 <i>Measurement protocol: Vibration frequency study</i> | 70 |
| 6.2.5 <i>Measurement protocol: Breathing study</i> | 70 |
| 6.2.6 <i>Probe development and fabrication</i> | 71 |
| APPENDIX..... | 72 |
| I. TECHNICAL DRAWING OF THE PROBE | 72 |
| II. EXAMPLE OF THE STIFFNESS CALCULATION..... | 73 |
| III. DATA TABLE | 74 |
| IV. INFORMATION SHEET..... | 78 |
| 與研究相關的資訊..... | 80 |
| V. INFORMED CONSENT FORM..... | 81 |
| 知情同意書..... | 83 |
| REFERENCES..... | 84 |

LIST OF ABBREVIATIONS

| | |
|-------|---|
| ADC | Apparent diffusion coefficient |
| APRI | Aspartate aminotransferase to platelets ratio index |
| AUROC | Area under receiver operating characteristic curve |
| BMI | Body mass index |
| DWI | Diffusion-weighted MRI |
| ECM | Extracellular matrix |
| HA | Hyaluronic acid |
| HBV | Hepatitis B virus |
| HCV | Hepatitis C virus |
| HSC | Hepatic stellate cell |
| ICC | Intraclass correlation coefficient |
| MRE | Magnetic resonance elastography |
| MRI | Magnetic resonance imaging |
| NASH | Non-alcoholic steatohepatitis |
| ROI | Region of interest |
| RTE | Real-time elastography |
| SSI | Supersonic shear imaging |
| TE | Transient elastography |

LIST OF FIGURES

| | |
|--|----|
| Figure 2.1 Anatomy of liver. (Zygotebody) | 7 |
| Figure 2.2 Change in the hepatic structure. (A) is the normal liver and (B) is the liver tissue with advanced fibrosis. (Bataller and Brenner 2005)..... | 9 |
| Figure 2.3 Liver biopsy is an invasive procedure that uses needle to remove a small amount of liver tissue. (http://www.skills.uct.ac.za/activities.htm)..... | 10 |
| Figure 2.4 B-mode ultrasound image of a patient with cirrhosis shows irregular liver surface and a hypo-echoic lesion. (Goyal et al. 2009)..... | 15 |
| Figure 2.5 Ultrasound images of the liver surface. (a) and (b) show a smooth and mildly irregular surfaces with a high frequency ultrasound transducer, respectively; (c) and (d) show an irregular and a highly irregular surfaces with a low frequency ultrasound transducer, respectively. This reveals the frequency of ultrasound does affect the diagnostic accuracy. (Nishiura et al. 2005) | 15 |
| Figure 2.6 DWI image and ADC map of liver. (a) is the control group image and (b) is the image for a patient with significant fibrosis. The ADC map shows the ADC values were higher in (a) as compared to (b), indicating the ADC value decreased as the severity of fibrosis increased. (Bakan et al. 2012)..... | 19 |
| Figure 2.7 RTE for liver stiffness measurement using conventional B-mode ultrasound probe for compression. It shows the stiffness distribution of tissue coded with color, red for soft tissue and blue for hard tissue. (Friedrich-Rust et al. 2007) | 22 |
| Figure 2.8 <i>In vivo</i> measurement results by Fibroscan: (a) is no fibrosis or mild fibrosis, (b) is severe fibrosis and (c) is cirrhosis. (Sandrin et al. 2003)..... | 25 |

Figure 2.9 MRE images of patient with cirrhosis. (a) shows the ROI of liver in MRI, (b) represents elasticity map of liver fibrosis and (c) represents the viscosity map of liver fibrosis. (Huwart et al. 2006)29

Figure 2.10 Supersonic shear source activation and propagation images at different time points. (Bercoff et al. 2004).....31

Figure 2.11 Color coded liver stiffness maps indicate 4 stages of fibrosis measured by SSI. (a) is the mild fibrosis; (b) is the severe fibrosis; (c) is significant fibrosis and (d) is cirrhosis. (Bavu et al. 2011)32

Figure 3.1 The developed transient elastography system with real-time B-mode ultrasound imaging, Liverscan , with specifically designed probe.....36

Figure 3.2 The schematic diagram represents the elements of Liverscan.....37

Figure 3.3 Illustration of imaging principle of the Liverscan. B-mode ultrasound images are generated in 25 frames per second and one of these B-mode images is replaced by M-mode ultrasound image to trace the propagation of the shear wave through liver tissue. The induced shear wave in liver causes disturbance in the ultrasound echo train. After tracing this disturbance, the transient elastography image can be formed and the stiffness can be calculated from the slope of the trace.....39

Figure 3.4 (a) Agar-gelatin phantom. A series of agar-gelatin phantoms with different stiffness were produced. Agar acts as the scatterer and gelatin is the matrix. The concentration of gelatin determines the stiffness of phantoms. (b) Agar-gelatin phantoms under mechanical indentation test. Totally 2 different locations were tested for averaging.....41

Figure 3.5 A typical force-deformation curve from indentation test in the last loading phase that shows a linear correlation. This indicates the fabricated agar-gelatin phantoms are purely elastic in this study.43

Figure 3.6 Established *in vivo* assessment protocol: Lie down in supine position with right arm in maximal abduction and placed behind head. The measurement locations are then identified with reference to the anatomical landmarks.45

Figure 3.7 (a) Assessment location for liver fibrosis using anatomical features of rib cage as reference. Generally, with the help of the landmark, the projection of rib case, we could identify the area of intercostal space between 7th and 8th ribs and 8th and 9th ribs to be the 1st and 2nd assessment locations. (b) The identification of measurement locations for the Fibroscan. (Google body)46

Figure 3.8 A typical measurement interface for the Liverscan. On the left, a real-time B-mode ultrasound image as guidance is provided. The elastography is displayed on the right side.47

Figure 4.1 A typical stiffness measurement result of an agar-gelatin phantom.....50

Figure 4.2 The correlation between the stiffness measured by the mechanical indentation test and that by the Liverscan. A significant correlation was found ($r=0.97, p<0.001$).....51

Figure 4.3 For both the Liverscan (a) and the Fibroscan (b), the mean and median values obtained were highly correlated ($r=0.0995, p<0.001$) and ($r=0.0996, p<0.001$), respectively.....53

Figure 4.4 The linear correlation between the *in vivo* liver stiffness measured by the Liverscan and that by the Fibroscan. A significant correlation was found in the results obtained from the two measurements ($r=0.886, p<0.001$).....54

Figure 4.5 Bland-Altman analysis shows agreement between the stiffness measured by the Liverscan and that by the Fibroscan. Only 3.6% of the values were outside limits of agreement, 1.96SD.....55

Figure 4.6 Some typical *in vivo* liver stiffness measurement results measured by the Liverscan, showing different stiffness measurements and indicating the measurement ability of the Liverscan. Left side is the B-mode ultrasound liver image and right side is the elastogram. We could identify the upper boundary and a blood vessel in the B-mode ultrasound image that allows selecting ROI. The slope of the trace in elastogram represents the liver stiffness.57

Figure 4.7 The liver stiffness measured by the Liverscan at two locations was correlated significantly ($r=0.946, p<0.001$).58

Figure 5.1 An *in vivo* liver stiffness measurement result with blood vessel (a) and without blood vessel (b) included in the ROI. In (a), the elastogram was distorted due to the presence of blood vessel in the ROI and this resulted in degraded trace measurement and overestimated liver stiffness, 28.5 kPa; (b) shows the measurement without blood vessel and correct stiffness measurement, 13.5 kPa.61

Figure A.1 Technical drawing of the probe.....72

LIST OF TABLES

| | |
|---|----|
| Table 3.1 The clinical characteristics of 20 patients with confirmed liver diseases. ... | 44 |
| Table A.1 The stiffness of phantoms measured by the mechanical indentation test and the Liverscan is listed below. The Young's modulus of phantoms measured by mechanical test was calculated based on Equation (1) with the force-deformation relationship obtained from the mechanical indentation test..... | 74 |
| Table A.2 Liver stiffness measured by the Liverscan and the Fibroscan is summarized below. Fibroscan obtains median values, while the Liverscan utilizes mean values. From the Fibroscan results, we can identify that the median values and mean values are very close. The correlation between the Liverscan and the Fibroscan was significant ($r=0.886$, $p<0.001$)..... | 75 |
| Table A.3 Liver stiffness measured at two locations for both male and female subjects. The first location was the area of intercostal space between 7 th and 8 th ribs and the second location was the area of intercostal space between 8 th and 9 th ribs. | 76 |

CHAPTER 1 INTRODUCTION

1.1 Background

Liver fibrosis has drawn great attention because of the common causes and severity. To enhance treatment and minimise the mortality rate, early screening is the most effective way. Generally, there are three ways routinely used to detect liver fibrosis including liver biopsy (Menghini 1970; Bravo et al. 2001); serum marker analysis (Plebani and Burlina 1991; Imbert-Bismut et al. 2001) and ultrasound imaging (Celle et al. 1988; Nishiura et al. 2005). Liver biopsy is recognized to be the most effective method to confirm the diagnosis of liver fibrosis. However, it is invasive that may cause severe complications (Perrault et al. 1978) and the accuracy is reduced because of the sampling error (Abdi et al. 1979) and repeatability problem (Regev et al. 2002). Serum marker analysis is a minimally invasive method that is routinely used in hospitals or clinics. It is relatively cheap, but its accuracy varies from one marker to another. It is also affected by the etiology of disease (Oberti et al. 1997). B-mode ultrasound imaging is commonly used as a screening tool for liver fibrosis. It is non-invasive and cheap in cost. However, ultrasound imaging is very operator-dependent that lacks accuracy and reliability.

Other than those commonly used methods, some promising and non-invasive methods are now being developed, including real-time elastography (RTE) (Friedrich-Rust et al. 2007; Morikawa et al. 2011), transient elastography (TE) (Sandrin et al. 2003; Castera et al. 2011), magnetic resonance elastography (MRE) (Kruse et al. 2000; Motosugi et al. 2010) and supersonic shear imaging (SSI) (Bercoff et al. 2003; Muller et al. 2009a). In spite of being promising and non-invasive, most of these methods

still have limitations that do not meet the criteria as a screening tool for liver fibrosis. RTE only provides relative elasticity instead of absolute elasticity. It is highly operator-dependent that may result in large variation of repeatability. MRE is with long-time data acquisition and of high cost including operation and maintenance. Therefore, the advantages of MRE are balanced. SSI is the latest one to this field and still lacks of sufficient *in vivo* clinical studies to evaluate its performance and advantages. Up to date, a device called Fibroscan (Sandrin et al. 2003; Verveer et al. 2012), which has been developed based on TE, seems to be the most promising one. For example, Fibroscan has high accuracy and repeatability that are supported by a large number of studies. It is of low cost and the measurement time is short. Considering its limitation of insufficient visual guidance, we developed another TE-based system, Liverscan (Mak et al. 2013), with real-time B-mode ultrasound imaging as guidance. In this study, we would like to validate the performance of the new system and develop a measurement protocol as to improve the measurement effectiveness and enhance the measurement accuracy and repeatability.

Liver fibrosis is very common due to infection of HBV, HCV or alcohol abuse. The importance of screening of potential patients or defined the fibrosis staging of patients is well recognized. As a screening tool, some sorts of factors are mostly preferred including radiation free, non-invasive, low cost and short measurement time. Ultrasound imaging, therefore, is a suitable diagnostic tool. The use of ultrasound imaging only is not satisfied to provide reliable diagnosis; TE with the combination of ultrasound imaging and mechanical vibration, however, appears to be able to meet the requirements as a screening tool and provide a reliable diagnostic result with the support from the results of considerable clinical studies. Fibroscan applies 1D

ultrasound imaging that provides limited visual information about the target liver tissue. From another view, the physician has to predict the target tissue based on his/her experience. This is the main limitation of the use of 1D ultrasound imaging; it would be preferable to apply 2D ultrasound imaging to provide the morphological information about liver tissue while taking elasticity measurement. Liverscan was thus developed with the implementation of 2D ultrasound imaging and mechanical vibration.

Liverscan and Fibroscan are both developed based on TE. Fibroscan has been validated comprehensively by considerable clinical studies; the correlation between stiffness of liver tissue and liver fibrosis stages has been established. In addition, other similar techniques like Supersonic Shear Imaging has just started its clinical trial that its performance has to be further validated. An early study has used Fibroscan to verify the results of Supersonic Shear Imaging (Bavu et al. 2011). Therefore, Fibroscan was selected to benchmark with Liverscan in this study.

1.2 Objectives of the study

As our team has developed a transient elastography system with real-time B-mode ultrasound imaging for liver fibrosis assessment, Liverscan, the aims of this study are

1. To design and fabricate a specific probe that can be used with a conventional B-mode ultrasound scanner to assess liver fibrosis non-invasively;
2. To validate the Liverscan using agar-gelatin phantoms with different stiffness with reference to indentation tests and *in vivo* subject measurements with reference to

the Fibroscan tests;

3. To establish a measurement protocol using the Liverscan including procedures for identifying the measurement locations, number of measurement locations and data processing methods.

1.3 Outline of the dissertation

Following the introduction chapter, Chapter 2 presents a literature review on the fundamental physiology of liver and liver fibrosis. The diagnostic methods for liver fibrosis are also presented and the limitations of these methods are pointed out.

Chapter 3 introduces the materials and methods used in this study. The details of the probe fabrication and principle of transient elastography system are presented. To validate the Liverscan, agar-gelatin phantoms were fabricated for stiffness measurements. The stiffness measured by the Liverscan was compared with that measured by the mechanical indentation test. For the *in vivo* measurement, a measurement protocol was developed and described in detail. The *in vivo* liver stiffness measurement was also conducted and compared with the Fibroscan. The location dependence for liver stiffness measurement is also described in this chapter.

In Chapter 4, the results of the corresponding studies in Chapter 3 are presented, including the correlations of the phantoms' stiffness between the Liverscan and the mechanical indentation test and of the *in vivo* liver stiffness between the Liverscan and the Fibroscan and the location dependence for stiffness measurement.

Chapter 5 discusses the system performance and results. The key feature of the Liverscan, real-time B-mode ultrasound imaging, is discussed to demonstrate the importance of the visual guidance as blood vessels may be included in the measurement region, affecting the accuracy. The system performances and the feasibility of the measurement protocol are also discussed.

Chapter 6 summarizes the performance of the Liverscan. Suggestions for further studies are also given.

CHAPTER 2 LITERATURE REVIEW

This chapter consists of two parts; the first part presents a literature review on the fundamental physiology of liver and liver fibrosis. The second part is the review on the diagnostic methods for liver fibrosis so as to indicate the limitations of the existing methods and the need for a non-invasive method with high accuracy and repeatability to act as a screening tool.

2.1 Anatomy of liver

Liver is a vital organ in body. It is soft, in reddish brown colour and in triangular shape. It weights approximately one fiftieth of an adult body weight, which is the largest internal organ in the body. Liver locates at the right upper part of the abdominal cavity and just below the diaphragm (Figure 2.1), protected by the rib cage partially. Liver consists of two unequal sized main lobes, separating by falciform ligament. The left lobe is smaller than the right one, only one sixth of the total liver size. The right lobe consists of three parts, namely right lobe proper, caudate lobe and quadrate lobe (Patton and Thibodeau 2010). Each lobe is made up of lobules and each lobule is made up of hepatic cells, which contribute to metabolism. The hepatic lobules are hexagonal or pentagonal cylinders in shape that allows the closely pack of the hepatic cells. Liver connects with hepatic artery, hepatic vein, hepatic portal vein and bile duct. It receives oxygenated blood through hepatic artery and deoxygenated blood through hepatic portal vein. At the sinusoids of the liver, the termination of the branches of hepatic artery and portal vein, the arterial and venous blood mixes together and flows into the central vein of each hepatic lobule. The bile canaliculi apposes to the hepatic cells and fuse to form bile duct, collecting bile from hepatic cells. Liver is a very vascular organ as hepatic artery and bile duct divide into many

branches that pass laterally and spread upwards and downwards through the liver (Ellis and Mahadevan 2010). The hepatic vein, however, is distributed different from that of hepatic artery and bile duct. It mainly consists of three veins including a left, right and central vein. They pass upwards and downwards into the inferior vena cava (Ellis and Mahadevan 2010). In terms of function, liver is one of the vital organs as it is responsible for maintaining the normal biological activities inside body including carbohydrate metabolism, detoxification, bile secretion and storage of several substances for body (Patton and Thibodeau 2010). Any sickness of the liver may lead to serious diseases such as liver fibrosis.

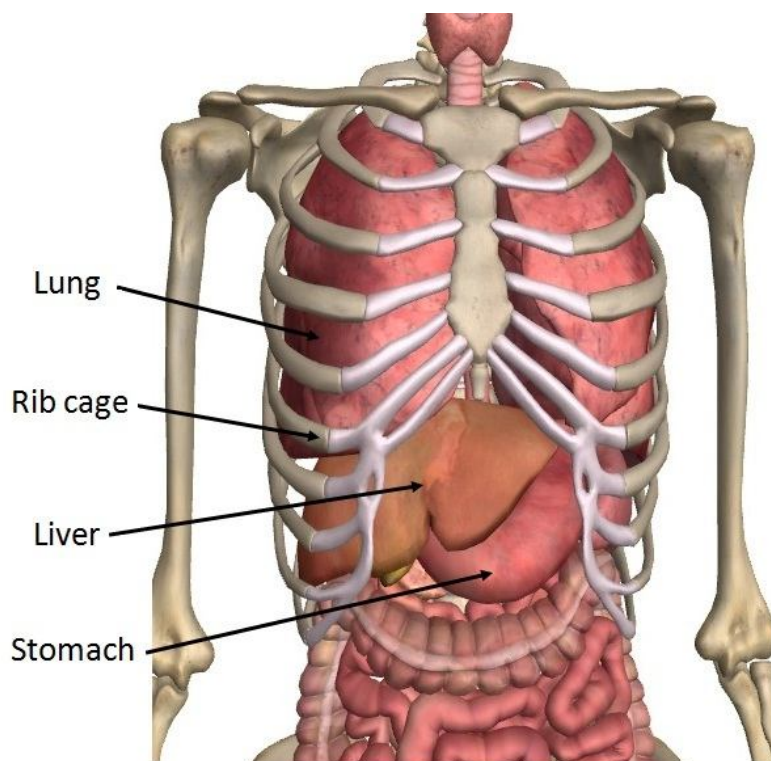


Figure 2.1 Anatomy of liver. (Zygotebdy)

2.2 Liver disease: Liver fibrosis

Liver fibrosis is a severe chronic disease. It results from excessive accumulation of

extracellular matrix (ECM) as the wound healing response to the repeated injury of the liver (Friedman 2003). The main causes of liver fibrosis are very common including hepatitis B virus (HBV) and hepatitis C virus (HCV) infection, alcohol abuse and non-alcoholic steatohepatitis (NASH) (Friedman 2003; Bataller and Brenner 2005). The progression of liver fibrosis may lead to cirrhosis. The complications of cirrhosis include liver failure, portal hypertension and hepatocellular carcinoma (Foucher et al. 2006b; Martini 2006). Cirrhosis is one of the top 10 causes of death in the western world (Martini 2006). Bosetti et al. (2007) reported the cirrhosis mortality rate in Chile was about 55 per 100,000 in men and 14 per 100,000 in women in early 1980s. In Scotland, the cirrhosis mortality rate was about 45 per 100,000 in men and 20 per 100,000 in women in 2002, which was the highest cirrhosis mortality rate in western European (Leon and McCambridge 2006).

Liver fibrosis is a kind of structural change of liver tissue due to chronic repeated injury (Figure 2.2). Briefly, the parenchymal cells will regenerate and replace the necrotic or apoptotic cells if liver is subjected to injury, for example injury from HBV. This process leads to an inflammatory response and a limited ECM deposition. In the case of repeated injury to liver tissue, that process is disturbed and results in tissue regeneration failure and excessive accumulation of ECM. In an advanced case, the accumulation of ECM is 6 times more than the normal amount of ECM (Bataller and Brenner 2005). The production of ECM is controlled by hepatic stellate cells (HSC) (Friedman et al. 1985). Under persisted injury, the HSCs are activated into myofibroblast-like cells. The activated HSCs accumulate at the site of injury and produce a large amount of ECM. In addition, they limit the ECM degradation (Bataller and Brenner 2005). As a result, the excessive ECM leads to the hepatic

tissue undergo structural change and results in fibrotic cells. If the ECM production and degradation could both be restored to normal, it is believed the fibrotic cells could be recovered. This could be one of the treatments of liver fibrosis in the future.

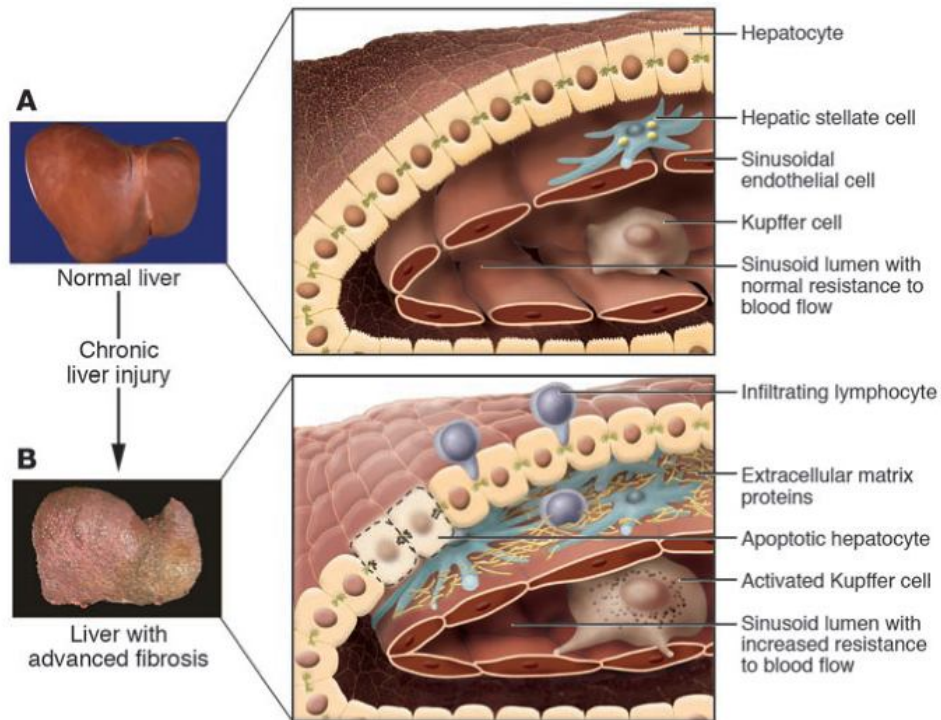


Figure 2.2 Change in the hepatic structure. (A) is the normal liver and (B) is the liver tissue with advanced fibrosis. (Bataller and Brenner 2005)

2.3 Assessment of liver fibrosis

2.3.1 Liver Biopsy

Liver biopsy is recognised to be the most effective method to diagnose liver fibrosis (Friedman 2003). It is a kind of invasive method that uses the needle to insert through the skin and muscle layer into liver to remove a small amount of liver tissue (Figure 2.3), about 1/50,000 of liver tissue (Afdhal and Nunes 2004). The removed liver

tissue is analyzed by hepatopathologist to identify the stage of fibrosis. In order to have a decent biopsy, the removed liver tissue should be at least 15 mm in length and consists of more than five portal tracts (Holund et al. 1980; Afdhal and Nunes 2004). Based on METAVIR scoring system (Bedossa and Poynard 1996), the fibrosis and activity level are graded, ranging from F0 to F4 representing no fibrosis, portal fibrosis, without septa, few septa, numerous septa without cirrhosis and cirrhosis for fibrosis and from A0 to A3 representing none, mild, moderate and severe for activity, respectively.



Figure 2.3 Liver biopsy is an invasive procedure that uses needle to remove a small amount of liver tissue. (<http://www.skills.uct.ac.za/activities.htm>)

As liver biopsy is routinely used, it seems that it is relatively safe since physicians have sufficient experience in performing this assessment. Some potential risks and complications, however, still occur, including pleurisy, perihepatitis and haemorrhage (Geller and Petrovic 2004). The complications relate to the relative contraindications

and the number of biopsies taken (Perrault et al. 1978; Afdhal and Nunes 2004). A more number of biopsy has to be taken; a higher chance of suffering from complications.

Apart from complications, liver biopsy is subjected to some sort of limitations. The most severe limitation is the sampling error (Regev et al. 2002; Friedman 2003). This is because fibrosis may be not uniformly distributed throughout the liver and the removed liver tissue, thus, contains no fibrotic tissue. Furthermore, the tissue removed by needle is small, about 1/50,000 of liver size (Afdhal and Nunes 2004); this further reduces the chance of removing the fibrotic tissue. Both reasons may lead to false negative diagnosis result. It is suggested to take three biopsies instead of one to improve accuracy. According to the study of Abdi et al. (1979), the diagnostic accuracy of cirrhosis increased from 80% with single biopsy taken to 100% with three taken. However, it is not reasonable to ask patients to conduct three biopsies in reality. In addition to the differences within one lobe, a difference of fibrosis grading also exists between lobes. A study carried out by Regev et al. (2002) showed that 33.1% of the subjects had difference of at least one grade between left and right lobes; there were 14.5% of subjects who were interpreted with cirrhosis in one lobe, but with stage 3 fibrosis in another lobe. As a result, biopsy may under or over estimate the fibrosis stage. Another limitation is the inter-observer variability among hepatopathologists (Bedossa et al. 1994; Regev et al. 2002). A study reported that this variation may be up to 20% for misclassifying the fibrosis stage (Friedman 2003). Another study revealed that there were variations between observers for assessing the disease activity for patients with HCV based on several selected features (Bedossa et al. 1994). Liver biopsy, therefore, seems to be more operator-dependent and may not be with

high accuracy.

Liver biopsy is the gold standard to assess the fibrosis stage, however, it may not be an effective method to screen the one who is under suspicious case or to monitor the treatment progression as it is invasive. The sampling error and inter-observer variability may lead to incorrect diagnosis, especially for those marginal cases. As a result, a non-invasive method with high accuracy and repeatability would be more preferable.

2.3.2 Serum Marker Analysis

Serum marker is a kind of biomarker. It refers to “measurement of one or more molecules within a blood or serum sample as a surrogate marker of fibrosis in liver” (Friedman 2003). Serum markers can be divided into two groups, namely indirect markers and direct markers. The indirect markers include AST/ALT ratio, platelet count, prothrombin index, PGA index and PGAA index (Afdhal and Nunes 2004). They have no direct relationship with the liver fibrosis stage (Wai et al. 2003; Huwart et al. 2007) and are based on a statistical approach to predict the liver fibrosis stage. The direct markers include cytokines, procollagen I, glycoproteins laminin and hyaluronic acid (HA) (Afdhal and Nunes 2004). It is believed that the direct markers are involved in the deposition or removal of ECM that relates to the liver fibrosis stage directly (Patel et al. 2003; Huwart et al. 2007).

For the indirect marker analysis, Oberti et al. (1997) reported that in a study involved 243 patients with chronic alcoholic or viral liver disease, the prothrombin index had the highest diagnostic accuracy, about 86% and similar performance in both diseased

groups. In contrast, AST/ALT ratio did not perform as well as prothrombin index and discrepancy existed between the two diseased groups, having an accuracy of 79% in viral liver disease; but only 65% accuracy in alcoholic liver disease (Oberti et al. 1997). This is because the etiology of liver disease affects the accuracy of indirect serum marker analysis. Another limitation of indirect marker analysis is its limited ability to categorize the fibrosis stage. It was reported that Fibrotest was able to classify patients with F2 or higher fibrosis stage with 75% sensitivity and 85% specificity (Angulo et al. 1999). Fibrotest, however, could only identify patients into F0-F1, F2-F4 and “cannot be categorized” groups. It was unable to have further fine categorization that limits its diagnostic precision. For the direct marker analysis, Oberti et al. (1997) reported that HA had the best accuracy of 86% in staging liver fibrosis, while others were not as accurate as HA. The etiology effect also existed among direct markers. For instance, Laminin performed better in patients who had alcoholic liver disease than in patients who had viral liver disease.

With the advantages of relatively simple operation and almost no complications, serum marker analysis becomes a routine procedure for assessing liver fibrosis in the clinic. Nevertheless, its accuracy may be affected since fibrosis is not specific to liver; other organs such as lung may also suffer from fibrosis. Therefore, serum marker analysis may not be an accurate method to confirm liver fibrosis; but suitable for routine use in clinic as a preliminary screening tool.

2.3.3 B-mode Ultrasound Imaging

B-mode ultrasound imaging with the major advantages of radiation free, non-invasiveness and cheap in cost is routinely used to image liver fibrosis preliminarily

in hospital. This facilitates ultrasound imaging to be a screening tool for liver fibrosis or other diseases. The evaluation of the B-mode ultrasound images is based on several factors, including liver size, bluntness of liver edge and nodularity of liver surface (Nishiura et al. 2005). In between, liver surface nodularity has been the most common indicator for grading fibrosis visually (Figure 2.4). Under the ultrasound image, fibrosis and cirrhosis is recognised by a coarse echo pattern and presence of regeneration nodules causing irregular outline on the liver surface (Saverymuttu et al. 1986). It is reported that ultrasound scanning was not very accurate in detecting the present of fibrosis, 57% sensitivity and 88% specificity (Saverymuttu et al. 1986). Since B-mode ultrasound imaging is able to provide 2D grey scale images only, it requires the operators or physicians to be well trained and experienced in scanning and interpreting images. This operator-dependent technique limits its repeatability and accuracy. The image quality, furthermore, depends on the frequency of ultrasound transducer. As illustrated in Figure 2.5, a high frequency ultrasound transducer is able to provide a smooth liver surface, sacrificing the depth information ((a) & (b)); while a low frequency ultrasound transducer can provide irregular liver surface only, maintaining depth information ((c) & (d)). The selection or the availability of proper ultrasound transducers is another important factor influencing the repeatability and accuracy. It has been demonstrated that high frequency ultrasound transducer was able to obtain acceptable results for cirrhosis assessment showing liver surface with dotted or irregular line or liver parenchyma with areas of different echogenicity (Simonovský 1999).

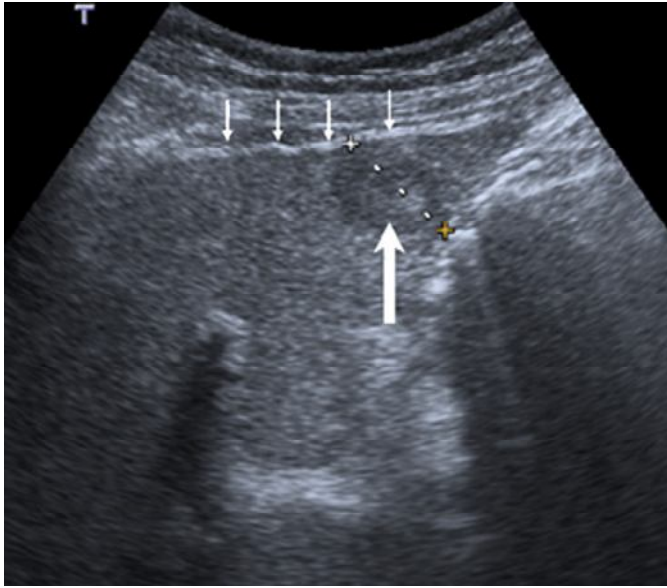


Figure 2.4 B-mode ultrasound image of a patient with cirrhosis shows irregular liver surface and a hypo-echoic lesion. (Goyal et al. 2009)

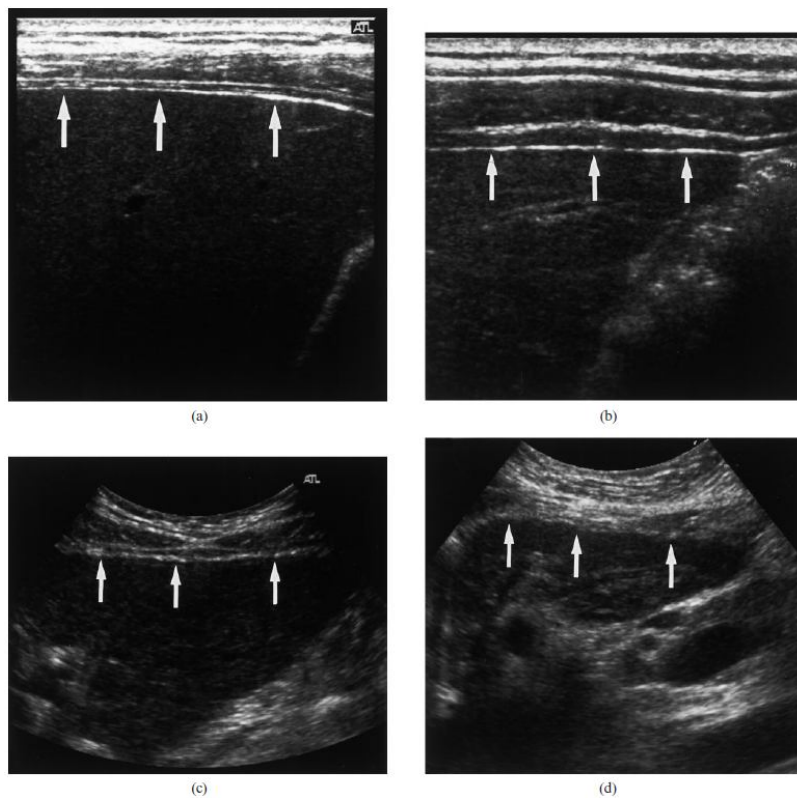


Figure 2.5 Ultrasound images of the liver surface. (a) and (b) show a smooth and mildly irregular surfaces with a high frequency ultrasound transducer, respectively; (c)

and (d) show an irregular and a highly irregular surfaces with a low frequency ultrasound transducer, respectively. This reveals the frequency of ultrasound does affect the diagnostic accuracy. (Nishiura et al. 2005)

To classify and grade liver fibrosis quantitatively, scoring systems (Gaiani et al. 1997; Nishiura et al. 2005) were developed based on the surface texture of liver. Nishiura et al. (2005) has reported that the developed scoring system was clinically useful for differentiating patients with minimal or no fibrosis from those with mild or severe fibrosis. It should be noted that the given scores were based on the image quality together with the experience of physicians, thus were very subjective. To tackle this limitation, some research groups have developed different algorithms based on the statistical data to examine liver fibrosis, including statistical analysis on ultrasound echo signals (Toyoda et al. 2009) and texture analysis of B-mode images (Wu et al. 1992). Only few of them have been applied for clinical use as most of them did not perform satisfactorily in terms of processing time, classification rate and clinical cases. The statistical analysis on ultrasound echo signal is a method that analyses the results of a statistical chi-square test of the echo amplitudes (Toyoda et al. 2009). It was performed on 148 patients with HCV using histologic fibrosis grade as a reference. This study demonstrated the statistical analysis method was able to grades liver fibrosis in patient with HCV; however, this method is not practical in real clinical setting since a considerable of time is needed to sample the RF signals which do not include the unnecessary structures such as blood vessel. For the texture analysis of B-mode images, different research groups have implemented different texture features including multiresolution fractal dimension (Wu et al. 1992), texture feature coding matrix (Horng 2003) and Fourier power spectrum (Abe et al. 1992); most of them

were not able to accuracy classification of liver fibrosis from F0 to F4 or were very time consuming processing. Vicas et al. (2011) have implemented a texture analysis tool consisting 12 texture algorithms and a logistic regression classifier for liver fibrosis staging and concluded the texture analysis system performed with limited staging ability for liver fibrosis.

With the use of B-mode ultrasound imaging only, it is useful to help for screening purpose since it consists of real-time and radiation free properties; it may not be sufficient for accurate diagnosis, but the 2D morphological information is helpful for screening. It is suggested B-mode ultrasound imaging can be integrated with other technique to assist liver fibrosis diagnosis quantitatively.

2.3.4 Magnetic Resonance Imaging

Conventional magnetic resonance imaging (MRI) is a radiation free imaging technique, which provides high contrast and resolution 2D and 3D imaging. These features enable MRI to be a diagnostic tool for liver fibrosis. It was reported that based on the specific image features including the narrowing of the hepatic vein (Numminen et al. 2005), caudate of the right lobe ratio (Awaya et al. 2002) and expanded gallbladder fossa (Ito et al. 1999), MRI was able to recognize cirrhosis. Other stages of fibrosis, nevertheless, were not possible. This explains why the research about liver fibrosis with the use of MRI was limited and MRI is not a routinely used tool for liver fibrosis measurement. With the advancement of technology, novel MRI applications have been developed that focus on the physiological and biomechanical properties of liver tissue as to increase the diagnostic accuracy and reliability. There are different kinds of imaging techniques for liver

fibrosis, including contrast-enhanced MRI (Elizondo et al. 1990; Chen et al. 2012), diffusion-weighted MRI (DWI) (Koinuma et al. 2005; Bakan et al. 2012) and magnetic resonance spectroscopy (Munakata et al. 1993; Fischbach and Bruhn 2008). Among these techniques, DWI seems to be the most promising one since most of the published research papers have applied DWI for study and proved DWI was feasible for liver fibrosis diagnosis.

Briefly, DWI assesses the freedom of diffusion of water protons in tissues. In fibrotic tissue, a reduction of water proton diffusion occurred since there is an accumulation of fibrosis which has lesser free unbound water. For the image of DWI, the signal intensity of tissue is inversely proportional to the freedom of water proton diffusion. This means the brighter pixel indicates tissue with reduced water proton diffusion. To quantitatively investigate the liver fibrosis with the use of DWI, apparent diffusion coefficient (ADC) is applied. Several studies have shown the obtained mean ADC from DWI measurement was lower in patients with cirrhosis (Koinuma et al. 2005; Annet et al. 2007; Taouli et al. 2007; Bakan et al. 2012) (Figure 2.6). In a previous study, 56 patients clinically diagnosed with cirrhosis underwent DWI, a significant reduction of ADC was found that indicates ADC decreased as the stage of liver fibrosis progressed (Koinuma et al. 2005). Lewin et al. (2007) reported that the area under receiver operating characteristic curve (AUROC) for identifying patients with significant fibrosis were 0.92 for DWI, 0.92 for TE, 0.79 for FibroTest, 0.87 for Aspartate aminotransferase to platelets ratio index (APRI), 0.86 for Forns index and 0.97 for hyaluronate. This indicates that DWI performed favorably with other non-invasive methods for patient with significant liver fibrosis.

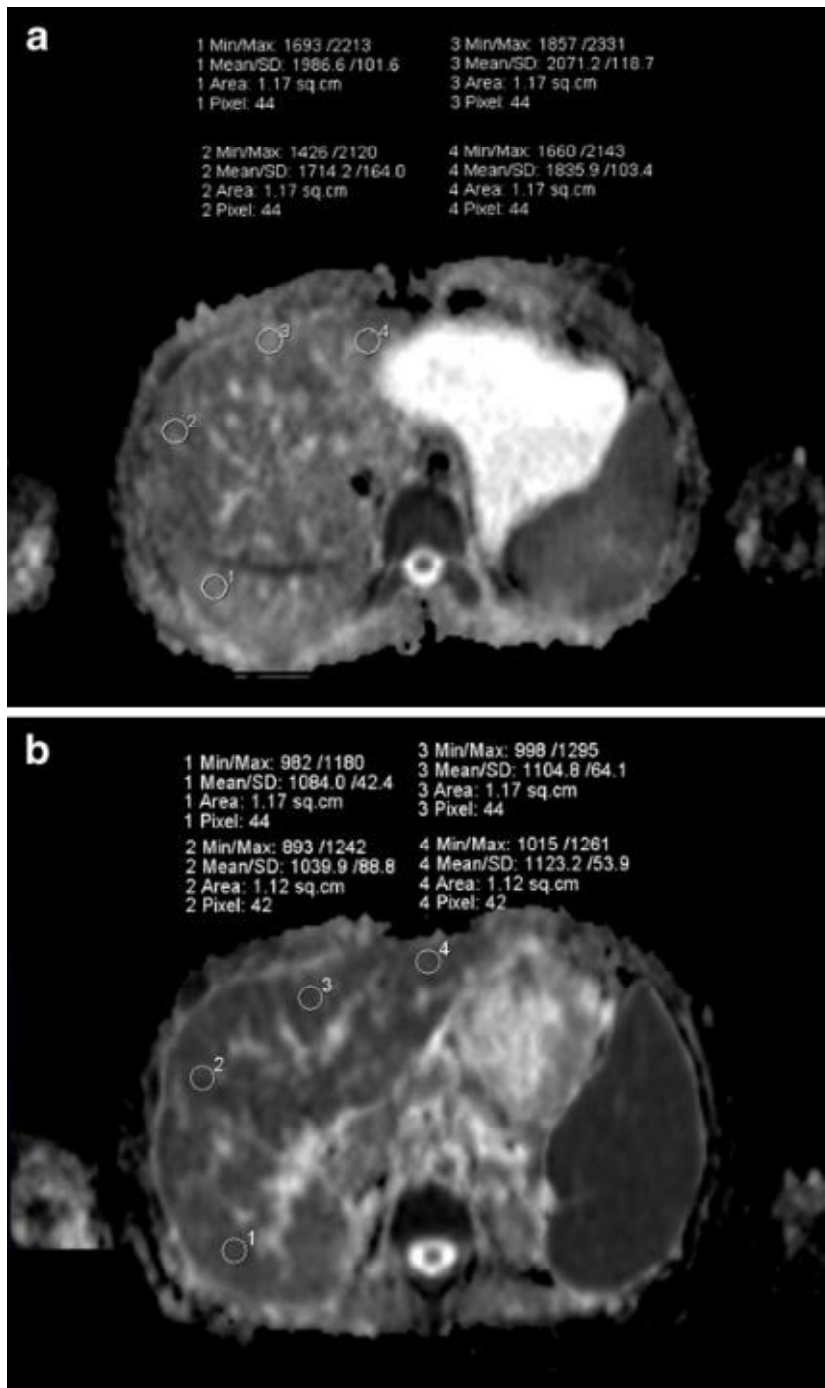


Figure 2.6 DWI image and ADC map of liver. (a) is the control group image and (b) is the image for a patient with significant fibrosis. The ADC map shows the ADC values were higher in (a) as compared to (b), indicating the ADC value decreased as the severity of fibrosis increased. (Bakan et al. 2012)

From the preliminary studies, DWI seems to be promising for liver fibrosis measurement, especially for significant fibrosis. DWI, however, has several limitations that reduce its ability to be a screening tool or routine measurement in clinical use. Up to recent studies, the sample size was limited in most of the studies, especially those with different liver fibrosis stages. The DWI has not been clinically validated and needs further investigation. Most of the studies reported DWI was able to identify patients with significant fibrosis, but not for early stages of liver fibrosis. The repeatability of its performance also needs to be further confirmed. It was reported that significant hepatic iron accumulation and hepatic steatosis may also affect the measurement accuracy (Talwalkar et al. 2008). MRI can provide high contrast and resolution, the drawback is the increased measurement time. DWI needs 45-60 minutes for a scanning (Talwalkar et al. 2008), which is very time consuming that reduces the acceptance from patients and limits the number of patients to be scanned in one day. In addition, the cost for MRI is higher than other non-invasive techniques such as ultrasound imaging.

DWI for MRI seems to be promising for significant liver fibrosis; but more studies are needed to prove its performance. Among those limitations, cost is a significant constraint, reducing its acceptability to the patients. In terms of financial consideration from government, DWI is also not favorable to be a routinely used tool in hospital.

2.3.5 Elasticity Measurement of Liver

2.3.5.1 Real-time elastography

Real-time elastography (RTE) (Friedrich-Rust et al. 2007) is a non-invasive method

for diagnosis of liver fibrosis. Basically, it is an imaging technique that reveals the elasticity of tissue by comparing and analyzing the degree of displacement of liver tissue before and under compression by a conventional ultrasound probe. Under compression, the stiffer tissue undergoes lesser change in shape; while softer tissue undergoes more deformation. The difference between stiffer and softer tissues is used to identify the relative stiffness, location and size of the harder objects such as fibrotic tissue in liver (Figure 2.7). RTE has been demonstrated to be clinically useful for detecting lesions in breast (Itoh et al. 2006; Thomas et al. 2006), prostate (Pallwein et al. 2007; Salomon et al. 2008) and thyroid (Lyshchik et al. 2005; Hong et al. 2009). For liver fibrosis, Friedrich-Rust et al. (2007) has shown the use of RTE to indicate the stiffness distribution of liver tissue for 79 patients with chronic viral hepatitis. It was reported that the correlation coefficient between the elasticity scores obtained by RTE and the histological fibrosis stage was 0.48; AUROCs for diagnostic accuracy were 0.75 for significant fibrosis, 0.73 for severe fibrosis and 0.69 for cirrhosis, which were not satisfactory for clinical application. Another study conducted by Kanamoto et al. (2009) has proved the AUROC for diagnostic accuracy was 0.951 for significant fibrosis. From the limited studies, RTE was demonstrated to be helpful for liver fibrosis diagnosis. It, nevertheless, only provides relative stiffness, showing the relative degree of tissue strain under compression. To quantitatively measure liver stiffness, a various algorithms were developed, which increased the measurement accuracy. Wang et al. (2012) has included 11 parameters to formulate the elastic index to correlate with fibrosis stage in RTE measurement, including 55 patients with liver fibrosis and chronic HBV and 20 healthy subjects. RTE with this quantitative method was demonstrated to be promising and accurate as the correlation between elasticity index and the histological fibrosis stage was 0.81 ($p < 0.001$) and AUROCs

of accuracy were 0.93 for fibrosis, 0.92 for significant fibrosis, 0.84 for severe fibrosis and 0.66 for cirrhosis.

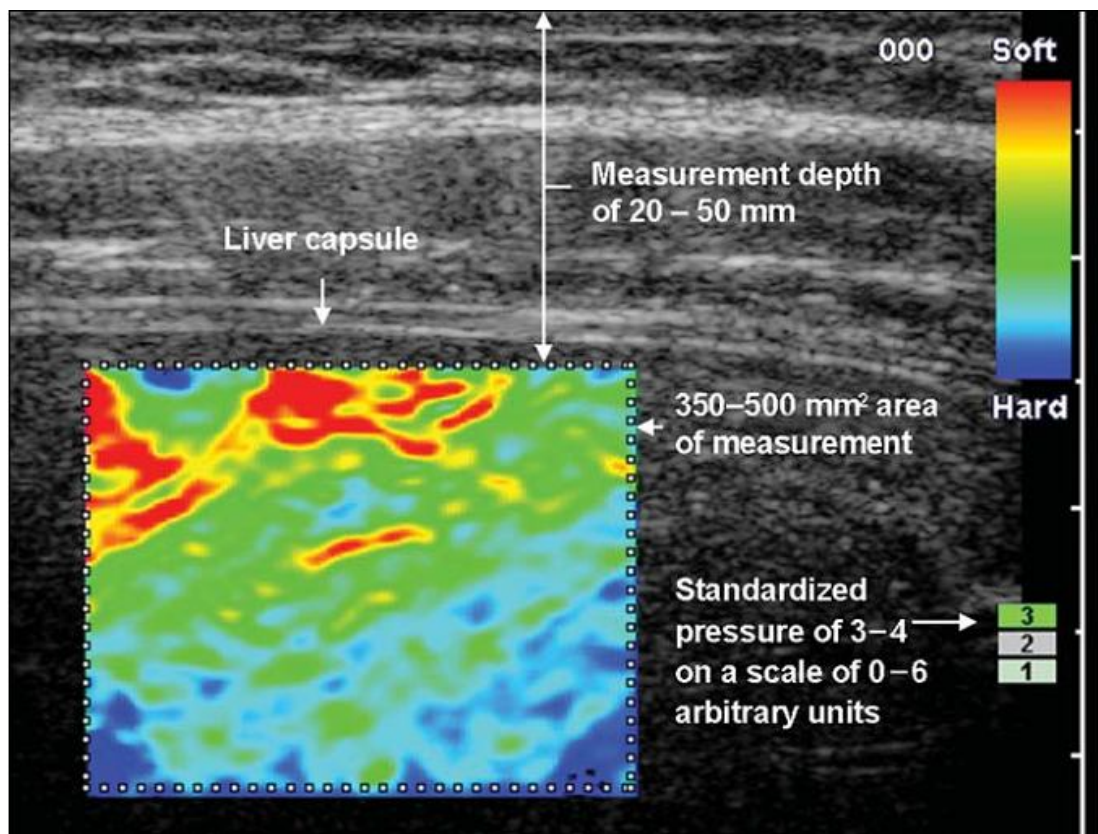


Figure 2.7 RTE for liver stiffness measurement using conventional B-mode ultrasound probe for compression. It shows the stiffness distribution of tissue coded with color, red for soft tissue and blue for hard tissue. (Friedrich-Rust et al. 2007)

Some promising results were published for RTE, but they were from the preliminary studies with limited subjects in specific fibrosis stages. In order to validate its clinical value, more studies with considerable subjects are needed. With the integration of quantitative methods, the performance seems to be improved (Koizumi et al. 2011; Morikawa et al. 2011; Wang et al. 2012). These quantitative methods are still under development and evaluation; in addition, the parameters difference among the

algorithms may cause variation in stiffness estimation. The measurement accuracy and effectiveness, therefore, will be reduced. Another limitation is the repeatability as RTE was highly operator-dependent; its intra-observer and inter-observer variability was criticized (Saftoiu et al. 2007; Friedrich-Rust et al. 2009). The selection of region of interest (ROI) was also dependent on the operator. It was suggested that the ROI of elastography should include the liver tissue and the surrounding tissue, otherwise the accuracy reduced (Saftoiu et al. 2007; Gulizia et al. 2008). Therefore, RTE may not be an effective method for liver fibrosis diagnosis.

RTE is a kind of technique based on ultrasound imaging; the main advantages are radiation free and low cost which facilitate RTE to be a potential screening tool for liver fibrosis. For grading of liver fibrosis, RTE seems to be unsuitable, especially in quantitative diagnosis. Further developments and more clinical studies are needed.

2.3.5.2 Transient Elastography

Transient elastography (TE) is a non-invasive method to diagnose liver fibrosis (Sandrin et al. 2002; Sandrin et al. 2003; Petta and Craxì 2012). TE combines ultrasound with vibration, modifying the probe with an ultrasound transducer installed on the axis of a mechanical vibrator. The induced low frequency shear wave propagates through liver tissue and is traced by the pulse-echo ultrasound acquisition method. The speed of shear wave is related to the liver tissue stiffness, a faster shear wave speed indicates a harder liver tissue that reveals the severity of fibrotic tissue.

Recently, a commercial device has been developed based on TE, called Fibroscan (Echosens, Paris, France). Fibroscan is able to measure the liver stiffness non-

invasively; in addition, the stiffness obtained from the Fibroscan had significant correlation with fibrosis grading according to the METAVIR scoring system in liver biopsy (Figure 2.8) (Sandrin et al. 2003; Foucher et al. 2006b). Before Fibroscan, different physical parameters have been investigated for potential fibrosis diagnosis. Backscattering property has been widely investigated, but results showed it was not effective for differentiating patient with cirrhosis or healthy liver in terms of backscatter coefficient quantitatively, as reported by Lu et al. (1999). Maybe the backscattering measurement can be affected by many factors. Considerable clinical studies have been conducted and demonstrated that the liver stiffness well correlated with the severity of liver fibrosis. An obvious biological reason for why stiffness correlates to the liver fibrosis severity is that more fibrotic tissue can make liver stiffer that can be explained by pressure-stiffness-fibrosis sequence hypothesis (Mueller and Sandrin 2010). The hypothesis states that when chronic liver diseases occur, the accumulation of interstitial liquid and inflammatory infiltrate result in an increased local stress causing stretch on the blood vessels and bile ducts. This stretch will stimulate the production of fibrotic tissue causing a stiffness increase as the liver is adapting its structure to mechanical stimulation.

Because of the novelty of the Fibroscan, there are a number of research groups using the Fibroscan to investigate its accuracy and repeatability for liver fibrosis measurement. In a meta-analysis including data from 50 studies, the TE's performance was evaluated using liver biopsy as reference. The histology of patients included HBV, HCV and NASH. The mean AUROCs for diagnosis of significant fibrosis, severe fibrosis and cirrhosis were 0.84, 0.89 and 0.94, respectively (Friedrich-Rust et al. 2008). With this large number of data analyses, they concluded

that AUROCs were representative and the diagnostic accuracy of TE was excellent. The accuracy of Fibroscan, moreover, should be higher than that of liver biopsy as the size of liver tissue measured by the Fibroscan is 100 times larger than that removed by biopsy. The tissue, thus, is more representative and in turns the results more accurate. For the intra-observer and inter-observer test, Fraquelli et al. (2007) reported that the measurements for patients with chronic liver diseases were highly reproducible as intraclass correlation coefficients (ICC) of inter and intra-observer tests were both 0.98. Another research group has also confirmed the repeatability of Fibroscan was excellent (Boursier et al. 2008). This indicates the Fibroscan is quite operator-independent and the accuracy is thus enhanced. In a recent study, Fibroscan was proved to be applicable to those patients with chronic HBV; the diagnostic performance of TE was similar between HCV and HBV, with AUROCs were 0.8 and 0.9 for significant fibrosis and cirrhosis (Leroy and Kim 2012).

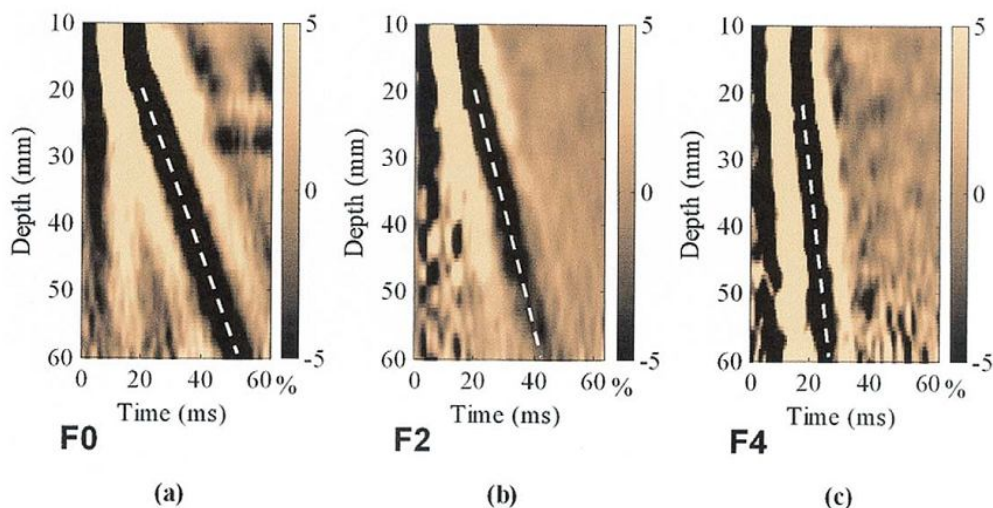


Figure 2.8 *In vivo* measurement results by Fibroscan: (a) is no fibrosis or mild fibrosis, (b) is severe fibrosis and (c) is cirrhosis. (Sandrin et al. 2003)

Apart from high accuracy and repeatability, non-invasiveness and radiation free are the most important advantages of the Fibroscan, enhancing it to be a screen tool for fibrosis measurement. It is believed the patients' acceptability should be high as being non-invasive and radiation free, the measurements do not cause any harm and complications. Patients could even have several scans in an examination to eliminate the uncertainty. The measurement time for Fibroscan is short, generally less than 10 minutes and the cost is low. Fibroscan thus provides a really helpful method for fibrosis measurement.

Fibroscan, nevertheless, has its limitations. The most important restraint is the Fibroscan does not have sufficient visual guidance to properly locate the ROI (Bavu et al. 2011; Kircheis et al. 2012; Orlacchio et al. 2012). This can be attributed to the use of A-mode ultrasound. Without the use of B-mode ultrasound to help to locate the ROI, it is easy to include blood vessels and bile duct, especially those large in size leading to inaccurate estimation of the fibrosis stage. This drawback has been specifically mentioned and evaluated in recent studies using other alternative ultrasound elasticity measurement techniques, including supersonic shear imaging (Bavu et al. 2011), ARFI (Kircheis et al. 2012), and real-time elastography (Orlacchio et al. 2012), which can provide real-time B-mode images of liver during the measurement of its elasticity. To tackle this limitation, a real-time assistance ultrasound tools have been developed, called TM- and A-scan modes (Audiere et al. 2009). The tools, basically, try to provide visual information of the liver and tissues around or within the liver. With the use of this real-time assistance, however, the visual information is still insufficient and difficult to observe. Other than limited visual guidance, Fibroscan is not applicable to the patients who are obese, having

narrow intercostal spaces or having ascites (Sandrin et al. 2003). Recently, a new probe (XL probe) was designed for obese patients in order to increase the range of BMI of patients. And it was reported the performance of the XL probe was comparable to that of standard probe (M probe), with reducing the measurement failure (de Ledinghen et al. 2012). However, the stiffness measured by XL probe was significantly lower than that measured by M probe (de Ledinghen et al. 2012; Myers et al. 2012) which made the existing cut-off values no longer valid for measurement using XL probe.

The Fibroscan is a kind of non-invasive method to make diagnosis of liver fibrosis. It has excellent repeatability and high accuracy. With the advantages of low cost, radiation free and short measurement time, the Fibroscan has high potential to be a screening tool routinely used in clinics or health centers. Instead of using TM- and A-scan modes as guidance, it is believed that the Fibroscan is able to perform much better, in terms of accuracy, repeatability and measurement time if real-time B-mode ultrasound imaging is applied.

2.3.5.3 Magnetic Resonance Elastography

Magnetic resonance elastography (MRE) (Huwart et al. 2006; Rustogi et al. 2012) seems to be another promising technique for measuring viscoelastic properties of liver tissue non-invasively. The principle of MRE is similar to that of TE, the main difference is the use of MRI instead of ultrasound. Briefly, MRE involves the induction of shear wave to propagate through liver tissue by an external vibrator. The shear wave propagation is related to the tissue stiffness. By the use of MRI with motion-sensitizing gradient technique, a phase shift caused by mechanical wave is

measurable. As a result, the phase map is generated and transformed into shear elasticity and viscosity maps as shown in Figure 2.9. MRE consists of several advantages as compared to TE, including 1) able to analyze relatively larger liver volume as to reduce the sampling error; 2) applicable to patients who are obese and have ascites and 3) able to make precise analysis by 3D displacement vector (Huwart and van Beers 2008). Based on limited preliminary studies, MRE was feasible for liver fibrosis measurement (Huwart et al. 2006; Rouviere et al. 2006; Yin et al. 2007). In a study which involved 35 normal volunteers and 50 patients with chronic liver disease, Yin et al. (2007) demonstrated that MRE was able to identify patients with moderate and severe fibrosis from those with mild fibrosis with 86% sensitivity and 85% specificity. Another research group has made comparison among MRE, TE and APRI and found that MRE had a higher successful rate than that of TE (94% vs 84%, $p=0.016$) (Huwart et al. 2008). The AUROC of MRE, in addition, was larger than that of TE, APRI and combination of TE and APRI ($p<0.05$). The ability of identifying fibrosis seems to be promising; but the repeatability is another concern. During recent years, MRE has been proved to be highly reproducible (Motosugi et al. 2010; Shire et al. 2011; Rustogi et al. 2012). Apart from assessing fibrotic liver, Venkatesh et al. (2008) claimed that MRE was promising for detecting solid liver tumours.

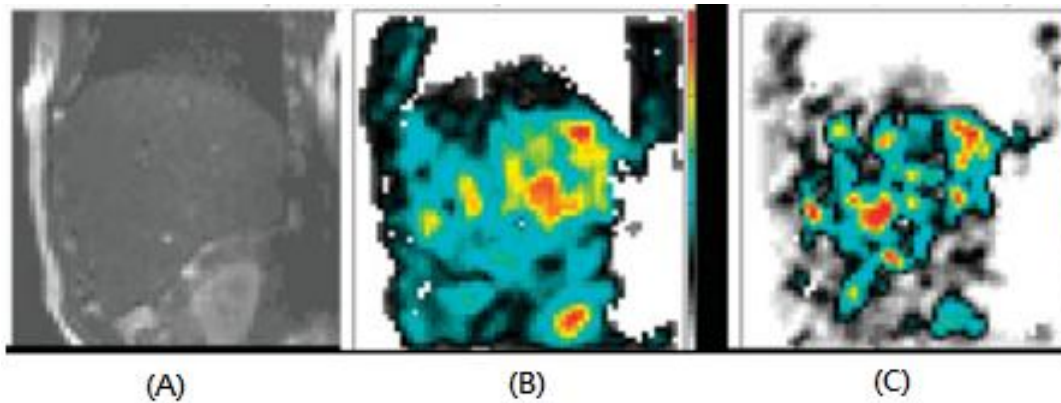


Figure 2.9 MRE images of patient with cirrhosis. (a) shows the ROI of liver in MRI, (b) represents elasticity map of liver fibrosis and (c) represents the viscosity map of liver fibrosis. (Huwart et al. 2006)

MRE seems to be comparable with TE. However, further investigation and clinical studies are needed to better understand its performance and limitations since those preliminary studies are still insufficient, due to the small number of normal subjects and patients with different stages of liver fibrosis and not enough comparisons with other techniques such as liver biopsy. In terms of the technical issues, the propagation of shear wave was not always homogenous throughout the liver and acquired slices, causing the problem with stiffness evaluation (Rustogi et al. 2012) and the need of correction for breathing movement (Huwart et al. 2007). The measurement time of MRE was long, at least 20 minutes (Huwart et al. 2007). This does not fulfil the basic criteria for screening purpose. The physical size of MRE is large and it needs to be installed in a specific room that restricts the locations for measurement, hospitals only. Apart from this, MRE is of high cost in terms of operation cost and maintenance cost. Both of these limiting factors confine the number of MRE system to be installed, most likely one to two MRE systems in a hospital.

In short words, MRE has great potential as a tool for grading liver fibrosis as it is comparable with the Fibroscan. To further test its feasibility for screening liver fibrosis, its advantages of MRE, nevertheless, are balanced by its long time measurement and high cost. It may be clinical effective, but not cost effective as a routinely used screening tool. More clinical studies are still needed.

2.3.5.4 Supersonic Shear Imaging

Supersonic shear imaging (SSI) (Bercoff et al. 2003; Bavu et al. 2011) is a kind of radiation force based technique for elasticity imaging. This imaging technique is similar to that of TE, both of them use ultrasound to track the shear wave propagation in the liver tissue to form the elastogram. The key difference is the way to induce shear wave. TE uses an external mechanical vibrator to induce shear wave; while SSI applies the focused ultrasound beam to induce shear wave. When low frequency shear wave is induced by acoustic radiation force remotely, the shear wave source moves with an ultra-fast speed to create successively focusing ultrasonic “pushing” beam at different pre-set depths. As shown in Figure 2.10, a series of shear wave is produced and they interfere constructively to form a shear wavefront as time increases. This wavefront propagates through liver tissue and causes disturbance to the liver tissue. Consequently, elastogram is formed as ultrasound is used to monitor the shear wavefront propagation at an ultrafast frame rate, about 3000 Hz.

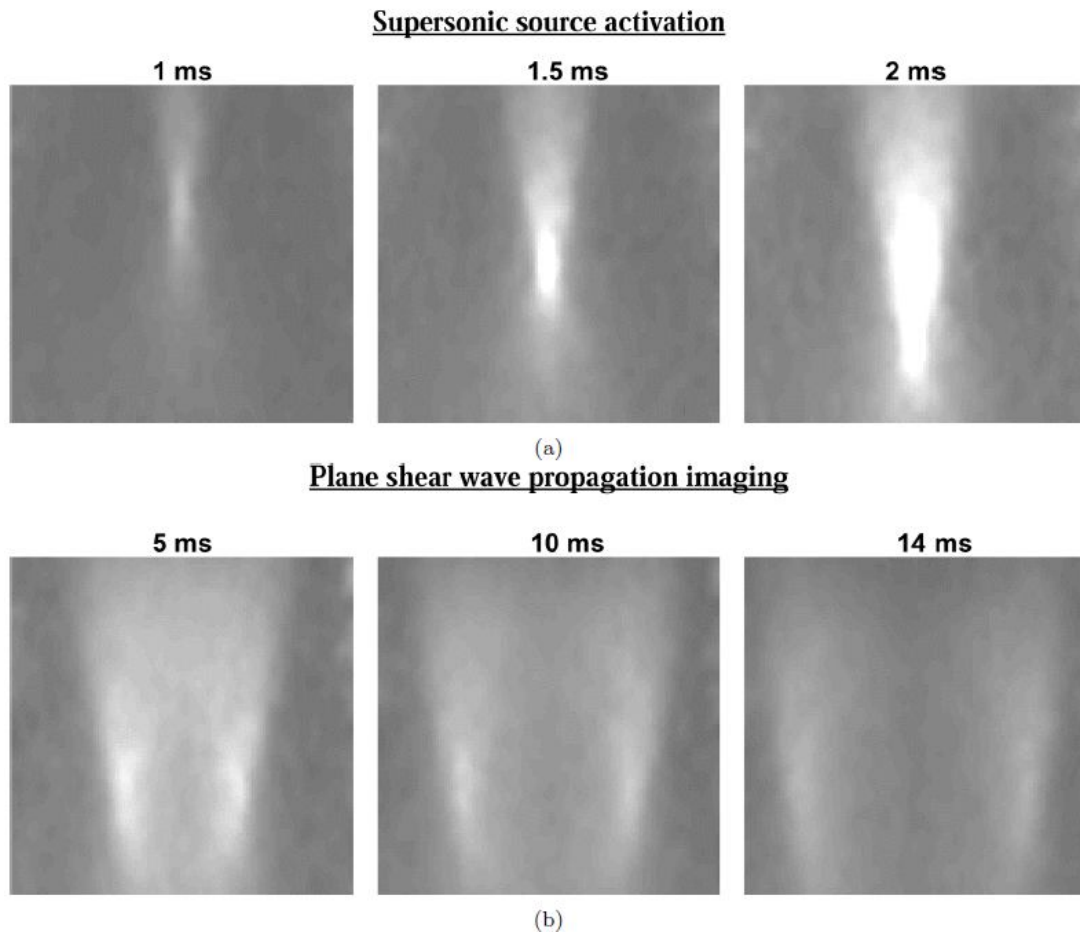


Figure 2.10 Supersonic shear source activation and propagation images at different time points. (Bercoff et al. 2004)

Based on a study conducted by Bercoff et al. (2004), SSI performed well for elasticity estimation on agar-gelatin phantom quantitatively, the inclusion and main body were measured with $4.1 \text{ kPa} \pm 12\%$ and $2 \text{ kPa} \pm 2\%$, respectively. It seems SSI has the ability to differentiate tissues with different stiffness. Apart from phantom test, *in vivo* assessment for soft tissue is also feasible. It was found that the stiffness value of the normal breast tissue measured by SSI agreed with that by MRE (Lorenzen et al. 2003). SSI also had the ability to identify malignant lesions for breast having significantly different stiffness as compared to normal tissue (Tanter et al. 2008). In a study including 15 normal subjects, the liver stiffness measured by SSI agreed with the

value of normal liver stiffness reported in literature (Muller et al. 2009b). The repeatability was also mentioned to be significant for those normal subjects. Recently, another publication involving 113 patients with HCV also presented the agreement between fibrosis staging and elasticity assessment using SSI and the Fibroscan (Bavu et al. 2011). The AUROCs of stiffness measurement by SSI were 0.948, 0.962 and 0.968 for patients with significant fibrosis and severe fibrosis and cirrhosis, respectively. From Figure 2.11, different stages of liver fibrosis are illustrated in the stiffness map, showing SSI has the potential ability to evaluate liver fibrosis.

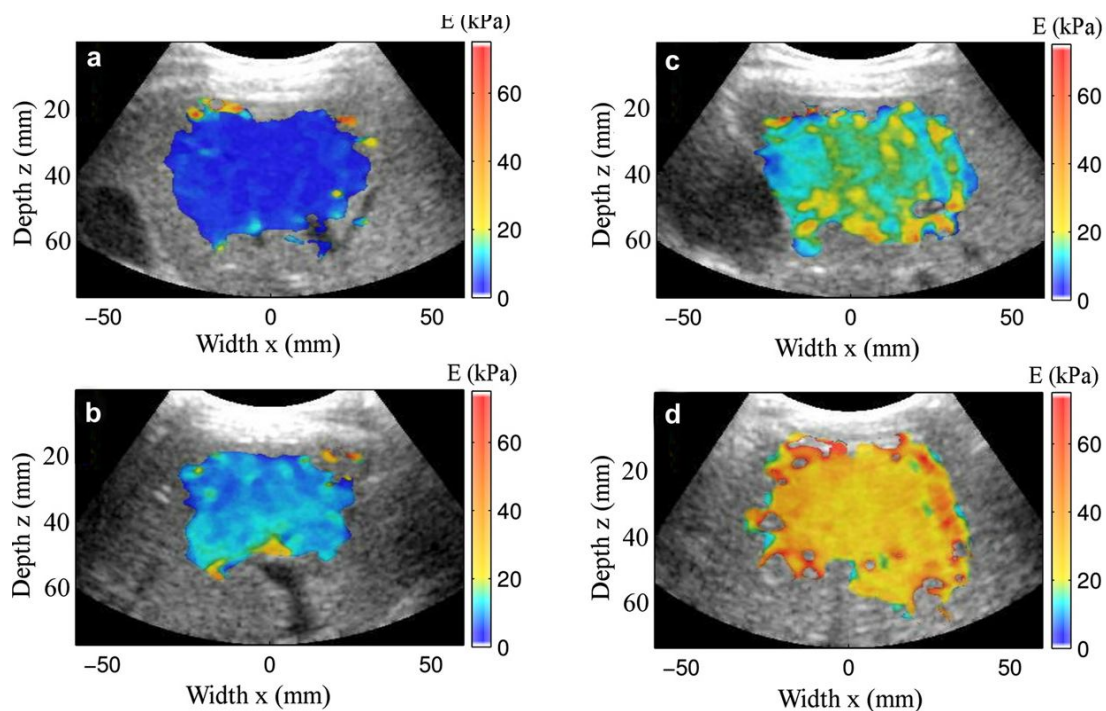


Figure 2.11 Color coded liver stiffness maps indicate 4 stages of fibrosis measured by SSI. (a) is the mild fibrosis; (b) is the severe fibrosis; (c) is significant fibrosis and (d) is cirrhosis. (Bavu et al. 2011)

Since SSI implies ultrafast frame rate, the measurement time is very short, less than 1s. In terms of cost, SSI is competitive to MRE; while less comparable to the Fibroscan.

Of these advantages, short time measurement and low cost are really helpful for screening purpose. The use of acoustic radiation force would be favourable since no external mechanical vibrator needed to generate shear wave. It is believed this can reduce the effect of shear wave attenuation due to thick fat tissue layer. The amplitude of shear wave induced by acoustic radiation force, however, should be smaller than that of external one. For instance, the amplitude of SSI was less than 10 μm (Tanter et al. 2008); while TE was about 50-60 μm (Gennisson et al. 2005). This implies that the ultrasound system needs to be very sensitive in order to monitor the small change of tissue displacement, increasing the cost of SSI in advance. Based on the literature review, SSI is promising but more qualitative and quantitative studies are required to advance its performance, especially those *in vivo* studies with different stages of liver fibrosis and with comparisons among different diagnostic techniques including liver biopsy and serum marker analysis. The repeatability of this method also needs to be addressed.

With the application of ultrasound imaging and acoustic radiation force, SSI seems to be simple in operation. It is believed that the cost of SSI would be more acceptable when compared with MRE. According to the literature review, SSI also has the potential being a tool for liver fibrosis diagnosis; but more clinical studies are needed to prove its accuracy and repeatability.

2.3.6 Summary

Liver fibrosis becomes more and more common due to the wide spread of HBV and HCV and the living style of citizens. The medical expenditure will increase dramatically if liver fibrosis deteriorates into cirrhosis or even liver cancer, increasing

the financial burden to the government and thus reducing the medical resources for the treatment. Therefore, an early screening for liver fibrosis is really demanded to increase the treatment effectiveness as well as to reduce the medical expenditure.

According to the above review, liver biopsy is still the gold standard and routinely used in hospital. It is, nevertheless, invasive that may not be favourable for screening. Serum marker analysis is minimally invasive and routinely used, but it may be affected by the etiologic effect which reduces its accuracy. Among those non-invasive methods, it seems the Fibroscan performs the most promisingly and meets the criteria for screening purpose. Fibroscan is cheap in cost since it is an ultrasound based technique. The measurement time is short (less than 10 minutes) and it is able to provide instant diagnostic result. From the review, the diagnostic performance of the Fibroscan appears to be excellent in terms of accuracy and repeatability based on the support from considerable studies. This enables the Fibroscan to grade liver fibrosis with no further biopsy needed. Fibroscan, nevertheless, lacks sufficient visual guidance to properly locate the liver tissue for measurement. This may confine the accuracy as the ROI may include blood vessels or bile duct. This is a key restriction of the Fibroscan.

Considering the key limitation of the Fibroscan, we developed another TE system with specifically designed probe to provide real-time B-mode ultrasound imaging as guidance for liver fibrosis measurement. In this study, we aimed to validate the performance of the system and develop a measurement protocol to improve the measurement effectiveness and enhance the measurement accuracy and repeatability.

CHAPTER 3 MATERIALS AND METHODS

This chapter introduces the materials and methods used in this study, including the details of probe fabrication, system validation with the use of agar-gelatin phantoms, the *in vivo* liver stiffness measurement based on the established measurement protocol and the study of measurement location dependence.

3.1 Probe development and fabrication

As illustrated in Figure 3.1, the measurement probe was designed and fabricated with a 4.5 MHz B-mode ultrasound transducer fixed along the axis of a mechanical vibrator. Different types of mechanical vibrators such as electromagnetic and pneumatic vibrators have been sourced with the consideration of size, power, etc. Some preliminary prototypes of the probe have built up by connecting the vibrators with the 2D ultrasound transducer to test the feasibility for generating suitable shear wave in the liver. When a suitable mechanical vibrator was identified, the plastic casing and internal supporting structures were designed and fabricated for assembly. For example, the mechanical vibrator was installed on the plastic casing (Figure A.1) which was fabricated using lathing machine. The dimensions of the probe are 70 mm in diameter and 170 mm in length. The material used for fabrication has also been considered, POM was selected, which is a biocompatible material in white colour. The mechanical vibrator was connected to a control box and an amplifier (Type 2718, Brüel & Kjær) to adjust frequency and amplitude of the vibration, respectively (Figure 3.2). When the mechanical vibrator vibrates, the ultrasound transducer will vibrate accordingly to generate shear wave. The frequency and amplitude were 100 Hz and about 5 mm at the surface of transducer in this study, which was the optimal setting for our system. When the shear wave propagated

through the liver tissue, pulse-echo ultrasound acquisition was used to trace the shear wave.

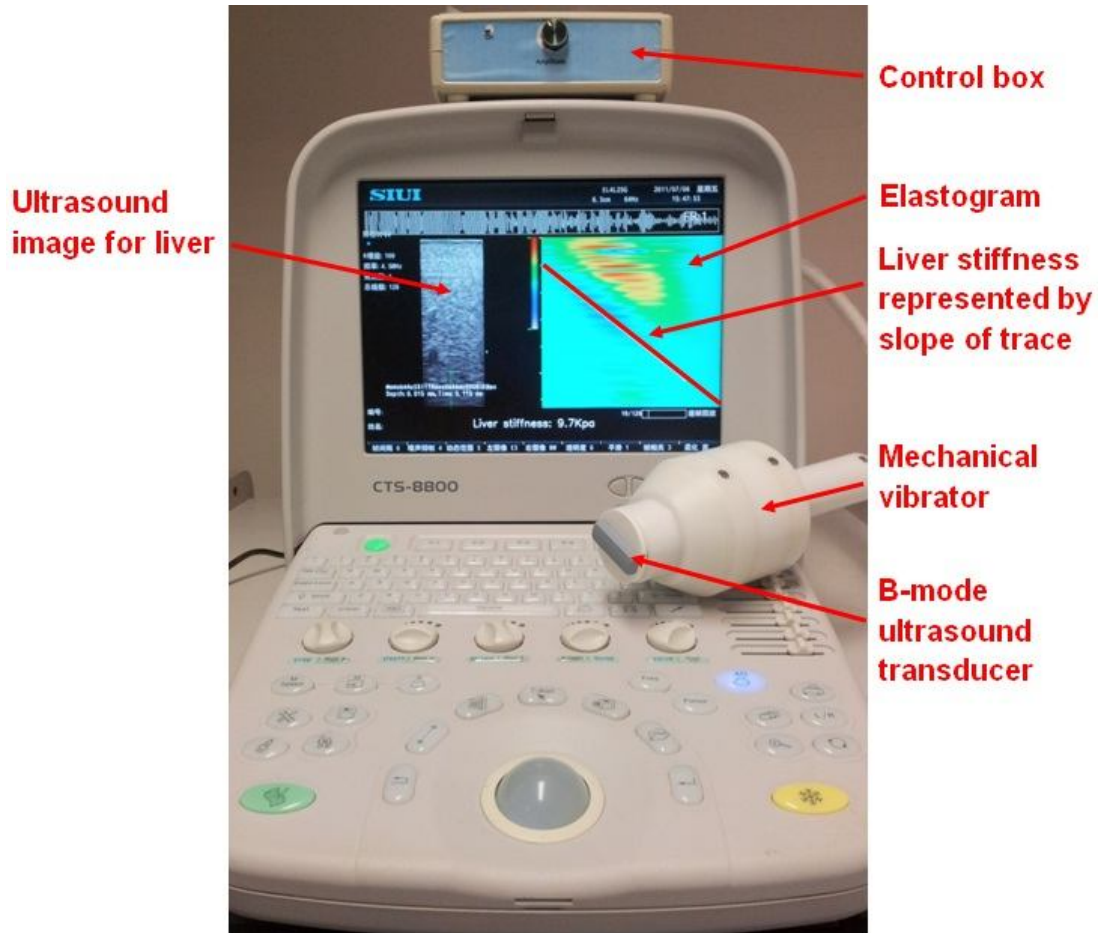


Figure 3.1 The developed transient elastography system with real-time B-mode ultrasound imaging, Liverscan , with specifically designed probe.

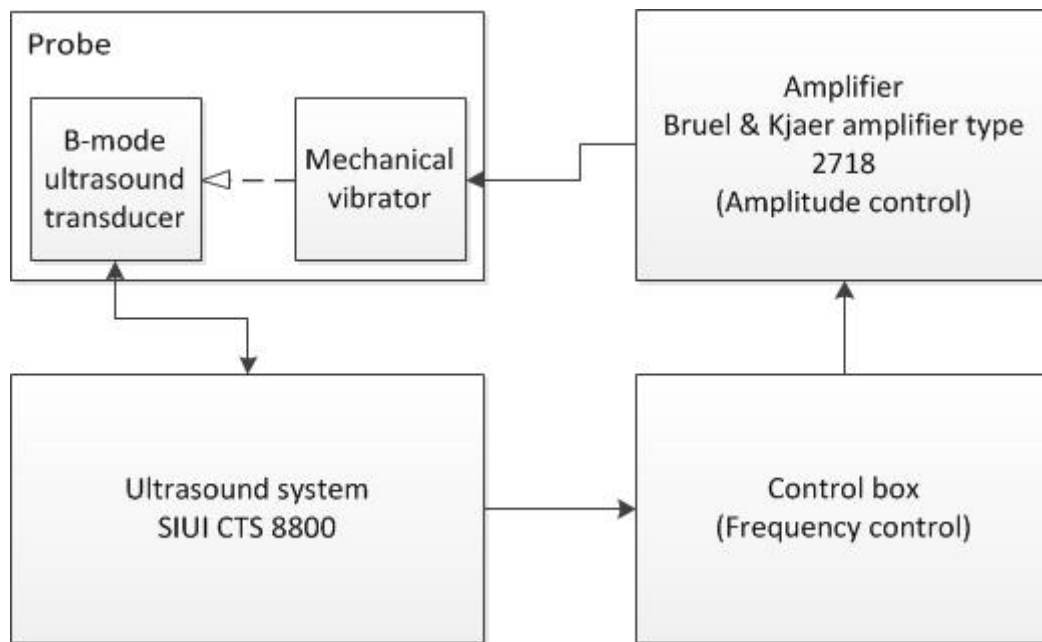


Figure 3.2 The schematic diagram represents the elements of Liverscan.

The frequency and amplitude was adjusted by the control box through the use of a computer interface that keys in the preferred frequency and the amplifier (Brüel & Kjaer amplifier type 2718) through an analog button, respectively. The displacement of the mechanical vibrator was 5 mm which could be measured using caliper. The probe was then held by a supporting structure that could move in vertical direction while the vibrator was in resting state. The probe was adjusted in height until the transducer surface be way 5 mm from the desk surface. The vibrator was activated, and the amplitude was adjusted by turning the analog button until the transducer head has just impacted to the desk surface. The voltage used to produce 5 mm displacement was then recorded.

The frequency and amplitude selected were 100 Hz and 5 mm, respectively that based on some in vivo preliminary trial. We have tested a number of different vibration frequencies from 50 to 200 Hz. We found that, 50 Hz of shear wave could not obtain

qualified result using our system, as the observed wave propagation patterns were too complicated for detection in some cases. Using a vibration frequency larger than 100 Hz, the shear wave propagation was influenced by the attenuation and could only be applicable to subjects with low BMI. The optimized vibration frequency was chosen to be 100 Hz instead of 50 Hz. For the amplitude, 5 mm was tried to be large enough to generate shear wave to propagate through liver with the consideration of safety and comfortableness.

3.2 Transient elastography system with real-time B-mode ultrasound imaging

The TE system was developed based on the modification of a conventional B-mode ultrasound system, SIUI CTS-8800 (Shantou Institute of Ultrasonic Instruments Co., Limited, Shantou, China) (Figure 3.1). Briefly, B-mode ultrasound imaging was generated in real-time to view the morphological information of the tissue before measurement. As illustrated in Figure 3.3, B-mode ultrasound images were generated in 25 frames per second and one of these B-mode images was replaced by M-mode ultrasound image which was formed by focusing the ultrasound beam at a selected fixed location and sampled with an ultra-high frame rate, up to 6000 frames/s. At the beginning of this M-mode frame, the vibration was generated. The propagation of the induced shear wave in tissue caused disturbance in the ultrasound echo train. The image was then processed to enhance the shear wave propagation trace. The tissue stiffness was calculated based on the following equation from the slope of the trace, which indicates the velocity of shear wave (Royer and Dieulesaint 2000):

$$E = 3\rho V^2 \quad (1)$$

where E is the Young's modulus; ρ is the mass density and V is the shear wave velocity. The slope of the trace is calculated by the software automatically. A higher

shear wave velocity indicates a harder liver tissue that reveals the severity of fibrosis.

The developed system was hereafter called as “Liverscan”.

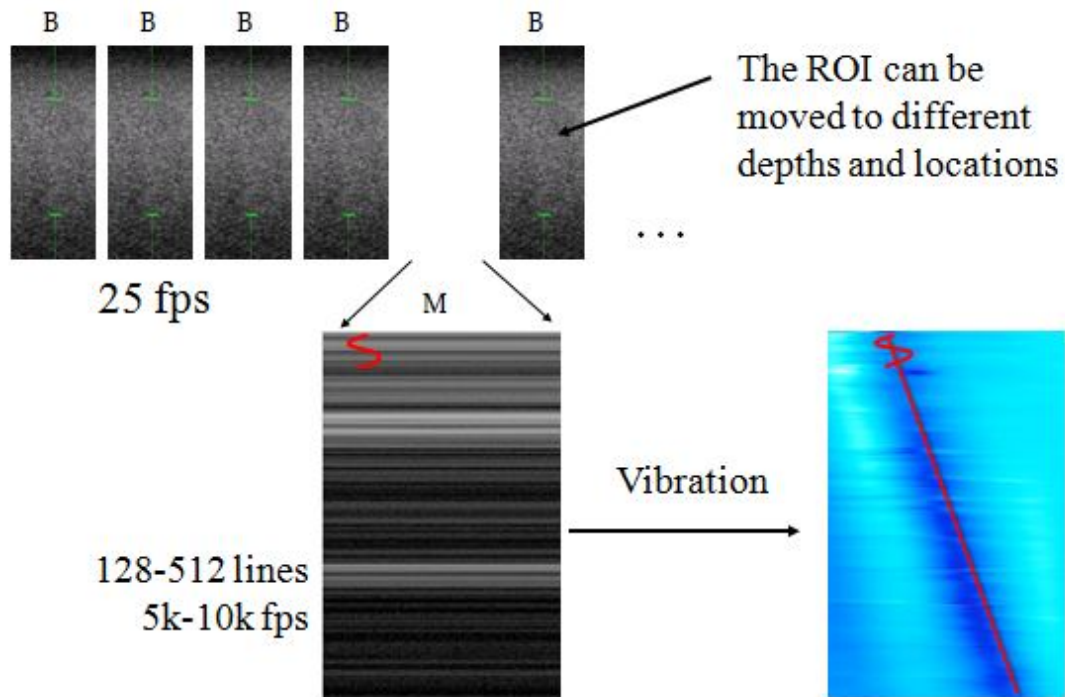


Figure 3.3 Illustration of imaging principle of the Liverscan. B-mode ultrasound images are generated in 25 frames per second and one of these B-mode images is replaced by M-mode ultrasound image to trace the propagation of the shear wave through liver tissue. The induced shear wave in liver causes disturbance in the ultrasound echo train. After tracing this disturbance, the transient elastography image can be formed and the stiffness can be calculated from the slope of the trace.

3.3 System validation using agar-gelatin phantoms

The capability of the system in measuring the soft tissue stiffness was firstly validated using custom-made agar-gelatin phantoms (Madsen et al. 2005; Gennisson and Cloutier 2006) with different stiffness (Figure 3.4 (a)). Agar (Fisher Scientific,

number A/1080/53, Loughborough, UK) and gelatin (Sigma-Aldrich, number G1890, St. Louis, MO) were used as scatterers and matrix, respectively. The agar remained constant in concentration, 1% by volume for each phantom; while the concentration of gelatin was used to control the stiffness, varying from 3% to 8% by volume. The mixture was heated to 50°C and then cooled down to 24°C as soon as possible to prevent sedimentation of agar as the mixture started to solidify at 24°C (Gennisson and Cloutier 2006). The phantoms were then covered by plastic wrap and stored in the refrigerator for 24 hours for further solidification. Before any measurements, it was ensured that the phantoms returned to room temperature. Totally 15 agar-gelatin phantoms, 80 mm in diameter and 64.1±8.2 mm in thickness of different stiffness were produced and tested by the Liverscan and the conventional mechanical indentation test in order to validate the developed system.



(a)



(b)

Figure 3.4 (a) Agar-gelatin phantom. A series of agar-gelatin phantoms with different stiffness were produced. Agar acts as the scatterer and gelatin is the matrix. The concentration of gelatin determines the stiffness of phantoms. (b) Agar-gelatin phantoms under mechanical indentation test. Totally 2 different locations were tested for averaging.

The agar-gelatin phantoms were tested by the Liverscan using the probe held by free hand, ensuring the ultrasound transducer was just in contact with the phantoms. The ROI of measurement was 31.5 mm in length and located about 10 mm below the phantom surface. 10 measurements were taken from each location and totally 2 locations were tested. The location selections were random. A trimmed mean, median 10 data was used to analyze the stiffness data as the sample taken in the study was small and the form of measurement distribution was unknown (Crow and Siddiqui

1967). To eliminate the variance from the extreme data, a trimmed mean can provide a more robust estimation.

For the comparison purpose, Instron[®] 5569 (Instron Corp., Norwood, MA, USA) was used to measure the force-deformation relationship for agar-gelatin phantoms in an indentation test, as shown in Figure 3.4 (b) in order to calculate the stiffness. A typical force-deformation curve of the agar-gelatin phantom is shown in Figure 3.5. The radius of a rigid steel indenter used was 5 mm (Lu and Zheng 2004). The indentation rate was 0.5 mms⁻¹ and 3 cycles of loading and unloading were conducted; only the data from last cycle of loading was captured for analysis. The applied maximum deformation on phantom was 4 mm to ensure the phantoms were in the range of elasticity. The indentation test was repeated at 3 different locations for averaging on each phantom. By using equation (2) (Hayes et al. 1972), the stiffness of those phantoms could be calculated.

$$E = \frac{(1-\nu^2)}{2a\kappa(\nu, a/h)} \frac{P}{W} \quad (2)$$

where ν is Poisson's ratio of agar-gelatin phantoms; a is indenter radius; h is thickness of phantom; $\kappa(\nu, a/h)$ is scaling factor, which tends to equal to 1 when the aspect ratio, a/h is small enough; P is the applied force and W is the indentation depth. In this study, ν was assumed to be 0.5 as agar-gelatin phantoms are an almost incompressible material (Glozman and Azhari 2010), and this assumption was consistent with that made for the measurement using transient elastography. The $a=5$ mm, $h=64.1\pm 8.2$ mm and thus $a/h=0.08\pm 0.01$, which was small enough that $\kappa=1$ could be used. P/W is force-deformation relationship obtained from a regression of the indentation test data.

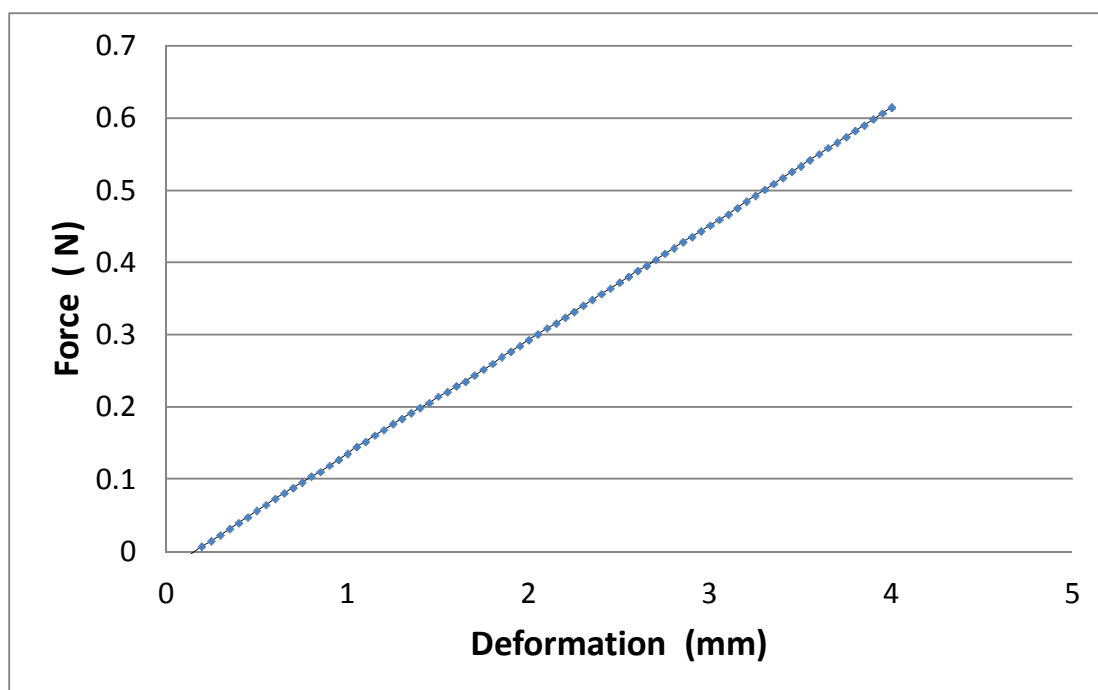


Figure 3.5 A typical force-deformation curve from indentation test in the last loading phase that shows a linear correlation. This indicates the fabricated agar-gelatin phantoms are purely elastic in this study.

3.4 Subjects

A total of 67 subjects were recruited in this study, including 34 male and 33 female subjects for different tests. Among these subjects, 20 of them had different kinds of liver diseases, and their clinical characteristics are summarized in Table 3.1. The mean age and the body mass index (BMI) of the subjects were 34 ± 13 years and $21.3 \pm 2.8 \text{ kgm}^{-2}$, respectively. After some initial trials, it was found that the Liverscan was not applicable to subjects having BMI over 27 kgm^{-2} , therefore, those subjects with BMI larger than this number were not recruited in this study. Among them, 26 and 23 subjects participated in inter- and intra-observer tests for the Liverscan, respectively. 28 subjects were tested using both the Liverscan and the Fibroscan. And,

all the 67 subjects participated in the test of location dependence using the Liverscan. Human ethical approval was obtained from the University committee and all the subjects were asked to sign the informed consent form before assessment.

Table 3.1 The clinical characteristics of 20 patients with confirmed liver diseases.

| No. of patients | Liver fibrosis | Liver cirrhosis | HBV | Fatty liver | Abnormal SGPT/ALT |
|-----------------|----------------|-----------------|-----|-------------|-------------------|
| 1 | | X | X | | |
| 1 | X | | | | |
| 14 | | | X | | |
| 1 | | | | X | |
| 3 | | | | | X |

3.5 *In vivo* assessment protocol and repeatability tests

For the *in vivo* measurement as illustrated in Figure 3.6, the subjects were asked to lie down in supine position with their right arms in maximal abduction and placed behind their heads. Then, an area close to the projection of the rib cage was identified, i.e. the intercostal space between the 7th and 8th ribs and about 5 cm in distance from the projection, as illustrated in Figure 3.7 (a). After suitable location was identified, measurement probe was applied. With the guidance of real-time B-mode ultrasound, we were able to observe and select the diagnostic depth and location of liver tissue without any large blood vessels by moving the ROI cursor. Totally 20 measurements were obtained and the trimmed mean, median 10 valid measurements were analyzed. In this study, all subjects fasted for at least 3 hours (Mederacke et al. 2009; Tempkin 2009) and rested for at least 15 minutes prior to measurement to ensure a resting state of live. A typical measurement interface showing the real-time B-mode

image and elastography located on the left and right sides of the interface, respectively, is demonstrated in Figure 3.8.



Figure 3.6 Established *in vivo* assessment protocol: Lie down in supine position with right arm in maximal abduction and placed behind head. The measurement locations are then identified with reference to the anatomical landmarks.

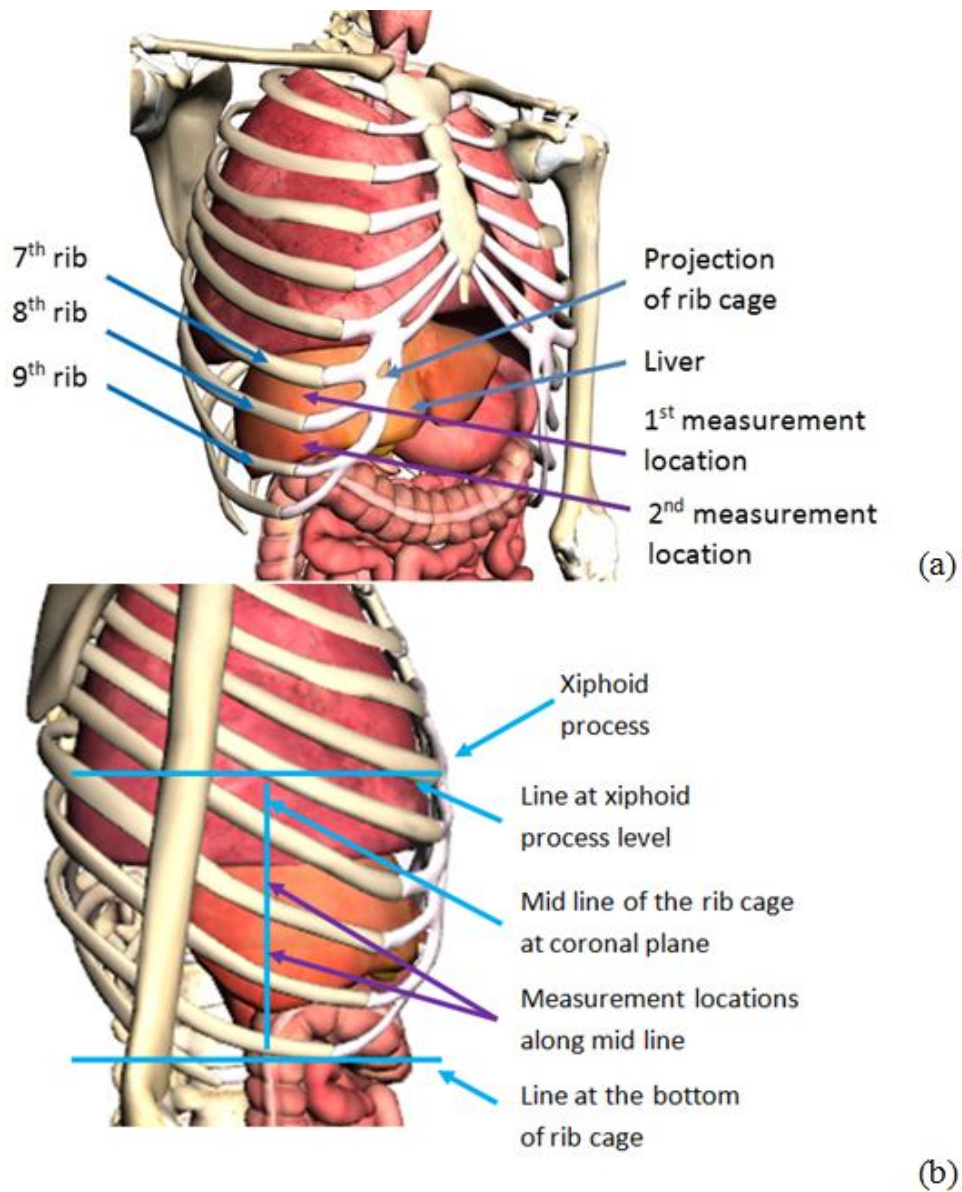


Figure 3.7 (a) Assessment location for liver fibrosis using anatomical features of rib cage as reference. Generally, with the help of the landmark, the projection of rib case, we could identify the area of intercostal space between 7th and 8th ribs and 8th and 9th ribs to be the 1st and 2nd assessment locations. (b) The identification of measurement locations for the Fibroscan. (Google body)

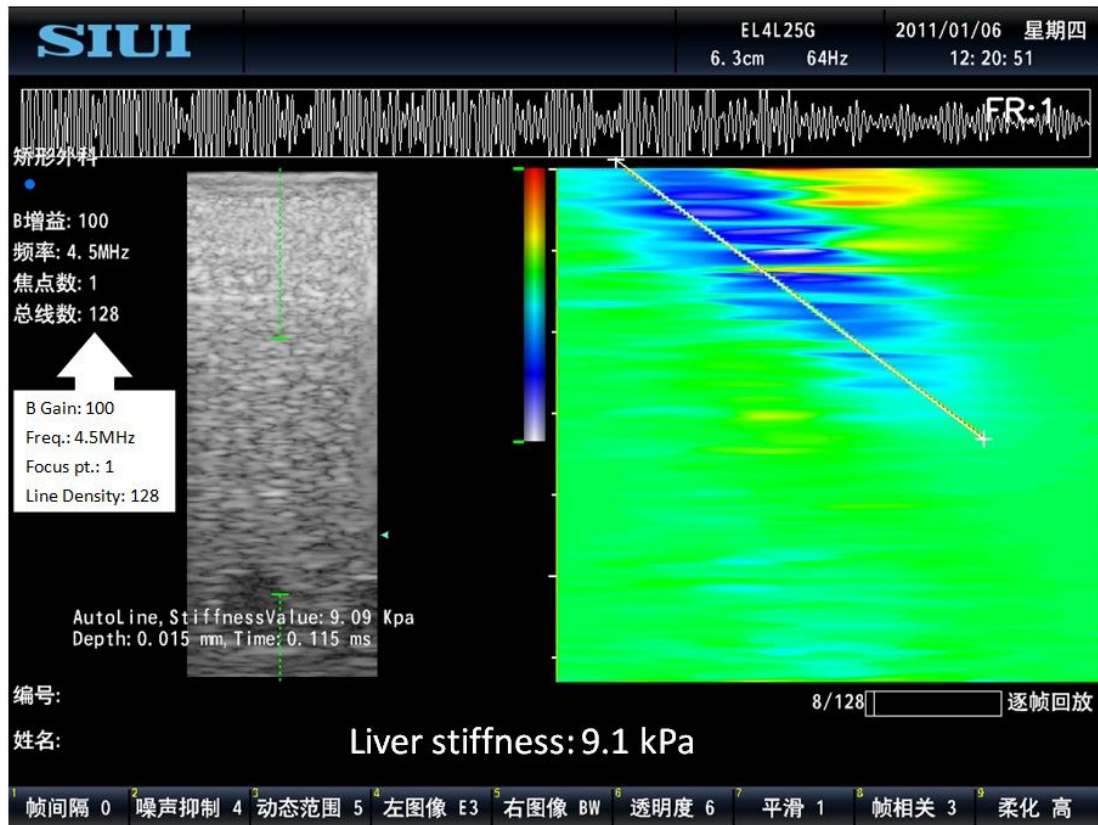


Figure 3.8 A typical measurement interface for the Liverscan. On the left, a real-time B-mode ultrasound image as guidance is provided. The elastography is displayed on the right side.

The repeatability tests were conducted to test whether the system was reproducible for the stiffness measurement. For the intra-observer test, the test was repeated by the same operator twice following the same protocol. A 5 minutes break was allowed between the two tests for each participant. The measurement was conducted by two operators in the inter-operator test, following the same measurement protocol and a 5 minutes break was also given between two tests.

3.6 Comparison between Liverscan and Fibroscan

To validate the Liverscan performance in measuring liver stiffness *in vivo*, a

comparison with the Fibroscan was made. After the measurement using the Liverscan, the subjects were tested by the Fibroscan. For the *in vivo* measurement of the Liverscan, all the subjects were tested based on the proposed measurement protocol at our laboratory. After that, the subjects were tested by the Fibroscan at the centre of The Hong Kong Health Check within one week. All the subjects fasted at least 3 hours before the measurement, and they were tested by the same operator at the centre. For the measurement protocol of the Fibroscan (Foucher et al. 2006b; Castera et al. 2008), briefly, the subjects were asked to lie down in the supine position with their right arms in maximal abduction and placed behind their heads. The identification of measurement locations is illustrated in Figure 3.7 (b), identifying the interval between xiphoid process and the last rib and then locating measurement locations along the mid line of sagittal plane within that interval. 10 valid measurements were obtained with the interquartile range not exceeding 30% of median value and success rate being at least 60%. The median value was used as the result.

3.7 Tests for location dependence of measurement

A location dependence test was also carried out in order to study the difference of liver stiffness measured at two independent locations, enhancing the measurement flexibility and effectiveness. In addition to the first location of intercostal space between 7th and 8th ribs, another location was selected for applying the measurement probe to test the location dependence, which was at the intercostal space between 8th and 9th ribs and just below the first location (Figure 3.7 (a)). Before any measurements, the locations of the two tests were identified first by following protocol. When the test on the 1st location was done, the probe was applied to the 2nd location immediately.

Reminding about the movement of the probe at two tested locations had been given to the participants before conducting the measurement as to reduce the motion artifact.

3.8 Statistical analysis

Statistical analysis software SPSS (Version 16, SPSS Inc., Chicago, IL, USA) was used for the data analysis. Linear correlations were employed to analyze the validation experiment using agar-gelatin phantoms with different stiffness tested by the Liverscan and the conventional mechanical indentation test and to study the relationship of liver stiffness measured by the Liverscan and the Fibroscan. In addition to linear correlation, Bland-Altman analysis was applied to confirm whether the liver stiffness values measured by the Liverscan would agree with those measured by the Fibroscan. Paired *t*-test was used to study the location dependence for liver stiffness measurement. The intra-class correlation coefficient (ICC) was used to test the repeatability of the intra-observer (ICC, Model 3) and inter-observer (ICC, Model 2) measurements (Rankin and Stokes 1998). A statistical level of $p < 0.05$ was used to indicate a significant difference or correlation.

CHAPTER 4 RESULTS

In this chapter, the main findings are presented, including the stiffness correlations between the Liverscan and the mechanical indentation test based on the phantom study, and between the Liverscan and the Fibroscan for the *in vivo* measurement. The result for the location dependence is also presented.

4.1 Agar-gelatin phantoms: Correlation between Liverscan and mechanical indentation test

Figure 4.1 is a typical measurement result of an agar-gelatin phantom. With the test of custom-made agar-gelatin phantoms with different stiffness, a significant linear correlation of stiffness between the mechanical indentation test and the Liverscan was found ($r=0.97$, $p<0.001$) (Figure 4.2), which indicated the stiffness measured by both methods was consistent and the Liverscan was able to measure soft tissue stiffness.

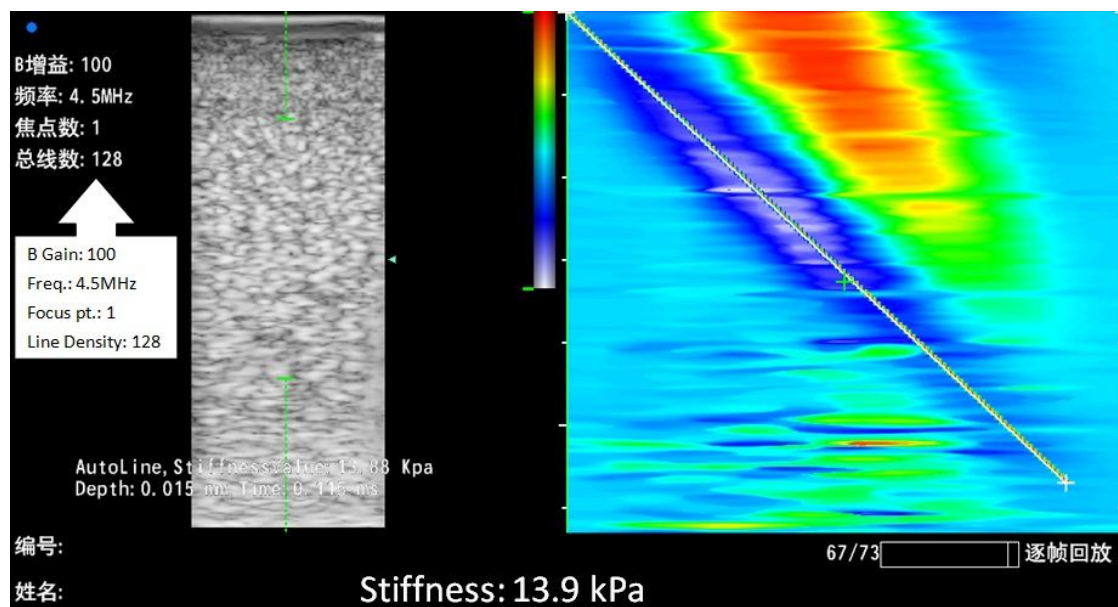


Figure 4.1 A typical stiffness measurement result of an agar-gelatin phantom.

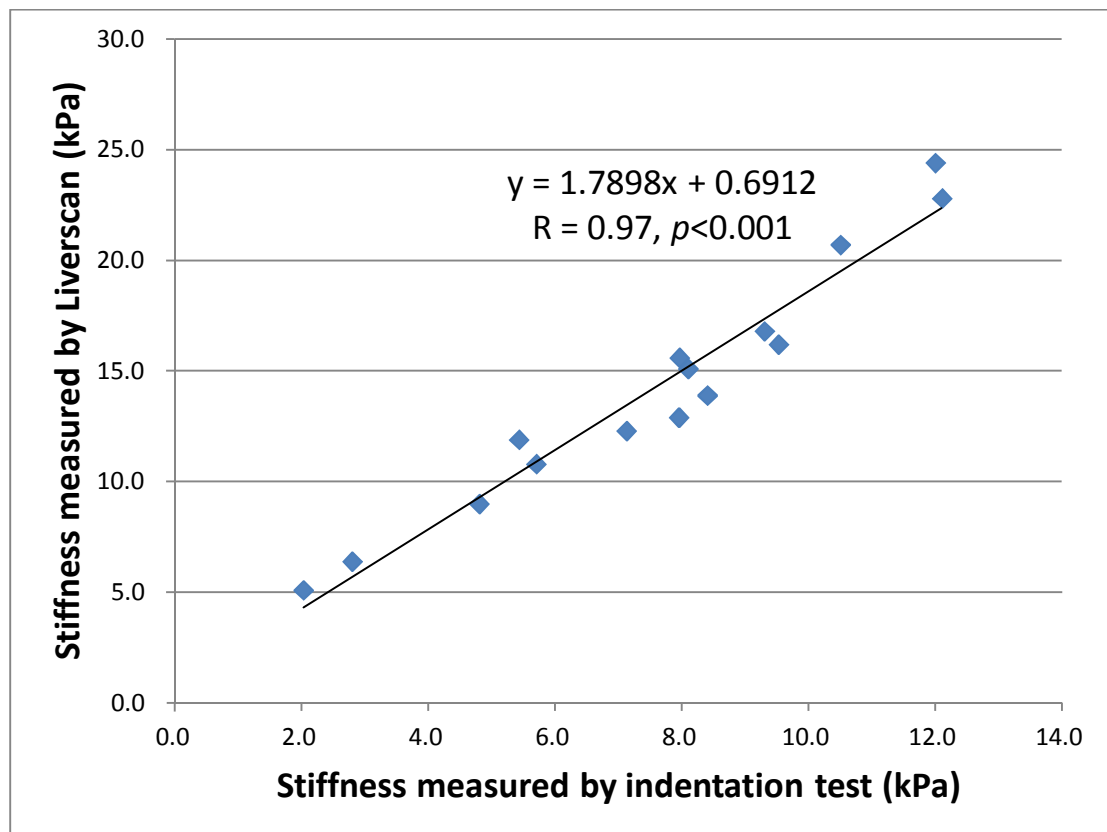


Figure 4.2 The correlation between the stiffness measured by the mechanical indentation test and that by the Liverscan. A significant correlation was found ($r=0.97$, $p<0.001$).

4.2 Intra- and inter- repeatability tests

For the repeatability of *in vivo* measurement, both intra- and inter-observer tests were repeatable significantly as ICC values were 0.987 ($p<0.001$) and 0.988 ($p<0.001$) for average measures, respectively. This revealed that our Liverscan was operator independent.

4.3 Correlation between Liverscan and Fibroscan for in vivo measurements

In the *in vivo* measurements, median values were obtained by the Fibroscan; while mean values were adapted by the Liverscan. Based on this study, it was confirmed that the median values and mean values obtained by the two methods were highly correlated for both Liverscan ($r=0.0995$, $p<0.001$) and Fibroscan ($r=0.996$, $p<0.001$) as shown in Figure 4.3. This finding implied that the uses of median or mean values got highly comparable results for stiffness measurement. Figure 4.4 shows a significant linear correlation of measured liver stiffness between the Liverscan and the Fibroscan ($r=0.886$, $p<0.001$). This indicated the Liverscan was able to perform *in vivo* liver stiffness measurement and able to identify different liver stiffness, ranging from 8.1 to 21.6 kPa for average measure. From the Bland-Altman analysis (Figure 4.5), it could be further confirmed that the liver stiffness measured by the Liverscan agreed with that measured by the Fibroscan. This finding suggested that the Liverscan performed comparably with the Fibroscan for *in vivo* stiffness measurement. Based on the cut-off value of normal liver stiffness from the Fibroscan (about 7.5 kPa) (Castera et al. 2005; Foucher et al. 2006b), 14.0 kPa was the calculated cut-off value for the Liverscan using the correlation as shown in Figure 4.4. Some typical *in vivo* stiffness values measured by the Liverscan are demonstrated in Figure 4.6.

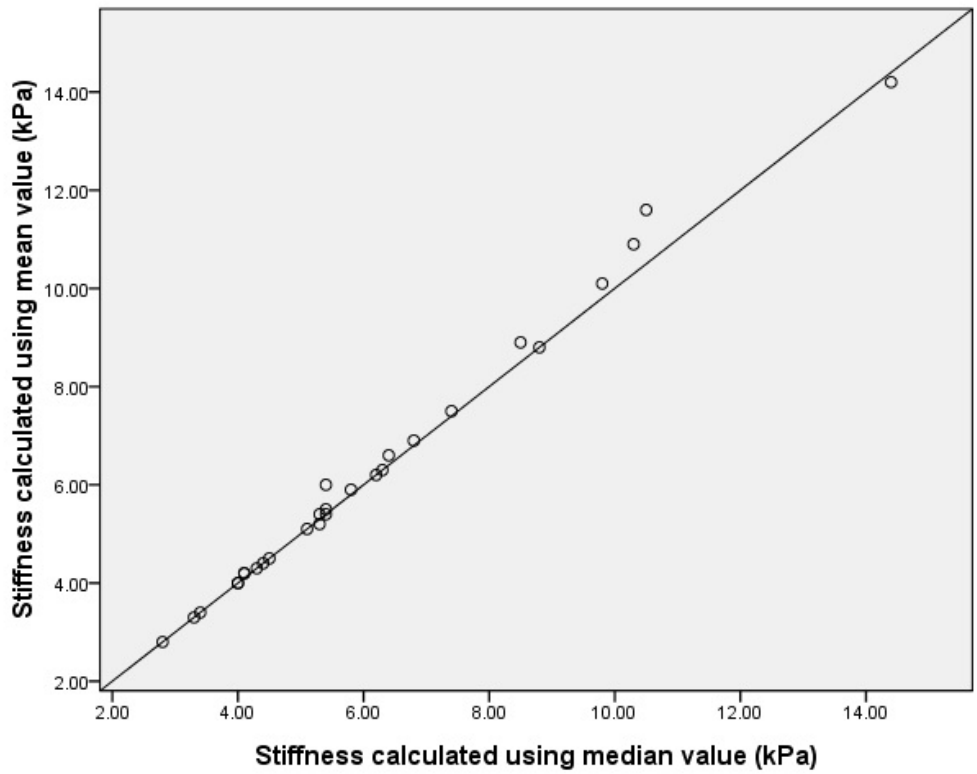
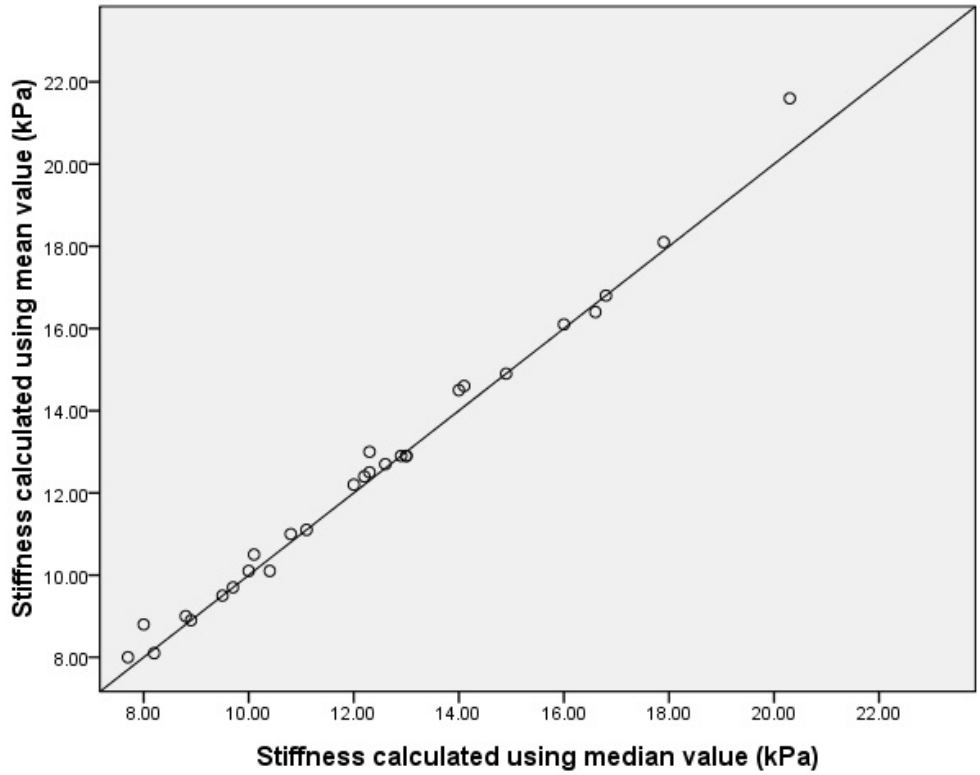


Figure 4.3 For both the Liverscan (a) and the Fibrosan (b), the mean and median values obtained were highly correlated ($r=0.0995$, $p<0.001$) and ($r=0.0996$, $p<0.001$), respectively.

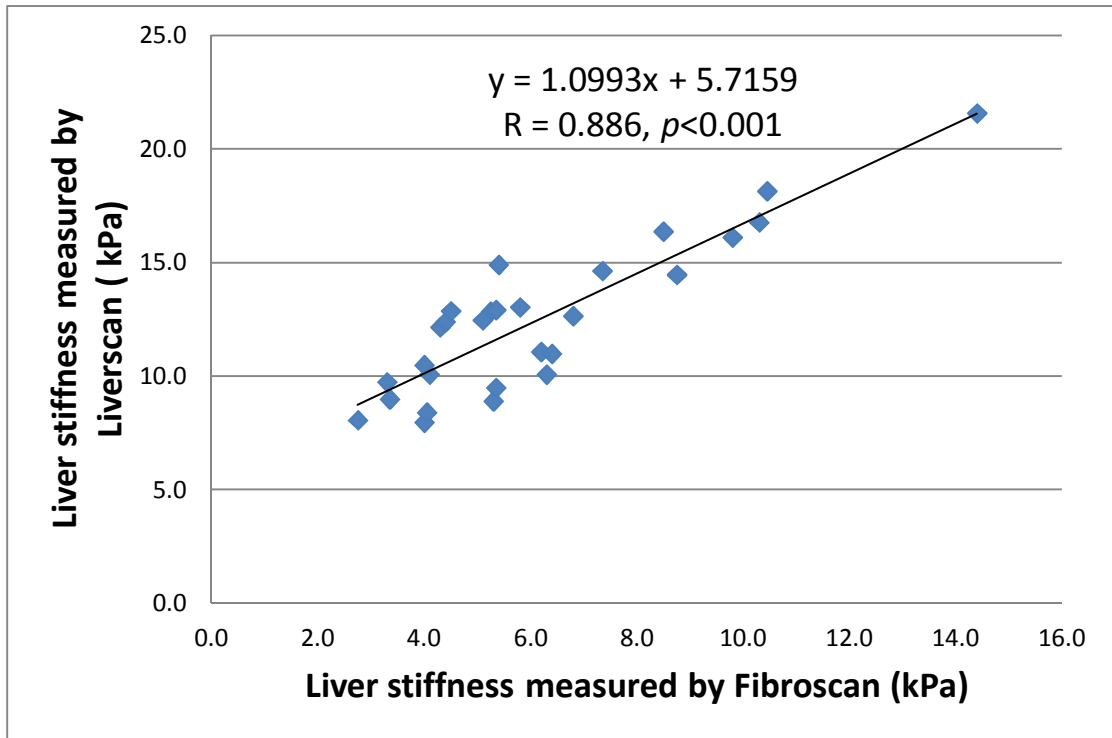


Figure 4.4 The linear correlation between the *in vivo* liver stiffness measured by the Liverscan and that by the Fibroscan. A significant correlation was found in the results obtained from the two measurements ($r=0.886, p<0.001$).

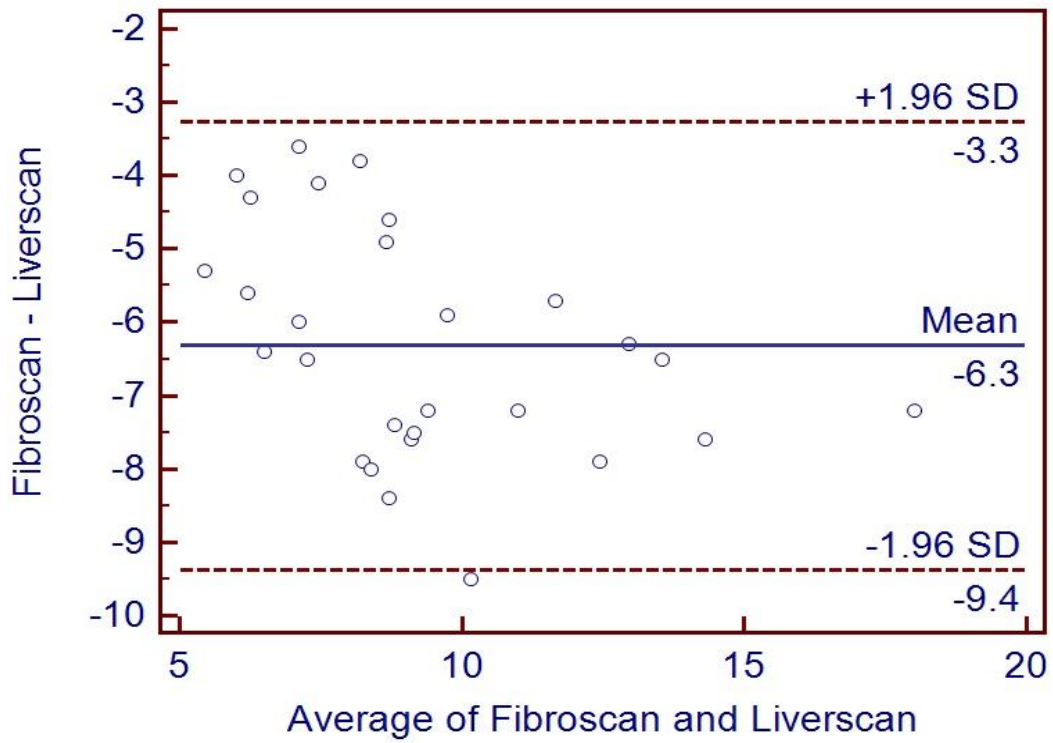
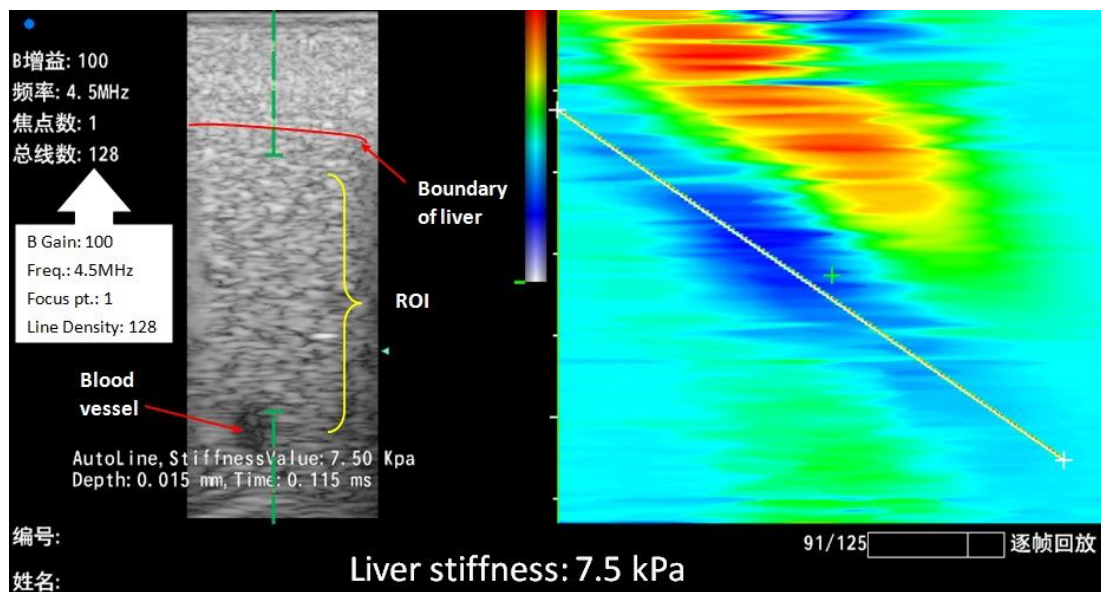
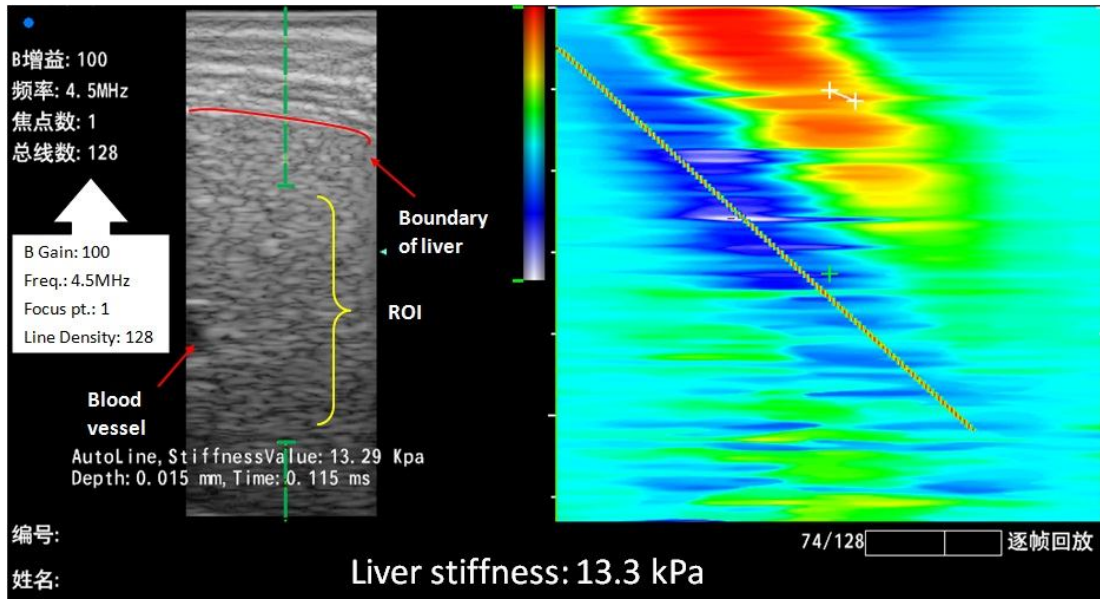


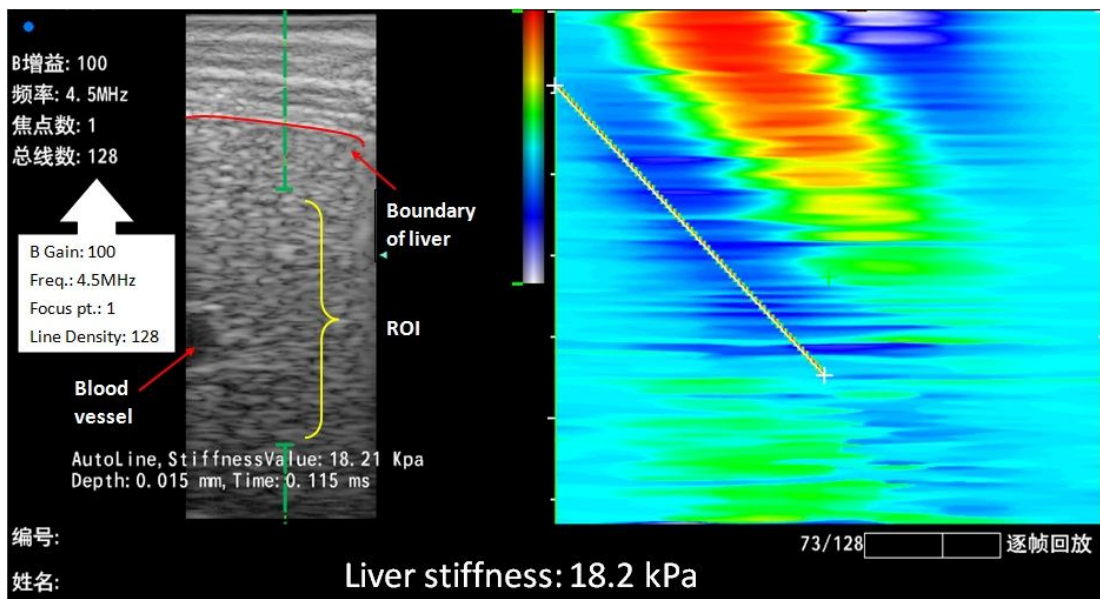
Figure 4.5 Bland-Altman analysis shows agreement between the stiffness measured by the Liverscan and that by the Fibroskan. Only 3.6% of the values were outside limits of agreement, 1.96SD.



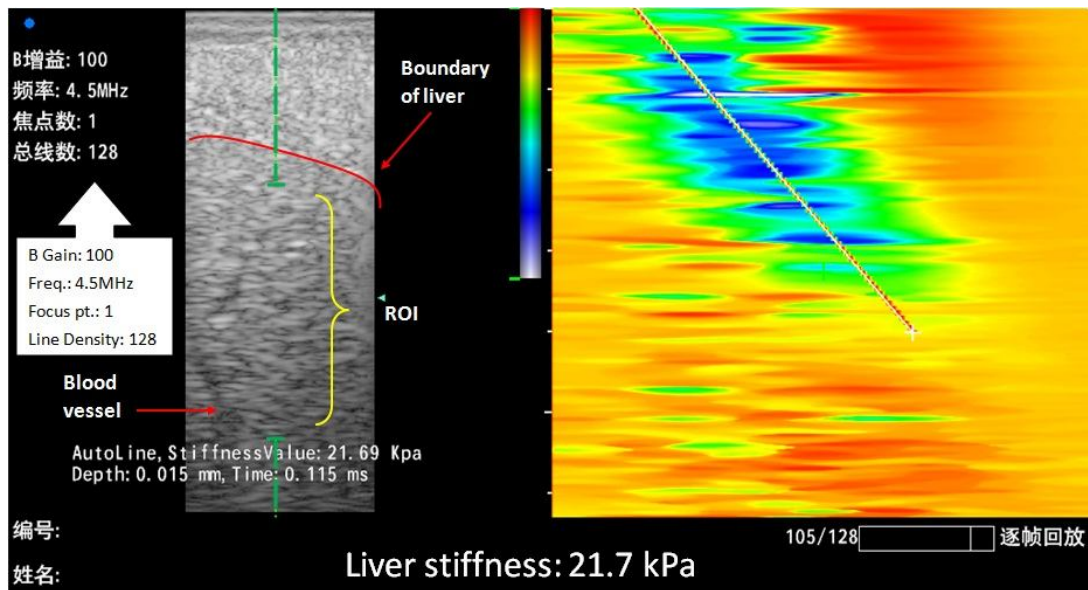
(a)



(b)



(c)



(d)

Figure 4.6 Some typical *in vivo* liver stiffness measurement results measured by the Liverscan, showing different stiffness measurements and indicating the measurement ability of the Liverscan. Left side is the B-mode ultrasound liver image and right side is the elastogram. We could identify the upper boundary and a blood vessel in the B-mode ultrasound image that allows selecting ROI. The slope of the trace in elastogram represents the liver stiffness.

4.4 Location dependence of measurement

To investigate the location dependence effect, two locations were selected for the measurement, in the areas between intercostal space 7th and 8th and between 8th and 9th. There was no significant difference in the results measured between these two locations ($p=0.178$). Figure 4.7, in addition, indicated the liver stiffness measured at two locations was correlated significantly ($r=0.946$, $p<0.001$). Therefore, it could be concluded that the location dependence was negligible and these two locations were both suitable to be included in the proposed measurement protocol to enhance the measurement flexibility and effectiveness. This finding also agreed with the Fibroscan

as its protocol also includes more than one location for measurement.

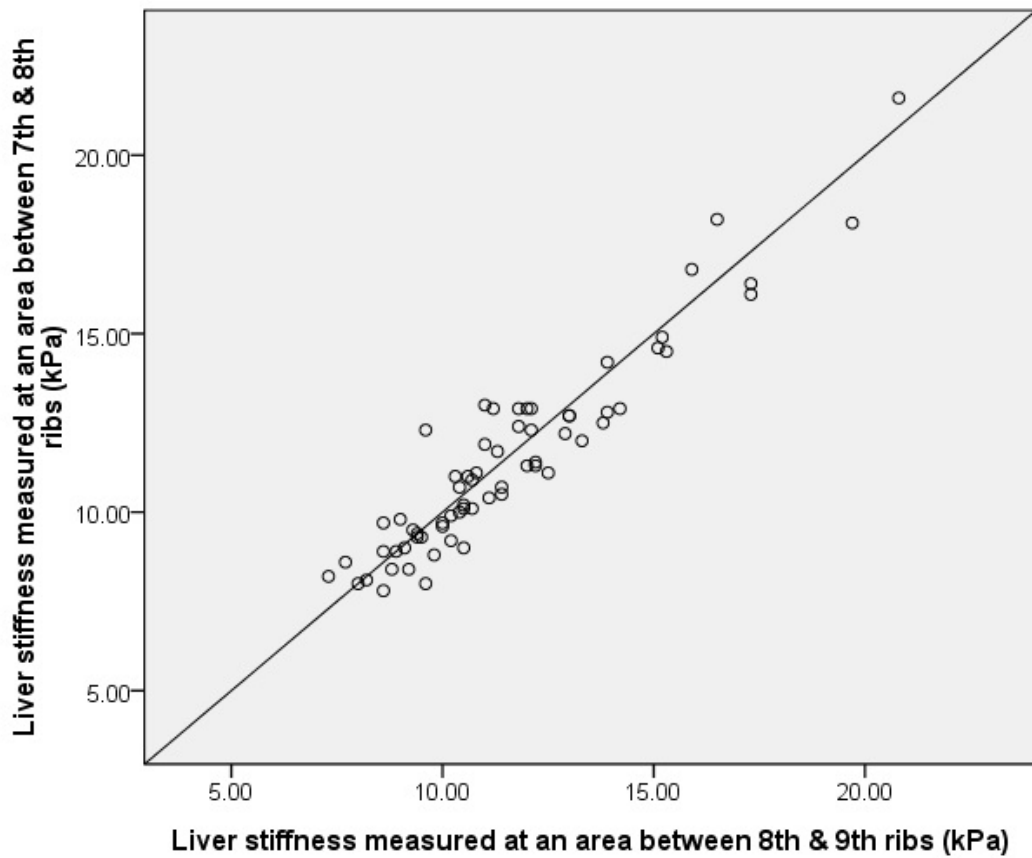


Figure 4.7 The liver stiffness measured by the Liverscan at two locations was correlated significantly ($r=0.946$, $p<0.001$).

CHAPTER 5 DISCUSSION

This chapter discusses the system performance and results of this study. The key feature of the Liverscan, the real-time B-mode ultrasound imaging used as visual guidance is discussed to demonstrate the importance of the visual guidance as blood vessels may be included in the measurement region which could affect the measurement accuracy.

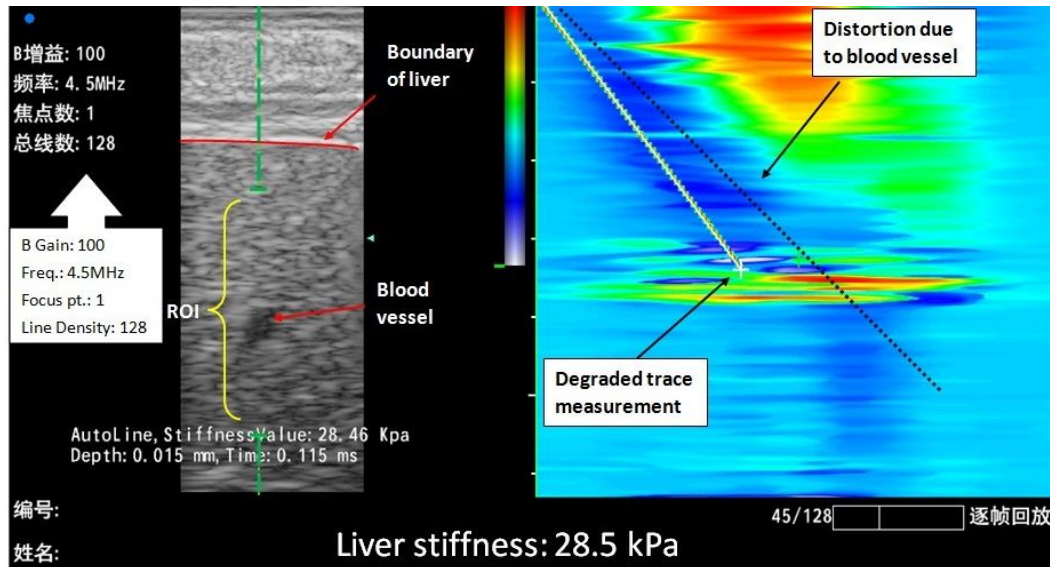
5.1 Summary of the study

In this study, we aimed to design and fabricate specific probe for the Liverscan to assess liver fibrosis non-invasively and to validate its performance systematically by comparing with the conventional mechanical indentation test based on agar-gelatin phantoms and with the Fibroscan for *in vivo* measurements, respectively. In addition, a measurement protocol for using the system was also established. Based on the stiffness results of agar-gelatin phantoms, we have demonstrated the Liverscan was able to measure and identify soft tissues with different stiffness. The repeatability of the Liverscan was excellent thus the operator dependent effect could be minimal. The significant linear correlation between the results by the Liverscan and the Fibroscan indicates that the performance of *in vivo* measurement of the Liverscan was comparable to that of the Fibroscan. We have also found that the effect of location dependence could be ignored for the Liverscan, that is, the areas of intercostal space between 7th and 8th ribs and between 8th and 9th ribs could both be included in the measurement protocol, therefore, the measurement flexibility and effectiveness could be enhanced.

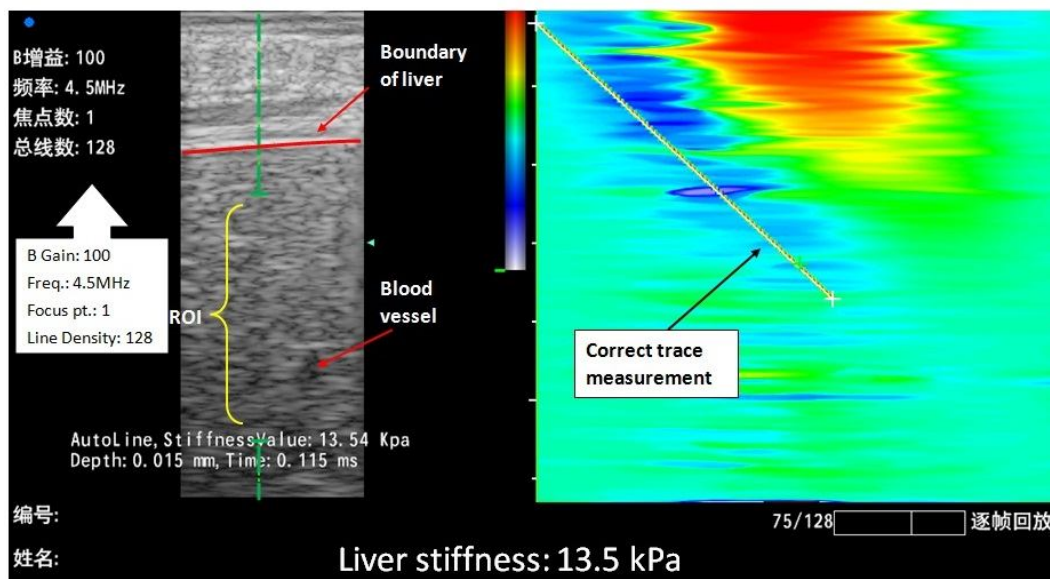
5.2 Real-time B-mode ultrasound guiding

Based on this study, real-time B-mode ultrasound imaging as guidance was very useful for the liver stiffness measurement. Under the guidance from real-time B-mode ultrasound imaging, we were able to locate the liver boundary and liver tissue as well to ensure the right target instead of other organs was located. During breathing, part of the liver may be covered by the diaphragm due to the motion of breathing. Without the guidance from B-mode ultrasound, it was difficult to confirm the measurement target to be liver, but not diaphragm. Additionally, with the help of real-time B-mode ultrasound, we were able to identify the locations of blood vessels within liver. As displayed in Figure 4.6 (a), a blood vessel located on the left side of ultrasound image could be observed. Thus, the ROI cursor was moved to avoid selecting that region for measurement. At this initial stage, we still cannot conclude whether the blood vessels included in the measurement would increase or decrease the stiffness result; however, an increased stiffness was obtained as shown in Figure 5.1. We can confirm that the measurement results would be affected by the presence of blood vessel which affected the accuracy of measurement. From Figure 5.1 (a), a blood vessel was included in the measurement ROI and thus the elastogram was distorted in the corresponding area of blood vessel, leading to the incorrect trace measurement. The distortion may be attributed to that the shear wave was not able to propagate in a liquid median. The accuracy of slope measurement was thus affected as the regressed measurement line was not able to cover all the area of the shear wave propagation trace. As shown in Figure 5.1 (b), when the ROI was moved away from the blood vessel, correct trace and stiffness measurement were obtained. Further investigation on the effect of blood vessel to the stiffness measurement is needed. With this key feature of the Liverscan, it was able to select the right ROI before any measurement, reducing the need of

repeated measurements due to measurement miscarry. Therefore, the measurement accuracy and efficiency were enhanced with the guidance from the B-mode ultrasound imaging of the Liverscan.



(a)



(b)

Figure 5.1 An *in vivo* liver stiffness measurement result with blood vessel (a) and without blood vessel (b) included in the ROI. In (a), the elastogram was distorted due to the presence of blood vessel in the ROI and this resulted in degraded trace

measurement and overestimated liver stiffness, 28.5 kPa; (b) shows the measurement without blood vessel and correct stiffness measurement, 13.5 kPa.

5.3 Evaluation of the stiffness measured by Liverscan

Although the stiffness results measured by the Liverscan correlated significantly with those measured by the mechanical indentation test and the Fibroscan, we could observe that the stiffness measured by the Liverscan was consistently larger than the values obtained by the other methods. This indicates the presence of systemic error which may be caused by the frequency difference among the indentation test, the Fibroscan and the Liverscan. According to the studies of Amador et al. (2011) and Gennisson and Cloutier (2006), a shear wave velocity increased with frequency from 50 Hz to 450 Hz on gelatin phantoms and from 50 Hz to 200 Hz on agar-gelatin phantoms, respectively. For the frequency increased from 50 Hz to 100 Hz, the increased velocity was both smaller than 0.5 ms^{-1} which was able to cause variation in stiffness estimation. In this study, the frequency for indentation test, which was 0.063 Hz according to the indentation rate of 0.5 mms^{-1} and maximum indentation of 4 mm, was much smaller than 50 Hz of the Fibroscan and 100 Hz of the Liverscan. Therefore, the stiffness measured by the indentation test was the smallest and the Liverscan was thus the largest. This systemic error was also reported in a study which compared the stiffness measurements using the Fibroscan and the MRE. The frequency difference was also considered to be the cause of stiffness difference for shear wave induction (Bavu et al. 2011). This could explain why the measured stiffness by the Liverscan was consistently larger than that by the others two methods.

Sandrin et al. (2002) suggested choosing 50 Hz shear wave for the Fibroscan, it was a compromise between a low frequency which promotes diffraction effect causing biases in velocity estimation (Dutt et al. 1996) and a higher frequency which enhances attenuation in soft tissue. The selection of 100 Hz for the Liverscan was based on the optimization of our system. We have tested a number of different vibration frequencies from 50 to 200 Hz. We found that, 50 Hz of shear wave could not obtain qualified results using our system, as the observed wave propagation patterns were too complicated for detection in some cases. Using a vibration frequency larger than 100 Hz, the shear wave propagation was influenced by the attenuation and could only be applicable to subjects with low BMI. The optimized vibration frequency was chosen to be 100 Hz instead of 50 Hz, which was used in the Fibroscan. The main reason for this may be the differences of shapes and surface areas of ultrasound transducers used in the two systems. Fibroscan uses 1D ultrasound transducer, which has a small sized circular surface; while the Liverscan utilizes 2D ultrasound transducer with a relatively larger rectangular surface. This surface area difference may affect the formation of shear wave in terms of amplitude and wavelength. For further evaluations of the system, more systemic tests on the effect of frequency difference on the velocity and also the effect of surface area and shape of ultrasound transducer on the waveform of shear wave need to be well studied.

The correlation between the results obtained using the Fibroscan and the Liverscan for the *in vivo* test was not as excellent as that between the indentation test and the Liverscan for the phantom test ($r=0.886$ vs. $r=0.97$). This may be due to the limited subject size, especially the patients with liver fibrosis in different stages, and the elastogram quality as well. We could observe from Figure 4.4, most of the tested

subjects were normal in liver stiffness and only 6 subjects were confirmed with liver fibrosis and 1 subject was a marginal case. This small patient size limited the range of stiffness to be tested, reducing the degree of correlation. As the patient group size was very small, a small deviation of the stiffness measurement in one or two patients may cause a relatively large change of the whole correlation. This might be one of the causes that reduced the comparability between the Liverscan and the Fibroscan. Elastogram quality was another reason. For the phantom test, the elastogram quality was consistently good and clear as the samples were homogenous. However, the elastogram quality was not always good for *in vivo* test. The main cause was the relatively high BMI or relatively thick fat tissue layer of some subjects. In this study, we found that it was more difficult to conduct test by the Liverscan on those with relatively high BMI and the elastogram quality was not as consistently good as those with normal BMI. Similar challenges are also faced by the Fibroscan (Foucher et al. 2006a; Castéra et al. 2010) , and the company has recently launched specially designed probes with lower ultrasound frequency and larger size (XL probe) for subjects with larger BMI. The quality of elastogram would cause variation in the stiffness measurement. As a result, the correlation of *in vivo* test was not as excellent as the phantom test.

5.4 Evaluation of the measurement protocol

In order to standardize the measurement, we have established a measurement protocol. Before any measurements, the subjects had to fast for at least 3 hours to ensure the liver was in rest status. Some previous studies showed liver stiffness increased significantly in patients with chronic liver disease after food intake (Mederacke et al. 2009; Yin et al. 2011). Although, there are limited studies related to liver stiffness

change after food intake, it has been confirmed that mesenteric blood flow increased significantly after a meal as compared to fasting state (Dauzat et al. 1994; Someya et al. 2008; Zardi et al. 2008). The increased blood flow would result in an increase of hepatic venous pressure gradient if the impedance to portal outflow remained constant (Yin et al. 2011). It was also reported that patients with cirrhosis experienced a 30-40% increase in hepatic venous pressure gradient after food intake (Osman et al. 2008). Therefore, we believe food intake would alter liver stiffness as hepatic venous pressure gradient increases. Apart from blood flow, an increased blood glucose level after meal may be another possible cause to alter liver stiffness chemically. Our preliminary study showed that the liver stiffness had a trend of increase at 30 min up to 120 min after the food intake according to the results obtained from 9 subjects (Mak et al. 2011). Further investigation on the influence of food intake for liver stiffness is needed with larger size of subjects.

In the measurement protocol, we had instructed an area of intercostal space between 7th and 8th ribs to be the measurement location. In this study, an area of intercostal space between 8th and 9th ribs was also tested to study the location dependence and to seek another feasible location in order to increase the efficiency. It was found that there was no significant difference between the results obtained from the two locations ($p=0.178$) and they were significantly correlated ($r=0.946$, $p<0.001$). This suggests that the stiffness values measured from the two locations well agreed, thus, the location dependence was negligible. This finding also demonstrated that the Liverscan was able to perform as well as the Fibroscan which can perform measurement on more than one location. Sometimes, this feature is critical as the anatomical structure of human body varies from one subject to another. For example,

it may be difficult to clearly identify the intercostals space between 7th and 8th ribs, and then we may take the second option for measurement. This improves the flexibility for measurement and thus increases the measurement efficiency.

As fibrotic tissue is scattered in liver, two or more measurement locations are more favorable in enhancing the accuracy. In real practices, the liver is moving during measurement because of the motion caused by the respiration. The stiffness result is actually the averaged stiffness of a relatively larger area of liver at a single measurement location. Taking measurements from two different locations could further increase the area of tissues to be measured, thus, the measurement accuracy is enhanced. In addition, measure at two locations help to confirm the stiffness for those marginal cases, like 13.9 kPa from one location. We, therefore, suggest that having two measurement locations is reasonable and helpful to confirm the measurement results for those marginal cases or the cases that are default to measure.

5.5 Stages of Liverscan Development

The development of Liverscan was a big project and contributed by many team members. In my MPhil study, I have contributed to 1) probe design and development, 2) parameter optimization, 3) establishment of measurement protocol, and 4) conduction of preliminary clinical trial. My team members have made contributions to the customization of ultrasound scanner program and image processing. My contributions are further elaborated along with the stages of Liverscan development as follow:

1. To source different type of mechanical vibrators such as the electromagnetic and pneumatic vibrators.

2. To build up prototypes of the probe by connecting the vibrators with the 2D ultrasound transducer. The prototypes were integrated with the ultrasound scanner, which was modified by team members to test the feasibility of the vibrators using phantom.
3. To give feedbacks on the problems of the ultrasound system, especially the processing algorithm to have better imaging result using those probe prototypes.
4. To design the structure of the probe with a selected mechanical vibrator based on the test results and to convert the design into a technical drawing for fabrication. The material of the probe has considered, non-toxic, biocompatible, and easy clean and wear resistance.
5. To fabricate the components of the probe based on the design including the casing and other installing parts.
6. To assemble the probe with mechanical vibrator and ultrasound transducer and to assemble the control box. The electronic circuit of the control box was developed by the team members.
7. To test the optimized setting for the system including the vibration frequency and amplitude.
8. To validated the measurement of Liverscan using phantoms with different stiffness.
9. To establish the measurement protocol based on trials on subjects using the system.
10. To carry out the preliminary clinical trial using the system.
11. To summary the findings and writing the papers.

CHAPTER 6 CONCLUSIONS AND FURTHER STUDIES

This chapter summarizes the performance of the Liverscan. Suggestions for further studies are also highlighted.

6.1 Conclusions

In this study, a custom-designed linear probe with vibration feature was successfully developed for the transient elastography system guided with real-time B-mode ultrasound imaging, Liverscan, for the assessment of liver fibrosis. The tissue stiffness measurement using the new probe was demonstrated reliable with very high inter- and intra-operator repeatability. Excellent correlation was found between the result obtained by the Liverscan and that obtained by the conventional indentation test on tissue-mimicking phantoms. The tests on subjects *in vivo* demonstrated that the liver stiffness values measured by the Liverscan and the Fibroscan agreed well. The real-time B-mode image guiding was demonstrated useful during the measurement. In addition, fasting and measurement locations have been included in the measurement protocol to measure liver stiffness properly. To conclude, this feasibility study has demonstrated that our Liverscan with specifically designed probe was able to measure liver with different stiffness and to identify the presence of fibrosis. Further studies are required to enhance the measurement system and to conduct tests with larger group of subjects.

6.2 Further studies

6.2.1 Size of subject group

One of the main limitations of this study is the small size of the subject group,

especially the patient group, which may reduce the correlation to the Fibroscan. Generally, it is suggested that future studies should have a subject size of up to hundreds and at least half of the subjects should be patients with different stages of liver fibrosis (Donner 1984). It is better to include subjects with a wider range of age and body size. This may help to understand whether age and body size would affect the result of measurement. As a feasibility study, the current research aims to show whether the Liverscan is able to make liver stiffness measurement and identify different liver stiffness using the Fibroscan as reference. In future studies, more subjects with various age, body size and liver fibrosis stages should be recruited to further validate the system performance quantitatively.

6.2.2 Comparison with biopsy

To validate the Liverscan preliminarily, the Fibroscan was used as reference since both of them were developed based on TE and the Fibroscan is commercially available device for measuring liver stiffness non-invasively. Other than the Fibroscan, we would like to make comparison with other methods, especially the “gold standard”, biopsy. We are planning to collaborate with physicians to further validate the performance of the Liverscan and make comparison with biopsy. Comments from physicians would also be helpful to refine the measurement protocol or the procedures.

6.2.3 Measurement protocol: Fasting study

In this study, the subjects were asked to fast at least 3 hours before any measurement for both the Liverscan and the Fibroscan. According to the results of our preliminary study with 9 normal subjects, we believed that liver stiffness may be altered due to the

increased blood flow and blood glucose level after food intake (Mak et al. 2011). It is suggested that relevant tests should be conducted to understand whether liver stiffness will be altered after a meal, by monitoring the blood flow by Doppler ultrasound and glucose level by glucose meter. Both normal subjects and patients with different degrees of liver fibrosis should be included in future studies. The results may help to further refine the fasting period as to standardize the measurement.

6.2.4 Measurement protocol: Vibration frequency study

The measured *in vivo* liver stiffness obtained by the Liverscan in this study tended to be larger than that by than that measured by the Fibroscan; this may be attributed to the frequency difference as discussed in discussion chapter. In this study, the vibration frequency was fixed at 100 Hz to test the feasibility of the measurement. Since the frequency dependence of measured stiffness relates to the viscoelasticity of tissues, it would be worthwhile to further investigate how the vibration frequency may affect the results obtained by the Liverscan. Tissue mimicking phantoms as well as patients with liver fibrosis can be tested with different vibration frequencies. It is also important to find a reliable formula to transfer the result measured by the Liverscan into an equivalent value for the Fibroscan if ultimately different vibration frequencies have to be used. If this can be achieved, the results obtained by the two systems can be easily compared in the further.

6.2.5 Measurement protocol: Breathing study

As mentioned earlier, the liver is moving passively under the motion of respiration during measurement. This kind of movement may help to expose the covered tissues,

thus improve the measurement accuracy. However, in terms of motion artifact, any motion during measurement is not preferable. In normal clinical practice, the patients will be asked to hold breathing during ultrasound scanning to help to capture clearer images for diagnosis. However, for the stiffness measurement purpose, holding breathing may have already altered liver stiffness. In order to have better understanding of the breathing effect, a study related to the effect of breathing movement on liver stiffness variation is needed in the future.

6.2.6 Probe development and fabrication

In this study, the measurement probe was developed and fabricated with a 4.5 MHz B-mode ultrasound transducer. During the clinical trial, we found that one probe was not applicable to all the participants, causing limitations for measurement. For instance, participants with BMI over 27 kgm^{-2} were excluded from the study as 4.5 MHz ultrasound and shear wave attenuated heavily. For such subjects, an ultrasound transducer with lower frequency such as 3.7 MHz and a stronger vibrator to generate larger magnitude shear wave may be needed. The measurement location is proposed to be the intercostal space. For some cases, especially for female subjects having narrow intercostal space that do not fit the placement of the whole ultrasound transducer, part of the transducer head impacts on the ribs causing interference to the shear wave and un-comfort to the subjects. For this case, an ultrasound transducer with smaller width is preferable to tackle the narrow intercostal space problem. Based on these experiences, we plan to fabricate a series of probes to meet the needs of various subjects.

APPENDIX

I. *Technical drawing of the probe*

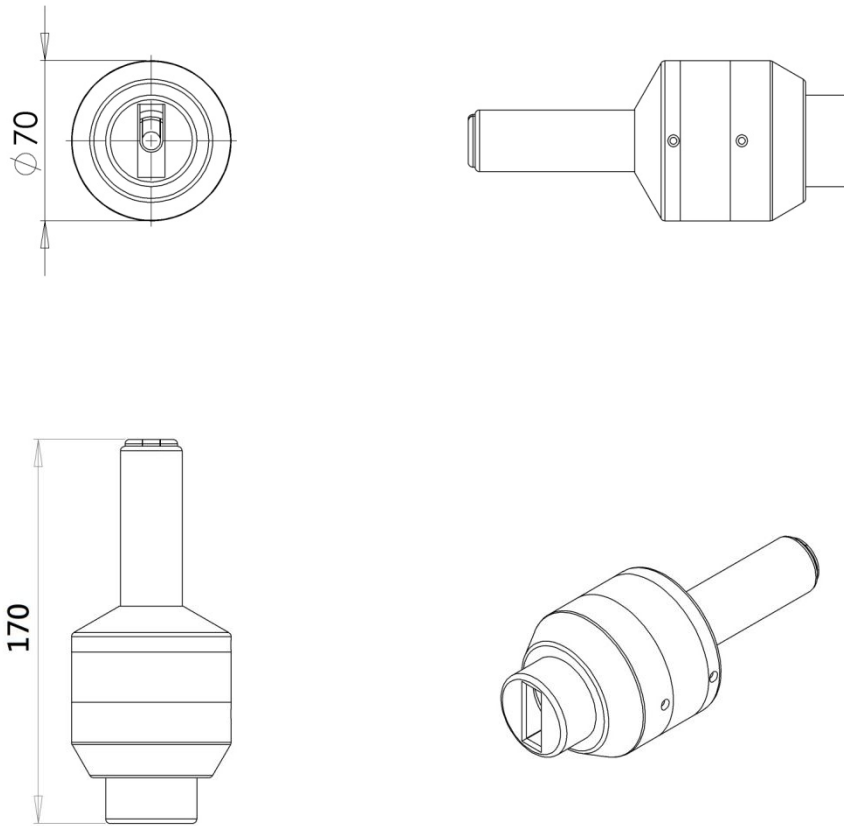


Figure A.1 Technical drawing of the probe.

II. Example of the stiffness calculation

For example, the slope of the trace obtained from the elastogram of Figure 4.6a was 1.58 ms^{-1} , the mass density of liver tissue is assumed to be 1000 kgm^{-3} ,

$$E = 3 \cdot 1000 \cdot 2^2, E = 7.5 \text{ kPa}$$

III. Data table

Table A.1 The stiffness of phantoms measured by the mechanical indentation test and the Liverscan is listed below. The Young's modulus of phantoms measured by mechanical test was calculated based on Equation (1) with the force-deformation relationship obtained from the mechanical indentation test.

| | Indentation test | | Liverscan | |
|-------------------|----------------------------|-----------|----------------------------|-----------|
| | Young's modulus/kPa | | Young's modulus/kPa | |
| | Mean | SD | Mean | SD |
| Phantom 1 | 2.0 | 0.1 | 5.1 | 0.4 |
| Phantom 2 | 4.8 | 0.2 | 9.0 | 0.6 |
| Phantom 3 | 5.7 | 0.5 | 10.8 | 0.7 |
| Phantom 4 | 7.1 | 0.1 | 12.3 | 1.0 |
| Phantom 5 | 8.0 | 0.2 | 12.9 | 0.6 |
| Phantom 6 | 8.4 | 0.2 | 13.9 | 0.6 |
| Phantom 7 | 9.5 | 0.2 | 16.2 | 0.8 |
| Phantom 8 | 10.5 | 0.5 | 20.7 | 1.7 |
| Phantom 9 | 12.0 | 0.3 | 24.4 | 1.3 |
| Phantom 10 | 2.8 | 0.1 | 6.4 | 1.1 |
| Phantom 11 | 5.4 | 0.1 | 11.9 | 1.0 |
| Phantom 12 | 9.3 | 0.2 | 16.8 | 1.2 |
| Phantom 13 | 8.1 | 0.4 | 15.1 | 0.7 |
| Phantom 14 | 8.0 | 0.4 | 15.6 | 0.8 |
| Phantom 15 | 12.1 | 0.2 | 22.8 | 0.6 |

Table A.2 Liver stiffness measured by the Liverscan and the Fibroscan is summarized below. Fibroscan obtains median values, while the Liverscan utilizes mean values. From the Fibroscan results, we can identify that the median values and mean values are very close. The correlation between the Liverscan and the Fibroscan was significant ($r=0.886, p<0.001$).

| | Liverscan | | | Fibroscan | | |
|-----------------|----------------------------|-------------|-----------|----------------------------|-------------|-----------|
| | Young's modulus/kPa | | | Young's modulus/kPa | | |
| | Median | Mean | SD | Median | Mean | SD |
| Male 1 | 11.1 | 11.1 | 0.9 | 6.2 | 6.2 | 1.0 |
| Male 2 | 7.7 | 8.0 | 0.5 | 4.0 | 4.0 | 0.5 |
| Male 3 | 20.3 | 21.6 | 3.6 | 14.4 | 14.2 | 2.8 |
| Male 4 | 12.3 | 13.0 | 2.3 | 5.8 | 5.9 | 1.2 |
| Male 5 | 12.0 | 12.2 | 0.9 | 4.3 | 4.3 | 0.7 |
| Male 6 | 12.2 | 12.4 | 1.2 | 4.4 | 4.4 | 0.5 |
| Male 7 | 12.9 | 12.9 | 0.8 | 5.3 | 5.4 | 0.9 |
| Male 8 | 16.6 | 16.4 | 1.0 | 8.5 | 8.9 | 1.2 |
| Male 9 | 17.9 | 18.1 | 1.7 | 10.5 | 11.6 | 2.5 |
| Male 10 | 8.9 | 8.9 | 0.4 | 5.3 | 5.2 | 0.3 |
| Male 11 | 10.4 | 10.1 | 0.9 | 4.1 | 4.2 | 0.7 |
| Male 12 | 9.5 | 9.5 | 0.4 | 5.4 | 6.0 | 2.4 |
| Male 13 | 9.7 | 9.7 | 0.6 | 3.3 | 3.3 | 0.2 |
| Male 14 | 12.6 | 12.7 | 1.2 | 6.8 | 6.9 | 1.0 |
| Male 15 | 16.0 | 16.1 | 1.0 | 9.8 | 10.1 | 2.5 |
| Male 16 | 10.1 | 10.5 | 1.5 | 4.0 | 4.0 | 0.3 |
| Male 17 | 16.8 | 16.8 | 0.7 | 10.3 | 10.9 | 0.8 |
| Male 18 | 14.1 | 14.6 | 1.8 | 7.4 | 7.5 | 1.0 |
| Male 19 | 13.0 | 12.9 | 0.6 | 4.5 | 4.5 | 0.4 |
| Female 1 | 10.0 | 10.1 | 1.0 | 6.3 | 6.3 | 1.0 |
| Female 2 | 8.2 | 8.1 | 0.6 | 2.8 | 2.8 | 0.4 |
| Female 3 | 8.8 | 9.0 | 0.8 | 3.4 | 3.4 | 0.4 |
| Female 4 | 8.0 | 8.8 | 0.9 | 4.1 | 4.2 | 0.5 |
| Female 5 | 14.0 | 14.5 | 0.8 | 8.8 | 8.8 | 1.7 |
| Female 6 | 10.8 | 11.0 | 0.8 | 6.4 | 6.6 | 0.8 |
| Female 7 | 14.9 | 14.9 | 0.7 | 5.4 | 5.4 | 0.6 |
| Female 8 | 13.0 | 12.9 | 0.9 | 5.4 | 5.5 | 0.6 |
| Female 9 | 12.3 | 12.5 | 1.4 | 5.1 | 5.1 | 0.6 |

Table A.3 Liver stiffness measured at two locations for both male and female subjects.

The first location was the area of intercostal space between 7th and 8th ribs and the second location was the area of intercostal space between 8th and 9th ribs.

| | Location 1 | | Location 2 | | Percentage difference/ % |
|----------------|---------------------|------|---------------------|-----|-----------------------------|
| | Liver stiffness/kPa | | Liver stiffness/kPa | | |
| | Mean | SD | Mean | SD | |
| Male 1 | 8.9 | 0.4 | 8.6 | 0.3 | 3.5 |
| Male 2 | 8.4 | 0.7 | 9.2 | 0.5 | -9.4 |
| Male 3 | 11.1 | 0.9 | 12.5 | 0.5 | -12.5 |
| Male 4 | 12.4 | 1.2 | 11.8 | 0.7 | 4.9 |
| Male 5 | 8.2 | 0.5 | 7.3 | 0.3 | 11.4 |
| Male 6 | 12.3 | 0.7 | 9.6 | 0.5 | 21.8 |
| Male 7 | 10.4 | 0.5 | 11.1 | 0.5 | -6.6 |
| Male 8 | 8.6 | 0.7 | 7.7 | 0.5 | 10.2 |
| Male 9 | 10.9 | 0.6 | 10.7 | 1.0 | 2.0 |
| Male 10 | 8.0 | 0.5 | 9.6 | 0.8 | -20.1 |
| Male 11 | 21.6 | 3.6 | 20.8 | 2.1 | 3.7 |
| Male 12 | 13.0 | 2.3 | 11.0 | 0.8 | 15.6 |
| Male 13 | 12.2 | 0.9 | 12.9 | 0.9 | -6.2 |
| Male 14 | 18.1 | 1.7 | 19.7 | 1.1 | -8.3 |
| Male 15 | 8.9 | 0.4 | 8.9 | 0.6 | -0.1 |
| Male 16 | 10.1 | 0.9 | 10.5 | 0.7 | -4.2 |
| Male 17 | 9.5 | 0.4 | 9.3 | 0.6 | 2.1 |
| Male 18 | 12.9 | 0.8 | 14.2 | 1.0 | -10.7 |
| Male 19 | 12.7 | 1.2 | 13.0 | 0.7 | -2.4 |
| Male 20 | 16.4 | 1.0 | 17.3 | 1.3 | -5.9 |
| Male 21 | 9.7 | 0.6 | 8.6 | 0.2 | 11.4 |
| Male 22 | 10.7 | 0.8 | 11.4 | 0.7 | -6.5 |
| Male 23 | 10.5 | 1.5 | 11.4 | 0.6 | -8.6 |
| Male 24 | 12.7 | 10.1 | 13 | 0.5 | -2.4 |
| Male 25 | 16.1 | 1.0 | 17.3 | 0.4 | -7.5 |
| Male 26 | 16.8 | 0.7 | 15.9 | 0.7 | 5.4 |
| Male 27 | 9.4 | 1.0 | 9.4 | 0.4 | 0.0 |
| Male 28 | 18.2 | 2.0 | 16.5 | 1.0 | 9.3 |
| Male 29 | 12.9 | 1.7 | 11.2 | 0.3 | 13.2 |
| Male 30 | 11.7 | 1.7 | 11.3 | 0.5 | 3.4 |
| Male 31 | 14.6 | 1.8 | 15.1 | 0.6 | -3.4 |

| | | | | | |
|------------------|------|-----|------|-----|-------|
| Male 32 | 10.2 | 1.4 | 10.5 | 0.5 | -2.9 |
| Male 33 | 12.9 | 0.6 | 12 | 0.4 | 7.0 |
| Male 34 | 11.4 | 0.8 | 12.2 | 0.7 | -7.0 |
| Female 1 | 9.2 | 0.6 | 10.2 | 1.2 | -11.0 |
| Female 2 | 9.0 | 0.5 | 10.5 | 0.8 | -16.3 |
| Female 3 | 9.8 | 0.7 | 9.0 | 0.7 | 8.1 |
| Female 4 | 9.3 | 0.4 | 9.4 | 0.8 | -1.2 |
| Female 5 | 9.3 | 0.4 | 9.5 | 0.4 | -1.6 |
| Female 6 | 9.6 | 0.3 | 10.0 | 0.4 | -3.9 |
| Female 7 | 8.8 | 0.4 | 9.8 | 0.5 | -10.8 |
| Female 8 | 14.5 | 0.8 | 15.3 | 0.6 | -5.5 |
| Female 9 | 11.0 | 0.8 | 10.3 | 0.8 | 6.3 |
| Female 10 | 10.1 | 1.0 | 10.7 | 0.7 | -6.2 |
| Female 11 | 8.1 | 0.6 | 8.2 | 1.1 | -2.1 |
| Female 12 | 8.4 | 0.9 | 8.8 | 0.3 | -4.4 |
| Female 13 | 9.0 | 0.8 | 9.1 | 0.7 | -0.9 |
| Female 14 | 14.9 | 0.7 | 15.2 | 0.8 | -1.7 |
| Female 15 | 11.3 | 0.9 | 12.2 | 0.6 | -8.0 |
| Female 16 | 12.9 | 0.9 | 12.1 | 0.9 | 6.3 |
| Female 17 | 11.0 | 0.7 | 10.6 | 0.7 | 3.6 |
| Female 18 | 9.7 | 0.8 | 10.0 | 0.7 | -3.1 |
| Female 19 | 10.7 | 1.0 | 10.4 | 0.9 | 2.8 |
| Female 20 | 12.8 | 1.9 | 13.9 | 1.2 | -8.6 |
| Female 21 | 11.1 | 1.2 | 10.8 | 1.1 | 2.7 |
| Female 23 | 14.2 | 1.1 | 13.9 | 1.4 | 2.1 |
| Female 24 | 12.9 | 1.2 | 11.8 | 1.2 | 8.5 |
| Female 25 | 11.3 | 1.3 | 12.0 | 0.9 | -6.2 |
| Female 26 | 11.9 | 0.8 | 11.0 | 0.3 | 7.6 |
| Female 27 | 9.9 | 1.0 | 10.2 | 0.9 | -3.0 |
| Female 28 | 12.0 | 1.4 | 13.3 | 1.2 | -10.8 |
| Female 29 | 12.5 | 1.4 | 13.8 | 1.5 | -10.4 |
| Female 30 | 8.0 | 0.9 | 8.0 | 0.7 | 0.0 |
| Female 31 | 7.8 | 1.3 | 8.6 | 0.6 | -10.3 |
| Female 32 | 12.3 | 0.9 | 12.1 | 1.2 | 1.6 |
| Female 33 | 10.0 | 0.9 | 10.4 | 1.4 | -4.0 |

IV. Information sheet

Project title: Liver fibrosis assessment using transient elastography guided with real-time B-mode ultrasound imaging

You are invited to participate on the study conducted by Mr. Tak-Man MAK, who is the student of The Hong Kong Polytechnic University doing his MPhil research study.

You will be required to sign the Consent form before any test of this study. The aims of this study are to validate the transient elastography system guided with real-time B-mode ultrasound imaging for liver fibrosis assessment and to find out the correlation between stiffness and liver fibrosis stage with the data obtained from our transient elastography system guided with real-time B-mode imaging.

The assessment of liver fibrosis using transient elastography system guided with real-time B-mode ultrasound imaging is a kind of non-invasive assessment. During the assessment, you need to lie down and put your right hand on the back of your head. The probe will be put on the skin surface located near the last rib and mechanical vibration will be sent from the probe to the liver in order to analyze the liver stiffness which in turn assess the fibrosis stage.

The assessment should not result in any undue discomfort. All information related to you will remain confidential and will be identifiable by codes only known to the researcher.

You can withdraw from the assessment and study at any time without any reason.

You will have no any penalty or consequence.

If you have any complaints about the conduct of this study, please do not hesitate to contact Ms Kathy Lui, Secretary of the Human Subjects Ethics Sub-Committee of The Hong Kong Polytechnic University in person or in writing (c/o Human Resources Office of the University).

If you would like to know more about this study, please contact Mr. Tak-Man MAK at 27667669. Thank you for participating in this study.

與研究相關的資訊

項目名稱：實時 B 超圖像引導下的瞬時彈性肝纖維化評估

我們誠邀你參與這項研究，這項研究會由香港理工大學碩士研究生麥德民先生負責。

在進行任何測試之前，你將被要求簽署知情同意書。本研究的目的是驗證實時 B 超圖像引導下的瞬時彈性肝纖維化評估系統的準確性，並跟據我們所獲得的數據找出肝臟彈性和肝纖維化階段的相關性。

實時 B 超圖像引導下的瞬時彈性肝纖維化評估系統是一種無創的評估。在評估時，你需要躺下以及把你的右手放在腦袋後。該系統的探測頭將會放在你右邊最後的肋骨皮膚之上，之後機械振動將從探測頭發送到肝臟，從而分析肝臟彈性以及評估肝纖維化階段。

評估應不會造成任何不必要的不適。有關你的所有信息將保持機密並以代碼來識別，只有相關的研究員才會知道你的信息。

你可以在任何時候和無需任何理由的情況下退出評估和研究，你將不會有任何罰款或後果。

如果你對這項研究有任何投訴，請親自或以書面形式與香港理工大學人類倫理小組委員會秘書雷女士聯繫（轉交大學人力資源處）。

如果你想了解更多有關此研究的資料，請與麥德民先生聯絡，電話 27667669。

感謝你參與本研究。

V. Informed consent form

Project title: Liver fibrosis assessment using transient elastography guided with real-time B-mode ultrasound imaging

I _____ (subject name) consent to participate the assessment entitled liver fibrosis assessment using transient elastography guided with real-time B-mode ultrasound imaging carried by Mr. Tak-Man MAK.

I have read and understand the information and test procedures about the assessments presented to me.

I have had the chance(s) to ask question(s) about the assessments and study and I have got satisfactory answer(s).

I realize I may not benefit personally from the part I will take during the assessments and study.

I realize I can withdraw from the assessments and study at any time without any reason. I will have no any penalty or consequence.

I realize that the assessment or study results may be published. For my own results, I realize they will be kept and processed in accordance with the provisions of the Personal Data (Privacy) Ordinance, and I will not be identified personally in any published work.

I realize the results of this study will be the properties of the Department of Health Technology and Informatics of The Hong Kong Polytechnic University.

Subject name: _____

Signature: _____

Witness name: _____

Signature: _____

Investigator name: _____

Signature: _____

Date: _____

知情同意書

項目名稱：實時 B 超圖像引導下的瞬時彈性肝纖維化評估

我_____（參與者名稱）同意參與由麥德民先生負責的實時 B 超圖像引導下的瞬時彈性肝纖維化評估。

我已閱讀並了解有關信息和測試程序。

我有機會提出關於這次評估和研究的問題，而且我已經得到了滿意的答复。

在這次評估和研究的過程中，我知道我不會得到個人好處。

我知道我可以在任何時候和無需任何理由的情況下退出評估和研究，我將沒有任何罰款或後果。

我知道評估或研究的結果有可能公佈。我知道有關的結果將按照個人資料（私隱）條例的規定去保存和處理，我將不會在任何發表的研究報告中被識別。

我知道這項研究結果將是香港理工大學醫療科技及資訊學系的資產。

參與者姓名 (正楷)：_____ 簽名：_____

見證者姓名 (正楷)：_____ 簽名：_____

研究者姓名 (正楷)：_____ 簽名：_____

日期：_____

REFERENCES

- Abdi W, Millan JC, Mezey E. Sampling variability on percutaneous liver biopsy. *Arch Intern Med* 1979;139:667-9.
- Abe C, Kahn CJ, Doi K, Katsuragawa S. Computer-aided detection of diffuse liver disease in ultrasound images. *Invest Radiol* 1992;27:71-7.
- Afdhal NH, Nunes D. Evaluation of liver fibrosis: A concise review. *Am J Gastroenterol* 2004;99:1160-74.
- Amador C, Urban MW, Shigao C, Qingshan C, Kai-Nan A, Greenleaf JF. Shear elastic modulus estimation from indentation and SDUV on gelatin phantoms. *IEEE Trans Biomed Eng* 2011;58:1706-14.
- Angulo P, Keach JC, Batts KP, Lindor KD. Independent predictors of liver fibrosis in patients with nonalcoholic steatohepatitis. *Hepatology* 1999;30:1356-62.
- Annet L, Peeters F, Abarca-Quinones J, Leclercq I, Moulin P, Van Beers BE. Assessment of diffusion-weighted MR imaging in liver fibrosis. *J Magn Reson Imaging* 2007;25:122-8.
- Awaya H, Mitchell DG, Kamishima T, Holland G, Ito K, Matsumoto T. Cirrhosis: Modified caudate–right lobe ratio. *Radiology* 2002;224:769-74.
- Bakan AA, Inci E, Bakan S, Gokturk S, Cimilli T. Utility of diffusion-weighted imaging in the evaluation of liver fibrosis. *Eur Radiol* 2012;22:682-7.
- Bataller R, Brenner DA. Liver fibrosis. *J Clin Invest* 2005;115:209-18.
- Bavu É, Gennisson J-L, Couade M, Bercoff J, Mallet V, Fink M, Badel A, Vallet-Pichard A, Nalpas B, Tanter M, Pol S. Noninvasive in vivo liver fibrosis evaluation using supersonic shear imaging: A clinical study on 113 hepatitis C virus patients. *Ultrasound Med Biol* 2011;37:1361-73.
- Bedossa P, Bioulacsage P, Callard P, Chevallier M, Degott C, Deugnier Y, Fabre M, Reynes M, Voigt JJ, Zafrani ES, Poynard T, Babany G. Intraobserver and

- interobserver variations in liver biopsy interpretation in patients with chronic hepatitis C. *Hepatology* 1994;20:15-20.
- Bedossa P, Poynard T. An algorithm for the grading of activity in chronic hepatitis C. *Hepatology* 1996;24:289-93.
- Bercoff J, Muller M, Tanter M, Fink M. Study of viscous and elastic properties of soft tissues using supersonic shear imaging. In: Yuhas DE, Schneider SC, ed. 2003 IEEE Ultrasonics Symposium Proceedings, Vols 1 and 2. New York: IEEE, 2003. pp. 925-8.
- Bercoff J, Tanter M, Fink M. Supersonic shear imaging: A new technique for soft tissue elasticity mapping. *IEEE Trans Ultrason Ferroelectr Freq Contr* 2004;51:396-409.
- Bosetti C, Levi F, Lucchini F, Zatonski WA, Negri E, La Vecchia C. Worldwide mortality from cirrhosis: An update to 2002. *J Hepatol* 2007;46:827-39.
- Boursier J, Konate A, Gorea G, Reaud S, Quemener E, Oberti F, Hubert-Fouchard I, Dib N, Cales P. Reproducibility of liver stiffness measurement by ultrasonographic elastometry. *Clin Gastroenterol Hepatol* 2008;6:1263-9.
- Bravo AA, Sheth SG, Chopra S. Liver biopsy. *N Engl J Med* 2001;344:495-500.
- Castéra L, Foucher J, Bernard P-H, Carvalho F, Allaix D, Merrouche W, Couzigou P, de Ledinghen V. Pitfalls of liver stiffness measurement: A 5-year prospective study of 13,369 examinations. *Hepatology* 2010;51:828-35.
- Castera L, Bernard PH, Le Bail B, Foucher J, Trimoulet P, Merrouche W, Couzigou P, de Ledinghen V. Transient elastography and biomarkers for liver fibrosis assessment and follow-up of inactive hepatitis B carriers. *Aliment Pharmacol Ther* 2011;33:455-65.
- Castera L, Forns X, Alberti A. Non-invasive evaluation of liver fibrosis using transient elastography. *J Hepatol* 2008;48:835-47.
- Castera L, Vergniol J, Foucher J, Le Bail B, Chanteloup E, Haaser M, Darriet M, Couzigou P, De Ledinghen V. Prospective comparison of transient

- elastography, fibrotest, APRI, and liver biopsy for the assessment of fibrosis in chronic hepatitis C. *Gastroenterology* 2005;128:343-50.
- Celle G, Savarino V, Picciotto A, Magnolia MR, Scalabrini P, Dodero M. Is hepatic ultrasonography a valid alternative tool to liver biopsy? Report on 507 cases studied with both techniques. *Dig Dis Sci* 1988;33:467-71.
- Chen BB, Hsu CY, Yu CW, Wei SY, Kao JH, Lee HS, Shih TTF. Dynamic contrast-enhanced magnetic resonance imaging with Gd-EOB-DTPA for the evaluation of liver fibrosis in chronic hepatitis patients. *Eur Radiol* 2012;22:171-80.
- Crow EL, Siddiqui MM. Robust estimation of location. *Journal of the American Statistical Association* 1967;62:353-89.
- Dauzat M, Lafortune M, Patriquin H, Pomier-Layrargues G. Meal induced changes in hepatic and splanchnic circulation: A noninvasive Doppler study in normal humans. *Eur J Appl Physiol* 1994;68:373-80.
- de Ledinghen V, Wong VWS, Vergniol J, Wong GLH, Foucher J, Chu SHT, Le Bail B, Choi PCL, Chermak F, Yiu KKL, Merrouche W, Chan HLY. Diagnosis of liver fibrosis and cirrhosis using liver stiffness measurement: Comparison between M and XL probe of FibroScan (R). *J Hepatol* 2012;56:833-9.
- Donner A. Approaches to sample size estimation in the design of clinical trials - A review. *Stat Med* 1984;3:199-214.
- Elizondo G, Weissleder R, Stark DD, Guerra J, Garza J, Fretz CJ, Todd LE, Ferrucci JT. Hepatic cirrhosis and hepatitis: MR imaging enhanced with superparamagnetic iron oxide. *Radiology* 1990;174:797-801.
- Ellis H, Mahadevan V. *Clinical anatomy : Applied anatomy for students and junior doctors*. Chichester: Wiley-Blackwell, 2010.
- Fischbach F, Bruhn H. Assessment of in vivo ¹H magnetic resonance spectroscopy in the liver: A review. *Liver Int* 2008;28:297-307.

- Foucher J, Castéra L, Bernard P-H, Adhoute X, Laharie D, Bertet J, Couzigou P, de Lédighen V. Prevalence and factors associated with failure of liver stiffness measurement using FibroScan in a prospective study of 2114 examinations. *Eur J Gastroenterol Hepatol* 2006a;18:411-2.
- Foucher J, Chanteloup E, Vergniol J, Castera L, Le Bail B, Adhoute X, Bertet J, Couzigou P, de Ledinghen V. Diagnosis of cirrhosis by transient elastography (FibroScan): A prospective study. *Gut* 2006b;55:403-8.
- Fraquelli M, Rigamonti C, Casazza G, Conte D, Donato MF, Ronchi G, Colombo M. Reproducibility of transient elastography in the evaluation of liver fibrosis in patients with chronic liver disease. *Gut* 2007;56:968-73.
- Friedman SL. Liver fibrosis - From bench to bedside. *J Hepatol* 2003;38:S38-S53.
- Friedman SL, Roll FJ, Boyles J, Bissell DM. Hepatic lipocytes: The principal collagen-producing cells of normal rat liver. *Proc Natl Acad Sci U S A* 1985;82:8681-5.
- Friedrich-Rust M, Ong MF, Herrmann E, Dries V, Samaras P, Zeuzem S, Sarrazin C. Real-time elastography for noninvasive assessment of liver fibrosis in chronic viral hepatitis. *Am J Roentgenol* 2007;188:758-64.
- Friedrich-Rust M, Ong MF, Martens S, Sarrazin C, Bojunga J, Zeuzem S, Herrmann E. Performance of transient elastography for the staging of liver fibrosis: A meta-analysis. *Gastroenterology* 2008;134:960-74.
- Friedrich-Rust M, Schwarz A, Ong M, Dries V, Schirmacher P, Herrmann E, Samaras P, Bojunga J, Bohle RM, Zeuzem S, Sarrazin C. Real-time tissue elastography versus Fibroscan for noninvasive assessment of liver fibrosis in chronic liver disease. *Ultraschall in Med* 2009;30:478,84.
- Gaiani S, Gramantieri L, Venturoli N, Piscaglia F, Siringo S, D'Errico A, Zironi G, Grigioni W, Bolondi L. What is the criterion for differentiating chronic hepatitis from compensated cirrhosis? A prospective study comparing ultrasonography and percutaneous liver biopsy. *J Hepatol* 1997;27:979-85.

- Geller SA, Petrovic LM. Examination of the Liver Biopsy. In: ed. Biopsy Interpretation of the Liver. Philadelphia, PA: Lippincott Williams & Wilkins, 2004. pp. 30.
- Gennisson JL, Cloutier G. Sol-gel transition in agar-gelatin mixtures studied with transient elastography. *IEEE Trans Ultrason Ferroelectr Freq Contr* 2006;53:716-23.
- Gennisson JL, Cornu C, Catheline S, Fink M, Portero P. Human muscle hardness assessment during incremental isometric contraction using transient elastography. *J Biomech* 2005;38:1543-50.
- Glozman T, Azhari H. A method for characterization of tissue elastic properties combining ultrasonic computed tomography with elastography. *J Ultrasound Med* 2010;29:387-98.
- Goyal N, Jain N, Rachapalli V, Cochlin DL, Robinson M. Non-invasive evaluation of liver cirrhosis using ultrasound. *Clin Radiol* 2009;64:1056-66.
- Gulizia R, Ferraioli G, Filice C. Open questions in the assessment of liver fibrosis using real-time elastography. *Am J Roentgenol* 2008;190:W370-W1.
- Hayes WC, Keer LM, Herrmann G, Mockros LF. A mathematical analysis for indentation tests of articular cartilage. *J Biomech* 1972;5:541-51.
- Holund B, Poulsen H, Schlichting P. Reproducibility of liver biopsy diagnosis in relation to the size of the specimen. *Scand J Gastroenterol* 1980;15:329-35.
- Hong YR, Liu XM, Li ZY, Zhang XF, Chen MF, Luo ZY. Real-time ultrasound elastography in the differential diagnosis of benign and malignant thyroid nodules. *J Ultrasound Med* 2009;28:861-7.
- Hornig M-H. Texture feature coding method for texture classification. *Optical Engineering* 2003;42:228-38.
- Huwart L, Peeters F, Sinkus R, Annet L, Salameh N, ter Beek LC, Horsmans Y, Van Beers BE. Liver fibrosis: Non-invasive assessment with MR elastography. *NMR Biomed* 2006;19:173-9.

- Huwart L, Sempoux C, Salameh N, Jamart J, Annet L, Sinkus R, Peeters F, ter Beek LC, Horsmans Y, Van Beers BE. Liver fibrosis: Noninvasive assessment with MR elastography versus aspartate aminotransferase-to-platelet ratio index. *Radiology* 2007;245:458-66.
- Huwart L, Sempoux C, Vicaut E, Salameh N, Annet L, Danse E, Peeters F, ter Beek LC, Rahier J, Sinkus R, Horsmans Y, Van Beers BE. Magnetic resonance elastography for the noninvasive staging of liver fibrosis. *Gastroenterology* 2008;135:32-40.
- Huwart L, van Beers BE. MR elastography. *Gastroenterol Clin Biol* 2008;32:68-72.
- Imbert-Bismut F, Ratziu V, Pieroni L, Charlotte F, Benhamou Y, Poynard T. Biochemical markers of liver fibrosis in patients with hepatitis C virus infection: A prospective study. *Lancet* 2001;357:1069-75.
- Ito K, Mitchell DG, Gabata T, Hussain SM. Expanded gallbladder fossa: Simple MR imaging sign of cirrhosis. *Radiology* 1999;211:723-6.
- Itoh A, Ueno E, Tohno E, Kamma H, Takahashi H, Shiina T, Yamakawa M, Matsumura T. Breast disease: Clinical application of US elastography for diagnosis. *Radiology* 2006;239:341-50.
- Kanamoto M, Shimada M, Ikegami T, Uchiyama H, Imura S, Morine Y, Kanemura H, Arakawa Y, Nii A. Real time elastography for noninvasive diagnosis of liver fibrosis. *J Hepatobiliary Pancreat Surg* 2009;16:463-7.
- Kircheis G, Sagir A, Vogt C, vom Dahl S, Kubit R, Haussinger D. Evaluation of acoustic radiation force impulse imaging for determination of liver stiffness using transient elastography as a reference. *World J Gastroenterol* 2012;18:1077-84.
- Koinuma M, Ohashi I, Hanafusa K, Shibuya H. Apparent diffusion coefficient measurements with diffusion-weighted magnetic resonance imaging for evaluation of hepatic fibrosis. *J Magn Reson Imaging* 2005;22:80-5.

- Koizumi Y, Hirooka M, Kisaka Y, Konishi I, Abe M, Murakami H, Matsuura B, Hiasa Y, Onji M. Liver fibrosis in patients with chronic hepatitis C: Noninvasive diagnosis by means of real-time tissue elastography - Establishment of the method for measurement. *Radiology* 2011;258:610-7.
- Kruse SA, Smith JA, Lawrence AJ, Dresner MA, Manduca A, Greenleaf JF, Ehman RL. Tissue characterization using magnetic resonance elastography: Preliminary results. *Phys Med Biol* 2000;45:1579-90.
- Leon DA, McCambridge J. Liver cirrhosis mortality rates in Britain from 1950 to 2002: An analysis of routine data. *Lancet* 2006;367:52-6.
- Leroy V, Kim SU. Can transient elastography be used for the management of chronic hepatitis B patients? *Liver Int* 2012;32:528-30.
- Lewin M, Poujol-Robert A, Boelle PY, Wendum D, Lasnier E, Viallon M, Guechot J, Hoeffel C, Arrive L, Tubiana JM, Poupon R. Diffusion-weighted magnetic resonance imaging for the assessment of fibrosis in chronic hepatitis C. *Hepatology* 2007;46:658-65.
- Lorenzen J, Sinkus R, Adam G. Elastography: Quantitative imaging modality of the elastic tissue properties. *Rofo-Fortschritte Auf Dem Gebiet Der Rontgenstrahlen Und Der Bildgebenden Verfahren* 2003;175:623-30.
- Lu MH, Zheng YP. Indentation test of soft tissues with curved substrates: A finite element study. *Med Biol Eng Comput* 2004;42:535-40.
- Lu ZF, Zagzebski JA, Lee FT. Ultrasound backscatter and attenuation in human liver with diffuse disease. *Ultrasound Med Biol* 1999;25:1047-54.
- Lyshchik A, Higashi T, Asato R, Tanaka S, Ito J, Mai JJ, Pellot-Barakat C, Insana MF, Brill AB, Saga T, Hiraoka M, Togashi K. Thyroid gland tumor diagnosis at US elastography. *Radiology* 2005;237:202-11.
- Madsen EL, Hobson MA, Shi HR, Varghese T, Frank GR. Tissue-mimicking agar/gelatin materials for use in heterogeneous elastography phantoms. *Phys Med Biol* 2005;50:5597-618.

- Mak T-M, Huang Y-P, Zheng Y-P. Liver fibrosis assessment using transient elastography guided with real-time B-mode ultrasound imaging: A feasibility study. *Ultrasound Med Biol* 2013;39:956-66.
- Mak TM, Yu X, Zheng YP. Liver fibrosis assessment using transient elastography guided with real-time B-mode ultrasound imaging: Investigation of food intake effect. *10th International Tissue Elasticity Conference* 2011;81.
- Martini FH. *Fundamentals of anatomy and physiology*. Englewood Cliffs, New Jersey: Prentice Hall, 2006.
- Mederacke I, Wursthorn K, Kirschner J, Rifai K, Manns MP, Wedemeyer H, Bahr MJ. Food intake increases liver stiffness in patients with chronic or resolved hepatitis C virus infection. *Liver Int* 2009;29:1500-6.
- Menghini G. One-second biopsy of the liver - Problems of its clinical application. *N Engl J Med* 1970;283:582-5.
- Morikawa H, Fukuda K, Kobayashi S, Fujii H, Iwai S, Enomoto M, Tamori A, Sakaguchi H, Kawada N. Real-time tissue elastography as a tool for the noninvasive assessment of liver stiffness in patients with chronic hepatitis C. *J Gastroenterol* 2011;46:350-8.
- Motosugi U, Ichikawa T, Sano K, Sou H, Muhi A, Koshiishi T, Ehman RL, Araki T. Magnetic resonance elastography of the liver: Preliminary results and estimation of inter-rater reliability. *Jpn J Radiol* 2010;28:623-7.
- Mueller S, Sandrin L. Liver stiffness: A novel parameter for the diagnosis of liver disease. *Hepatic Med Evid Res* 2010;2:49-67.
- Muller M, Gennisson JL, Deffieux T, Tanter M, Fink M. Quantitative viscoelasticity mapping of human liver using supersonic shear imaging: Preliminary in vivo feasibility study. *Ultrasound Med Biol* 2009a;35:219-29.
- Muller M, Gennisson JL, Deffieux T, Tanter M, Fink M. Quantitative viscoelasticity mapping of human liver using supersonic shear imaging: Preliminary in vivo feasibility study. *Ultrasound Med Biol* 2009b;35:219-29.

- Munakata T, Griffiths RD, Martin PA, Jenkins SA, Shields R, Edwards RHT. An in vivo³¹P MRS study of patients with liver cirrhosis: Progress towards a non-invasive assessment of disease severity. *NMR Biomed* 1993;6:168-72.
- Myers RP, Pomier-Layrargues G, Kirsch R, Pollett A, Duarte-Rojo A, Wong D, Beaton M, Levstik M, Crotty P, Elkashab M. Feasibility and diagnostic performance of the FibroScan XL probe for liver stiffness measurement in overweight and obese patients. *Hepatology* 2012;55:199-208.
- Nishiura T, Watanabe H, Ito M, Matsuoka Y, Yano K, Daikoku M, Yatsunami H, Dohmen K, Ishibashi H. Ultrasound evaluation of the fibrosis stage in chronic liver disease by the simultaneous use of low and high frequency probes. *Br J Radiol* 2005;78:189-97.
- Numminen K, Tervahartiala P, Halavaara J, Isoniemi H, Höckerstedt K. Non-invasive diagnosis of liver cirrhosis: Magnetic resonance imaging presents special features. *Scand J Gastroenterol* 2005;40:76-82.
- Oberti F, Valsesia E, Pilette C, Rousselet MC, Bedossa P, Aube C, Gallois Y, Rifflet H, Maiga MY, PenneauFontbonne D, Cales P. Noninvasive diagnosis of hepatic fibrosis or cirrhosis. *Gastroenterology* 1997;113:1609-16.
- Orlacchio A, Bolacchi F, Antonicoli M, Coco I, Costanzo E, Tosti D, Francioso S, Angelico M, Simonetti G. Liver elasticity in NASH patients evaluated with real-time elastography (RTE). *Ultrasound Med Biol* 2012;38:537-44.
- Osman O, Huseyin A, Cagatay C, Veysel T, Sena T, Adnan G, Nese I, Feyyaz B, Davut T, Canan E, Nurdan T. Role of echo Doppler ultrasonography in the evaluation of postprandial hyperemia in cirrhotic patients. *World J Gastroenterol* 2008;14:260-4.
- Pallwein L, Mitterberger M, Struve P, Pinggera G, Horninger W, Bartsch G, Aigner F, Lorenz A, Pedross F, Frauscher F. Real-time elastography for detecting prostate cancer: Preliminary experience. *BJU Int* 2007;100:42-6.

- Patel K, Lajoie A, Heaton S, Pianko S, Behling CA, Bylund D, Pockros PJ, Blatt LM, Conrad A, McHutchison JG. Clinical use of hyaluronic acid as a predictor of fibrosis change in hepatitis C. *J Gastroenterol Hepatol* 2003;18:253-7.
- Patton KT, Thibodeau GA. *Anatomy & physiology*. St. Louis, Mo: Mosby Elsevier 2010.
- Perrault J, McGill DB, Ott BJ, Taylor WF. Liver biopsy: Complications in 1000 inpatients and outpatients. *Gastroenterology* 1978;74:103-6.
- Petta S, Craxi A. Assessment by Fibroscan of fibrosis in nonalcoholic fatty liver disease: XL versus M probe? *Hepatology* 2012;55:1309-.
- Plebani M, Burlina A. Biochemical markers of hepatic fibrosis. *Clin Biochem* 1991;24:219-39.
- Rankin G, Stokes M. Reliability of assessment tools in rehabilitation: An illustration of appropriate statistical analyses. *Clin Rehabil* 1998;12:187-99.
- Regev A, Berho M, Jeffers LJ, Milikowski C, Molina EG, Pyrsopoulos NT, Feng ZZ, Reddy KR, Schiff ER. Sampling error and intraobserver variation in liver biopsy in patients with chronic HCV infection. *Am J Gastroenterol* 2002;97:2614-8.
- Rouviere O, Yin M, Dresner MA, Rossman PJ, Burgart LJ, Fidler JL, Ehman RL. MR elastography of the liver: Preliminary results. *Radiology* 2006;240:440-8.
- Royer D, Dieulesaint E. *Elastic waves in solids*. Berlin: Springer, 2000.
- Rustogi R, Horowitz J, Harmath C, Wang Y, Chalian H, Ganger DR, Chen ZME, Bolster BD, Shah S, Miller FH. Accuracy of MR elastography and anatomic MR imaging features in the diagnosis of severe hepatic fibrosis and cirrhosis. *J Magn Reson Imaging* 2012;35:1356-64.
- Saftoiu A, Gheonea DI, Ciurea T. Hue histogram analysis of real-time elastography images for noninvasive assessment of liver fibrosis. *Am J Roentgenol* 2007;189:W232-W3.

- Salomon G, Koellermann J, Thederan I, Chun FKH, Budaeus L, Schlomm T, Isbarn H, Heinzer H, Huland H, Graefen M. Evaluation of prostate cancer detection with ultrasound real-time elastography: A comparison with step section pathological analysis after radical prostatectomy. *Eur Urol* 2008;54:1354-62.
- Sandrin L, Fourquet B, Hasquenoph JM, Yon S, Fournier C, Mal F, Christidis C, Ziolo M, Poulet B, Kazemi F, Beaugrand M, Palau R. Transient elastography: A new noninvasive method for assessment of hepatic fibrosis. *Ultrasound Med Biol* 2003;29:1705-13.
- Sandrin L, Tanter M, Gennisson JL, Catheline S, Fink M. Shear elasticity probe for soft tissues with 1-D transient elastography. *IEEE Trans Ultrason Ferroelectr Freq Contr* 2002;49:436-46.
- Saverymuttu SH, Joseph AEA, Maxwell JD. Ultrasound scanning in the detection of hepatic fibrosis and steatosis. *Br Med J* 1986;292:13-5.
- Shire NJ, Yin M, Chen J, Railkar RA, Fox-Bosetti S, Johnson SM, Beals CR, Dardzinski BJ, Sanderson SO, Talwalkar JA, Ehman RL. Test-retest repeatability of MR elastography for noninvasive liver fibrosis assessment in hepatitis C. *J Magn Reson Imaging* 2011;34:947-55.
- Simonovský V. The diagnosis of cirrhosis by high resolution ultrasound of the liver surface. *Br J Radiol* 1999;72:29-34.
- Someya N, Endo MY, Fukuba Y, Hayashi N. Blood flow responses in celiac and superior mesenteric arteries in the initial phase of digestion. *American Journal of Physiology - Regulatory, Integrative and Comparative Physiology* 2008;294:R1790-R6.
- Talwalkar JA, Yin M, Fidler JL, Sanderson SO, Kamath PS, Ehman RL. Magnetic resonance imaging of hepatic fibrosis: Emerging clinical applications. *Hepatology* 2008;47:332-42.
- Tanter M, Bercoff J, Athanasiou A, Deffieux T, Gennisson JL, Montaldo G, Muller M, Tardivon A, Fink M. Quantitative assessment of breast lesion viscoelasticity:

- Initial clinical results using supersonic shear imaging. *Ultrasound Med Biol* 2008;34:1373-86.
- Taouli B, Tolia AJ, Losada M, Babb JS, Chan ES, Bannan MA, Tobias H. Diffusion-weighted MRI for quantification of liver fibrosis: Preliminary experience. *Am J Roentgenol* 2007;189:799-806.
- Tempkin BB. *Ultrasound scanning: Principles and protocols*. St. Louis, Missouri: Saunders, 2009.
- Thomas A, Fischer T, Frey H, Ohlinger R, Grunwald S, Blohmer JU, Winzer KJ, Weber S, Kristiansen G, Ebert B, Kummel S. Real-time elastography - An advanced method of ultrasound: First results in 108 patients with breast lesions. *Ultrasound Obstet Gynecol* 2006;28:335-40.
- Toyoda H, Kumada T, Kamiyama N, Shiraki K, Takase K, Yamaguchi T, Hachiya H. B-Mode Ultrasound With Algorithm Based on Statistical Analysis of Signals: Evaluation of Liver Fibrosis in Patients With Chronic Hepatitis C. *Am J Roentgenol* 2009;193:1037-43.
- Venkatesh SK, Yin M, Glockner JF, Takahashi N, Araoz PA, Talwalkar JA, Ehman RL. MR elastography of liver tumors: Preliminary results. *Am J Roentgenol* 2008;190:1534-40.
- Verveer C, Zondervan PE, ten Kate FJW, Hansen BE, Janssen HLA, de Knegt RJ. Evaluation of transient elastography for fibrosis assessment compared with large biopsies in chronic hepatitis B and C. *Liver Int* 2012;32:622-8.
- Vicas C, Lupsor M, Badea R, Nedevschi S. Usefulness of textural analysis as a tool for noninvasive liver fibrosis staging. *Journal of Medical Ultrasonics* 2011;38:105-17.
- Wai CT, Greenson JK, Fontana RJ, Kalbfleisch JD, Marrero JA, Conjeevaram HS, Lok ASF. A simple noninvasive index can predict both significant fibrosis and cirrhosis in patients with chronic hepatitis C. *Hepatology* 2003;38:518-26.

- Wang J, Guo L, Shi X, Pan W, Bai Y, Ai H. Real-time elastography with a novel quantitative technology for assessment of liver fibrosis in chronic hepatitis B. *Eur J Radiol* 2012;81:e31-e6.
- Wu CM, Chen YC, Hsieh KS. Texture features for classification of ultrasonic liver images. *Medical Imaging, IEEE Transactions on* 1992;11:141-52.
- Yin M, Talwalkar JA, Glaser KJ, Manduca A, Grimm RC, Rossman PJ, Fidler JL, Ehman RL. Assessment of hepatic fibrosis with magnetic resonance elastography. *Clin Gastroenterol Hepatol* 2007;5:1207-13.
- Yin M, Talwalkar JA, Glaser KJ, Venkatesh SK, Chen J, Manduca A, Ehman RL. Dynamic postprandial hepatic stiffness augmentation assessed With MR elastography in patients with chronic liver disease. *Am J Roentgenol* 2011;197:64-70.
- Zardi EM, Dobrina A, Uwechie V, Caccapaglis F, Rollo M, Laghi V, Ambrosino G, Lumachi F. Postmeal portal flow variations in HCV-related chronic hepatitis and liver cirrhosis with and without hyperdynamic syndrome. *In Vivo* 2008;22:509-12.